CONFERENCE PROGRAM

2ND International PEEK Meeting

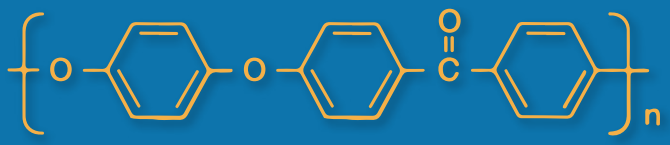

WASHINGTON, D.C.
April 23-24

2015

PEEK Practice Newsletters

- Complimentary semi-annual newsletter summary of medical PEEK literature
- Hand-picked selection of the most recent, clinically relevant literature
- Save time and accelerate the speed of innovation

REGISTER AT:
invibio.com/newsletter

Invibio®
BIOMATERIAL SOLUTIONS

Stay at the Forefront of Medical PEEK Innovation

Online Reference for PEEK Implants

- Complimentary reference for polyaryletherketones used in medical devices
- Highlights recent developments in clinically relevant PEEK research
- Stimulate biomaterial investigations related to medical grade PEEK

REGISTER AT:
medicalpeek.org/register

Medical PEEK Lexicon

2ND International PEEK Meeting

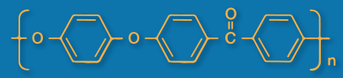

Dear Participant,

The purpose of the meeting is to bring together engineers, scientists, regulators and clinicians from academia, industry and government agencies. Leading edge research on advancements in medical grade PEEK technology and clinical applications will be presented:

- Identifying and closing gaps in the regulatory science
- Innovations in orthopedic bearings and tribology
- PEEK composites for bone on-growth
- Advances in spinal rods and artificial disc applications
- Advances in formulations for dental, trauma and arthroscopic implants
- Structural composites and woven fiber applications
- Advances in biologic aspects of wear debris

Abstracts were evaluated by the Scientific Committee for inclusion in the program, either as a podium presentation or a poster.

SCIENTIFIC COMMITTEE

Steven Kurtz, Ph.D.
CONFERENCE ORGANIZER
Drexel University & Exponent, Inc.

Ryan Roeder, Ph.D.
Notre Dame University

Prof. Joanne Tipper, Ph.D.
University of Leeds

Kenneth McDermott, Ph.D.
FDA OSEL (Office of Science and Engineering Laboratories)

Kate Kavlock, Ph.D.
FDA CDRH (Center for Devices and Radiological Health)

John Bowsher, Ph.D.
FDA CDRH

SPONSORED BY
Invibio® BIOMATERIAL SOLUTIONS

ORGANIZED BY
IRC IMPLANT RESEARCH CENTER
Exponent®

2ND INTERNATIONAL PEEK MEETING AGENDA

Thursday Morning, April 23

WELCOME

8:00 am	On-site Registration Opens	
9:00 am	Welcome, Opening Remarks & Advances Since 2013	*Steven Kurtz*

SESSION I: Regulatory Science of PEEK and PEEK Composites

Moderators: Ken McDermott, Ph.D., FDA & John Bowsher, Ph.D., FDA

9:12 am	**Invited Talk 1:** Primer on PEEK and International Standards	*Steven Kurtz, Ph.D.*
9:24 am	**Invited Talk 2:** Processing and Properties of PEEK and PEEK-CFR Composites	*Craig Valentine*
9:36 am	**Invited Talk 3:** Coating Technologies of PEEK – What Works, What Doesn't	*Francesco Robotti, Ph.D.*
9:48 am	**Invited Talk 4:** Bioactive PEEK Composites – Porous PEEK and HA PEEK	*Ryan Roeder, Ph.D.*
10:00 am	**Regulatory Roundtable 1:** Unanswered Questions in Processing of Novel PEEK Coatings and Composites	*Kate Kavlock, Ph.D., FDA*
10:30 am	**Morning Coffee Break**	
11:00 am	**Invited Talk 5:** Retrieval Update on PEEK Devices	*Steven Kurtz, Ph.D.*
11:12 am	**Invited Talk 6:** Deformation, Creep, Fatigue and Fracture of PEEK and CFR-PEEK	*Clare Rimnac, Ph.D.*
11:24 am	**Invited Talk 7:** Tribology of PEEK	*Thomas Grupp, Ph.D.*
11:36 am	**Invited Talk 8:** Biologic Response to PEEK and CFR-PEEK Debris	*Joanne Tipper, Ph.D.*
11:48 am	**Regulatory Roundtable 2:** Unanswered Questions in Spine and Orthopaedic Bearing Surfaces	*John Bowsher, Ph.D., FDA*
12:17 pm	**Lunch & Poster Session 1**	

2ND INTERNATIONAL PEEK MEETING AGENDA

Thursday Afternoon, April 23

SESSION II: Orthopaedic Applications of PEEK
Moderators: John Bowsher, Ph.D., FDA and Steven Kurtz, Ph.D.

2:00 pm	**Podium Talk 1:** Early Results of a New Rotating Hinge Knee Implant	*Alexander Giurea, M.D.*
2:15 pm	**Podium Talk 2:** Inflammatory Effects of Different Carbon-Fiber Reinforced PEEK Particles *In Vivo*	*Sandra Utzschneider, M.D., Ph.D.*
2:30 pm	**Podium Talk 3:** PEEK Femoral Component in TKA: Bone Remodeling and Device Performance during Gait and Squatting	*Lennert de Ruiter, Ph.D.*
2:45 pm	**Podium Talk 4:** The Tribological Performance of PEEK Polymer on Polymer Bearings	*Doruk Baykal, Ph.D.*
3:00 pm	**Podium Talk 5:** The Influence of Surface Roughness, Lubricant Protein Concentration and Temperature on the Wear of UHMWPE Articulating against PEEK-OPTIMA®	*R. Cowie, Ph.D.*

3:15 pm **Afternoon Coffee Break**

SESSION III: Engineering PEEK Bioactivity
Moderators: Ryan Roeder, Ph.D., and Kate Kavlock, Ph.D., FDA

3:45 pm	**Podium Talk 6:** Enhanced Osteogenesis on PEEK Polymer Using Injection Mould Nanopatterning	*Ali Brydone, Ph.D.*
4:00 pm	**Podium Talk 7:** *In Vitro* and *In Vivo* Evaluation of Surface Porous PEEK for Orthopaedic Applications	*Brennan Torstrick, Ph.D.*
4:15 pm	**Podium Talk 8:** Characterization of the *In Vitro* Antimicrobial and *In Vivo* Antibiofilm Properties of a PEEK-Silver Zeolite Composite In Spine	*Paul Kraemer, M.D.*
4:30 pm	**Podium Talk 9:** PEEK-β-TCP-TiO2: A Smart Biocompatible Composite with Osteoconductive Properties	*M-F. Harmand, Ph.D.*
4:45 pm	**Podium Talk 10:** Evaluation of HA/PEEK Material in An Ovine Cervical Fusion Model: A Pilot Study	*William Walsh, Ph.D.*

5:00 pm **Day 1 Meeting Adjourns**

Drexel transportation – transition to Reception and Dinner

6:30 pm **Reception and Dinner Begins**

2ND INTERNATIONAL PEEK MEETING AGENDA

Friday Morning, April 24

8:00 am On-site Registration Opens, Breakfast

SESSION IV: Novel Fabrication Techniques and Structure-Property Relationships in PAEKS
Moderators: Clare Rimnac, Ph.D., and Hany Demian, FDA

9:00 am	**Invited Talk 9:** Additive Manufacturing of PAEK Polymers	*Oana Ghita, Ph.D.*
9:20 am	**Podium Talk 11:** Correlation Between Crystallinity and Mechanical Properties of PEEK for Orthopaedic Applications	*Marco Regis*
9:35 am	**Podium Talk 12:** Morphology and Impact Strength of PEEK containing Hydroxyapatite Micro- and Nano-fillers	*Stephen Spiegelberg, Ph.D.*
9:50 am	**Podium Talk 13:** PEEK-OPTIMA® LT1 for High Temperature Laser Sintering (HT-LS)	*Silvia Berretta, Ph.D.*

10:05 am **Morning Coffee Break**

SESSION V: Novel Clinical Applications of PEEK
Moderators: Joanne Tipper, Ph.D., and John Bowsher, Ph.D., FDA

10:20 am	**Invited Talk 10:** Development of a PEEK-on-Ceramic Artificial Disc	*David Hovda*
10:40 am	**Podium Talk 14:** Antibiotic Drug Release PEEK Clip to Combat Surgical Site Infection in Spinal Fusion Surgery	*Alex Sevit*
10:55 am	**Podium Talk 15:** Antithrombogenic Modification on PEEK with Bioinspired Phospholipid Polymer Grafting	*K. Ishihara, Ph.D.*
11:10 am	**Invited Talk 11:** CFR PEEK in Orthopaedic Trauma – Pre-Clinical Data	*Joanne Wilson, Ph.D.*
11:25 am	**Podium Talk 16:** Seeing is Believing: Treatment of Proximal Humerus Fractures Using a Novel Radiolucent Implant	*Kyros Ipaktchi, M.D.*
11:25 am	**Podium Talk 17:** A Computational Investigation into the Use of Carbon Fibre Reinforced PEEK Laminates for Orthopaedic Applications	*Elizabeth Gallagher, Ph.D.*

12:00 pm **Meeting Adjourns**

2ND International PEEK Meeting

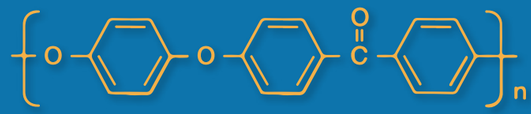

WASHINGTON, D.C.
April 23-24
2015

Reference	Abstract Title	First Author	Page
BIOACTIVE			
Podium Talk 6	Enhanced Osteogenesis on PEEK Polymer Using Injection Mould Nanopatterning	*Brydone, A.*	00
Podium Talk 7	*In Vitro* and *In Vivo* Evaluation of Surface Porous PEEK for Orthopaedic Applications	*Torstrick, F.*	00
Podium Talk 9	PEEK-β-TCP-TiO2: A Smart Biocompatible Composite with Osteoconductive Properties	*Harmand, M-F.*	00
Podium Talk 15	Antithrombogenic Modification on PEEK with Bioinspired Phospholipid Polymer Grafting	*Ishihara, K.*	00
Poster 003	Mechanical Properties of Surface Porous PEEK	*Evans, N.*	00
Poster 005	Enhanced PEEK *In Vivo* Osseointegration by Accelerated Neutral Atom Beam Processing	*Khoury, J.*	00
Poster 007	Silver Doped Titanium Oxide - PDMS Hybrid Coating Inhibits *Staphylococcus aureus and Staphylococcus epidermidis Growth on PEEK*	*Tran, N.*	00
Poster 040	Increased Bone Fusion on PEEK Implants Coated with Nano-Hydroxyapatite: A Histomorphometric Study in Rabbit Bone	*Johansson, P.*	00
DENTAL			
Poster 008	Plasma Treatment of Machined PEEK and CFRPEEK Implants: Wettability and Osteoblast Proliferation	*Moon, P.*	00
Poster 009	The Effect of Processing Conditions on the Flexural Strength of Polyetheretherketone (PEEK) Used as Innovative Denture Base Material	*Muhsin, S.*	00
Poster 010	The Application of PEEK in Dental Implant Suprastructures: A Finite Element Analysis	*Schwitalla, A.*	00
Poster 039	Polyetheretherketon (PEEK) Telescopic Denture Retained on Implants and Teeth for Maxilla Rehabilitation	*Spintig, T.*	00
ORTHO			
TBD	Carbon-Fiber-Reinforced PEEK as an alternative bearing material in artificial knee arthroplasty	*Grupp, T.*	00
Podium Talk 1	Early Results of a New Rotating Hinge Knee Implant	*Giurea, A.*	00
Podium Talk 2	Inflammatory Effects of Different Carbon-Fiber Reinforced PEEK Particles *In Vivo*	*Utzschneider, S.*	00
Podium Talk 3	PEEK Femoral Component in TKA: Bone Remodeling and Device Performance during Gait and Squatting	*de Ruiter, L.*	00
Poster 015	Investigation of Fretting-Corrosion Behavior of PEEK-Metal Interfaces and Comparison with Metal-Metal Interfaces	*Kocagoz, S.*	00
Poster 016	Improved Bone Remodelling Stimulus with a Novel PEEK Implant for Total Knee Replacement	*Rankin, K. E*	00
Poster 042	Intracorporeal Ultrasonic Welding of PEEK Implants	*Bonutti, P.*	00
PEEK PROPERTIES			
Podium Talk 11	Correlation Between Crystallinity and Mechanical Properties of PEEK for Orthopaedic Applications	*Regis, M.*	00
Podium Talk 12	Morphology and Impact Strength of PEEK containing Hydroxyapatite Micro- and Nano-fillers	*Spiegelberg, S.*	00
Podium Talk 13	PEEK-OPTIMA® LT1 for High Temperature Laser Sintering (HT-LS)	*Berretta, S.*	00
Poster 017	The Role of Thermal History on the Semicrystalline Morphology and Impact Strength of PEEK	*Bellare, A.*	00
Poster 019	Mechanical and Structural Analyses of TiO_2 and HA Coated Peek Biomaterial	*Sargin, F.*	00
Poster 041	Thin Film Self-Reinforced Composite PEEK: Characterization and Evaluation as a Potential Orthopedic Biomaterial	*Ouellette, E.*	00

Reference	Abstract Title	First Author	Page
SPINE			
Invited Talk 10	Development of a Peek-Ceramic Cervical Disc	*Hovda, D.*	00
Podium Talk 10	Evaluation of HA/PEEK Material in An Ovine Cervical Fusion Model: A Pilot Study	*Walsh, W.*	00
Podium Talk 14	Antibiotic Drug Release PEEK Clip to Combat Surgical Site Infection in Spinal Fusion Surgery	*Sevit, A.*	00
Poster 022	Evaluation of Viscoelastic Properties of an Oblong PEEK Rod Construct in a Spondylolisthesis Reduction Model	*Julien, P.*	00
Poster 024	Tribological Studies of PEEK on PEEK Facet Resurfacing Devices	*Siskey, R.*	00
Poster 038	A Novel PEEK Titanium Structural Composite for Spinal Devices	*Fang, S.*	00
TRAUMA			
Podium Talk 16	Seeing is Believing: Treatment of Proximal Humerus Fractures Using a Novel Radiolucent Implant and Its Effect on Reduction Accuracy, Healing Rate, and Functional Outcome	*Hak, D.*	00
Podium Talk 17	A Computational Investigation into the Use of Carbon Fibre Reinforced PEEK Laminates for Orthopaedic Applications	*Gallagher, E.*	00
Poster 027	PEEK Bone Plate Structures for Mandibular Fracture Fixation	*Lovald, S.*	00
Poster 028	Biomechanical Performance of Shape-Memory PEEK Soft Tissue Fixation Devices	*Smith, K.*	00
TRIBOLOGY			
Podium Talk 4	The Tribological Performance of PEEK Polymer on Polymer Bearings	*Baykal, D.*	00
Podium Talk 5	The Influence of Surface Roughness, Lubricant Protein Concentration and Temperature on the Wear of UHMWPE Articulating against PEEK-OPTIMA®	*Cowie, R.*	00
Podium Talk 8	Characterization of the In Vitro Antimicrobial and In Vivo Antibiofilm Properties of a PEEK-Silver Zeolite Composite In Spine	*Sankar, S.*	00
Poster 029	The Use of PEEK-on-UHMWPE and CFR-PEEK-on-UHMWPE as a Bearing Combination in Total Knee Arthroplasty	*Adesina, T.*	00
Poster 031	PEEK-OPTIMA® as an Alternative Bearing Material to Cobalt Chrome in Total Knee Replacement	*Cowie, R.*	00
Poster 033	PEEK-based Materials as Hip Replacement Bearing Surfaces: A Comparison of Wear and Wear Particles Generated by Injection Molded PEEK-based Materials with Cross Linked Polyethylene Sliding Against Metal and Ceramic Counterfaces.	*Hammouche, S.*	00
Poster 034	Wear Resistance of PMPC-Grafted CFR-PEEK Cups Against Ceramic Femoral Heads	*Kyomoto, M.*	00

PEEK / β-TCP / TiO_2: a smart biocompatible composite with osteoconductive properties

M-F. Harmand[(1)], C. Sédarat[(2)], J-P. Cougoulic[(3)]

(1) LEMI –Technopole Bordeaux Montesquieu – Martillac – France (2) Faculty of Odontology – University of Bordeaux – France

(3) Private Practice – Pornichet – France

info@lemi.fr

Introduction: Polyetheretherketone (PEEK) is a well-known aromatic, rigid semi-crystalline thermoplastic with excellent mechanical properties and bone-like stiffness, with good biocompatibility. Moreover for biomedical applications, particularly in the area of load-bearing orthopedic applications, PEEK is able to be repeatedly sterilized, and shaped by machining or injection molding. Devices using PEEK's unique combination of properties have found considerable success in spine, cardiovascular and dental applications. However, PEEK exhibits poor osteoconductive properties that severely limit the potential applications in orthopedic or dental fields. To overcome this lack of efficacy, an innovative PEEK-based composite was developed as a dispersion of β-tricalcium phosphate (β-TCP) (10% w/v) and Titanium oxide (anatase) (10% w/v) within a PEEK matrix. The PEEK/β-TCP/TiO_2 demonstrated excellent mechanical properties, with elastic modulus comparable to that of natural cortical bone: tensile strength of 98 MPa, flexural modulus of 4.7 GPa and a flexural strength of 161 MPA. Moreover, based on the recommendations of ISO 10993-1 (2009) "Biological evaluation of medical devices", cytotoxicity, acute systemic toxicity, irritation, sensitization and mutagenicity (Ames test, chromosome aberrations using human lymphocytes and sister chromatid exchange) were performed and demonstrated composite biocompatibility. In this study, we present the cytocompatibility using human osteoblasts, and rabbit implantation results demonstrating the bioactive nature of the material.

Materials and Methods:
In vitro study: Discs (15.5 mm in diameter) of the composite exhibiting a smooth surface were γ-ray sterilized (25kGy) and placed in 24-well tissue culture plates (Nunc). Human osteoblasts (HAB) arising from alveolar bone were cultured directly on the material at $5x10^3$ cells/cm^2 for assessment of adhesion, proliferation, and alkaline phosphatase (ALP) activity over 27 days. Viable cells were counted using trypan blue exclusion test. ALP activity was measured with a commercial kit. HAB adhesion was recorded by SEM.

In vivo study: Two different implants were tested, cpTi and PEEK composite (2 mm in diameter, 6 mm length). They were inserted in drilled femoral diaphysis perpendicular to the femur axis of New Zealand White rabbits. 5 rabbits were euthanized at 4, 12 and 24 weeks. Bone segments containing the implants were prepared for SEM analysis (sections parallel to the long axis of the implants).

Results:
In vitro results: SEM showed that HAB adhere and proliferate on the material. At 27 days, the material was covered by a multilayer of HAB (Fig.1). A slight increase in cell adhesion has been observed with regards to negative control: + 12% at 3h. HAB proliferated better on the compound than on the negative control. At 27 days, cell density was 17% higher than on the negative control. A significant enhancement of ALP activity, an early marker of HAB differentiation was observed (+21% at day 27).
In vivo results: as soon as week 4, apposition by "invagination" of newly-formed bone along the PEEK composite implant surface was observed without any soft tissue interposition (Fig.2). Comparable result was obtained with cpTi. These first results were confirmed at 12 and 24 weeks with more intensity.

Discussion: Human alveolar osteoblasts growth and phenotype expression (ALP) were slightly enhanced in direct contact with the composite: this could be the consequence of a better cell adhesion process, and/or related to the release of Ca^{++} ions from the material surface. Human osteoblast proliferation, gene expression of BMP-2 and -4, and collagen type I synthesis were shown *in vitro* to be stimulated by increased extracellular Ca^{++} [1,2]. Following implantation in the rabbit bone, both PEEK composite and cpTi presented an increase in bone thickness in contact with the implant accompanied with apposition of new bone along the implant surface.
Both *in vitro* and *in vivo* results show obvious osteoconductive properties of PEEK composite. This was confirmed by the successful development of a clinical application in the field of dental implants.

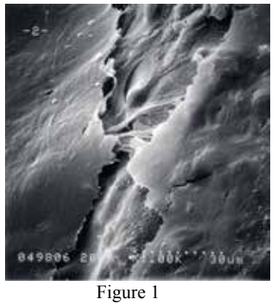

Figure 1

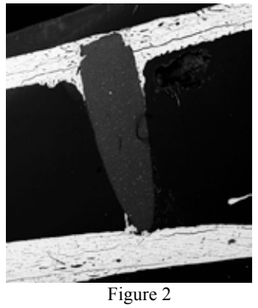

Figure 2

References:
[1]. Huang Z. et al (2001) J Biol Chem; 276: 21351-21358
[2]. Nakade O. et al (2001) J Bone Miner Metab; 19(1):13-19.

Enhanced osteogenesis on PEEK polymer using injection mold nanopatterning

Brydone, AS[1,2], Meek, RDM[2], Dalby, MJ[3], Gadegaard, N[1]
[1]Division of Biomedical Engineering, University of Glasgow, Glasgow, UK
[2]Department of Orthopaedic Surgery, Southern General Hospital, Glasgow, UK
[3]Centre for Cell Engineering, University of Glasgow, UK
alibrydone@gmail.com

Introduction: Poly-ether-ether-ketone (PEEK) is a popular orthopedic biomaterial [Kurtz 2007]. Previous studies, however, have demonstrated PEEK is relatively inert (i.e. has no bioactivity) which reduces integration with bone and limits its application in orthopedic surgery [Gittens 2014, Briem 2005]. Without osseointegration implants may loosen or migrate, and cause pain, deformity or disability to the patient [Branemark 2006].

Surface topography can affect cell adhesion, proliferation, and differentiation [Dalby 2007, Biggs 2009 and 2010]. Nanofabrication techniques such as electron beam lithography can create highly defined and reproducible bioactive topographies that may enable osseointegration of orthopedic implants [Gadegaard 2003, 2006, Prodanov 2013]. Also, plasma treatment has been used to modify surface chemistry and topography to improve human osteoblast cyto-compatibility [Briem 2005, Poulsson 2011].

The aim of this project was to determine if injection mold nanopatterning and plasma treatment can be used to enhance osteogenesis *in vitro*, and thus make PEEK bioactive.

Methods and Materials: PEEK (LT1 Optima, Invibio Biomaterials Solutions Ltd, Thornton-Cleveleys, UK) substrates were fabricated by injection mold nanopatterning (using molds created by electron beam lithography and nickel electroplating [Gadegaard 2003 and 2006]. The 'osteoinductive' near-square (NSQ) nanopattern (120 nm diameter pits, with 300 ± 50 nm centre-centre spacing) was compared to planar (FLAT) PEEK samples [Curtis 2004, Dalby 2007]. NSQ and FLAT PEEK surfaces were plasma treated at 20°C at 200W and 0.2 mbar O_2 for 0, 30, 60, 120, 300 or 600 seconds.

Atomic force microscopy (AFM) and scanning electron microscopy were used to characterize the surface topography. Water contact angle measurements were taken using a telescopic goniometer.

Human bone marrow stromal cells (hBMSCs, also referred to as mesenchymal stem cells, skeletal stem cells, or osteoprogenitor cells in the literature) were harvested from patients undergoing primary hip replacement operations. Mononuclear cells were isolated from the blood cells using Ficoll-Paque density gradient. 10,000 hBMSCs/cm^2 were seeded onto the PEEK substrates and maintained in a humidified atmosphere of 5% CO_2 at 37˚C in basal culture media changed three times weekly.

The cells were fixed and stained after 6 weeks using alizarin red S (ARS) stain (for calcium) and the von Kossa technique (for phosphate) and analyzed using CellProfiler cell image analysis software to determine: (1) cell-surface coverage; (2) cell number; and (3) particle analysis of either calcium (ARS stain) or phosphate (von Kossa technique)[Kamentsky 2011].

Results: AFM revealed distinct topographical differences in the FLAT PEEK compared to NSQ nanopatterned PEEK. After plasma treatment, nanopits became wider and less well defined, and the FLAT substrates became rougher (fig. 1).

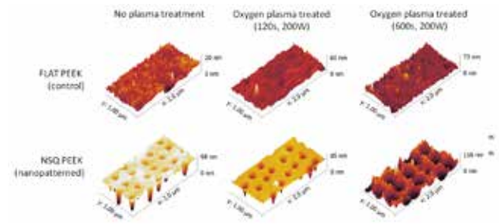

Fig. 1. AFM images showing the etching effect of oxygen plasma on FLAT and NSQ PEEK with increased duration of treatment.

ARS stain showed that oxygen plasma treatment increased cell coverage from 38.5% on FLAT and 36.0% on NSQ to over 70% on the plasma treated FLAT and NSQ surfaces. Also, oxygen plasma treatment resulted in an increased number of cells on the FLAT and NSQ surfaces ($P < 0.05$). Calcium expression (quantified relative to the number of cells) was increased on the untreated NSQ surface compared to oxygen plasma treated NSQ PEEK (fig. 2)(not significant).

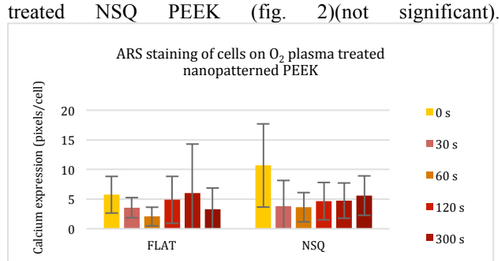

Fig. 2. Relative calcium expression (using ARS stain) on FLAT and NSQ nanopatterned PEEK.

Von Kossa staining revealed more cell-surface coverage on the FLAT substrates (69.1%) compared to NSQ (31.9%) without oxygen plasma treatment. After oxygen plasma treatment there was an increase in cell coverage on all samples (75-81%). Also, an increased number of cells were detected on the FLAT and NSQ surfaces that had been oxygen plasma treated ($P < 0.005$).

Phosphate expression relative to cell number, was increased (seven-fold) on NSQ PEEK ($P < 0.05$) compared to FLAT PEEK (fig. 3). Furthermore, after oxygen plasma treatment relative phosphate expression on NSQ PEEK significantly decreased ($P < 0.05$).

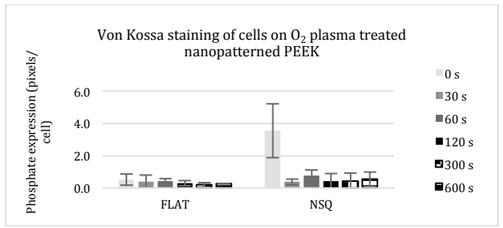

Fig. 3. Relative phosphate expression (using von Kossa staining technique) on FLAT and NSQ nanopatterned PEEK.

Discussion: It was hypothesized that improving the wettability of PEEK using oxygen plasma treatment would improve hBMSC adhesion and enhance osteogenesis as has been demonstrated with other cell types [Briem et al. 2005, Poulsson 2011]. In this study, oxygen plasma treatment significantly increased hBMSC cell attachment on PEEK surfaces by two to four fold as demonstrated by both ARS and von Kossa staining. Although hBMSCs adhere to untreated NSQ PEEK in much smaller numbers, the cells that remained expressed a relatively much larger amount of calcium. This indicates that the remaining cells attained a more osteoblastic phenotype and that the NSQ nanopatterned PEEK surface induces hBMSC differentiation and stimulates osteogenesis. Interestingly, the relative calcium expression per cell was reduced by oxygen plasma treatment, thus indicating the osteogenic effect of the nanopattern had been reversed.

This project has demonstrated that oxygen plasma treatment can improve cell adhesion and injection mold nanopatterning enhances osteogenesis on PEEK. Injection mold nanopatterning can be used to modify complex three-dimensional structures and therefore this technology has the potential to be translated into clinical application and improve osteointegration of PEEK implants *in vivo* [Brydone 2012].

References:

Biggs MJ, Richards RG, Gadegaard N, McMurray RJ, Affrossman S, Wilkinson CD, Oreffo RO, Dalby MJ. Interactions with nanoscale topography: adhesion quantification and signal transduction in cells of osteogenic and multipotent lineage. J Biomed Mater Res A 2009; 91(1): 195-208.

Biggs MJ, Richards RG, Dalby MJ. Nanotopographical modification: a regulator of cellular function through focal adhesions. Nanomedicine 2010; 6(5): 619-33.

Boscariol MR, Moreira AJ, Mansano RD, Kikuchi IS, Pinto TJA. Sterilization by pure oxygen plasma and by oxygen-hydrogen peroxide plasma: an efficacy study. Int J Pharmaceutics 2008; 353: 170-5.

Brånemark R, Brånemark PI, Rydevik B, Myers RR. Osseointegration in skeletal reconstruction and rehabilitation: a review. J Rehabil Res Dev. 2001; 38(2): 175-81.

Briem D, Strametz S, Schroder K, Meenen NM, Lehmann W, Linhart W, et al., Response of primary fibroblasts and osteoblasts to plasma treated polyetheretherketone (PEEK) surfaces. J Mater Sci Mater Med 2005; 16 (7): 671-677.

Brydone AS, Morrison DSS, Stormonth-Darling J, Meek RDM, Tanner KE, Gadegaard N. Design and fabrication of a 3D nanopatterned PEEK implant for cortical bone regeneration in a rabbit model. Eur Cells Mater. 2012, 24, 39.

Curtis ASG, Gadegaard N, Dalby MJ, Riehle MO, Wilkinson CDW, Aitchison G. Cells react to nanoscale order and symmetry in their surroundings. IEEE Transactions on Nanobioscience 2004; 3(1): 61-5.

Dalby MJ, Gadegaard N, Tare R, Andar A, Riehle MO, Herzyk P, Wilkinson CD, Oreffo RO. The control of human mesenchymal cell differentiation using nanoscale symmetry and disorder. Nat Mater 2007; 6(12): 997-1003.

Gadegaard N, Thoms S, Macintyre DS, McGhee K, Gallagher J, Casey B, Wilkinson CDW. Arrays of nano-dots for cellular engineering. Microelectron Eng 2003; 67-68: 162-168.

Gadegaard N, Martines E, Riehle MO, Seunarine, K. Applications of nano-patterning to tissue engineering. Microelectronic Engineering 2006; 83(4-9): 1577-81.

Gittens RA, Olivares-Navarrete R, Schwartz Z, Boyan BD. Implant osseointegration and the role of microroughness and nanostructures: lessons for spine implants. Acta Biomater. 2014; 10(8): 3363-71.

Kamentsky L, Jones TR, Fraser A, Bray M, Logan D, Madden K, Ljosa V, Rueden C, Harris GB, Eliceiri K, Carpenter AE. Improved structure, function, and compatibility for CellProfiler: modular high-throughput image analysis software. Bioinformatics 2011; 27(8): 1179-80.

Kurtz SM, Devine JN. PEEK biomaterials in trauma, orthopedic, and spinal implants. Biomaterials 2007; 28(32): 4845-69.

Moriera AJ, Mansano RD, Pinto TJA, Ruas R, Zambon LS, Silva MV, Veronck PB. Sterilization by oxygen plasma. Applied Surface Science 2004; 235: 151-5.

Moisan M, Barbeau J, Moreau S, Pelletier J, Tabrizian M, Yahia LH. Low-temperature sterilization using gas plasmas: a review of the experiments and an analysis of the inactivation mechanisms. Int J Pharmaceutics 2001; 226: 1-21.

Poulsson AHC, Richards GR. Surface modification techniques of polyetheretherketone, including plasma surface treatment. In: Kurtz SM, editor. PEEK Biomaterials Handbook. Oxford: Elsevier Inc; 2012. p. 145-161.

Prodanov L, Lamers E, Domanski M, Luttge R, Jansen JA, Walboomers XF. The effect of nanometric surface texture on bone contact to titanium implants in rabbit tibia. Biomaterials 2013; 34(12): 2920-7.

Mechanical Properties of Surface Porous PEEK

Nathan T. Evans[1], F. Brennan Torstrick[1], Christopher S.D. Lee[2], Kenneth M. Dupont[3], David L. Safranski[3], W. Allen Chang[2], Annie E. Macedo[1], Angela Lin[1], Jennifer M. Boothby[1], Robert E. Guldberg[1], Ken Gall[1]
[1]*Georgia Institute of Technology, Atlanta, GA,* [2]*Vertera, Inc., Atlanta, GA,* [3]*MedShape, Inc., Atlanta, GA*
nevans3@gatech.edu

Introduction: Polyether-ether-ketone (PEEK) is a polymer widely used in load-bearing orthopaedic and spinal applications due to its outstanding mechanical properties, chemical resistance, radiolucency, and favorable biocompatibility [1-3]. However, due in part to its hydrophobic and low energy surface, PEEK has recently been associated with poor osseointegration that could lead to clinical failure and increase the risk of revision. One method commonly used to increase the osseointegration of implants is the introduction of porosity. Porosity has been shown to stimulate a more favorable osteoconductive response and create a mechanical interlock at the bone-implant interface that leads to greater implant stability [4, 5]. However, porosity can decrease mechanical properties by reducing the effective load bearing cross-sectional area and introducing stress concentration sites for strain localization and damage, decreasing both strength and ductility. Therefore, a tradeoff generally exists between the osseointegrative capacity of implants via porosity and the corresponding mechanical integrity to bear physiologic loads [6, 7]. Limiting porosity to PEEK's surface, however, could promote osseointegration and maintain bulk mechanical properties. In this study we characterize a novel surface porous PEEK structure created using a melt extrusion and salt-leaching process and examine the effect of the various structures on the mechanical properties.

Methods and Materials: Surface porous PEEK (PEEK-SP) samples were created by extruding medical grade PEEK (Zeniva® 500, Solvay Advanced Polymers) through the spacing of sodium chloride crystals (Sigma Aldrich) under heat and pressure. After cooling, embedded sodium chloride crystals were leached in water leaving behind a porous surface layer. To control for pore size, sodium chloride was sieved into ranges of 200-312 µm, 312-425 µm, and 425-508 µm using #70, #50, #40, and #35 U.S. mesh sieves. Samples processed using each size range are referred to as PEEK-SP-250, PEEK-SP-350, and PEEK-SP-450, respectively. Injection molded PEEK samples (PEEK) were used as smooth controls. Pore layer characterization was performed using µCT (µCT 50; Scanco Medical) at 10 µm voxel resolution with the scanner set at a voltage of 55 kVp and a current of 200 µA (n=15) as well as SEM imaging (SEM, Hitachi S-3700N VP-SEM). Tensile tests were performed according to ASTM D638 at room temperature using a MTS Satec 20 kip (89 kN) servo-controlled, hydraulically-actuated test frame. Fatigue tests were run on the same Satec test frame in axial stress control at a frequency of 1 Hz. Fatigue tests were run at increasingly lower stresses below the ultimate stress of the samples to generate S-N curves and determine the endurance limits of the respective samples. For monotonic and fatigue results, two representations of stress for PEEK-SP were calculated: the first using load-bearing area, A_{LB}, and the second using total area, A_T. Interfacial shear testing was adapted from ASTM F1044-05 using 3M™ Scotch-weld™ 2214 Non-Metallic Filled as adhesive and a 30 kN load cell (Instron).

Results: Pore morphology reliably correlated to sodium chloride crystal size and cubic nature as shown in **Fig. 1** and **Table 1**. The pore layers were over 65% porous and highly interconnected (>99%).

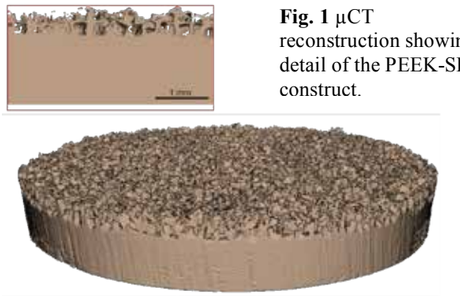

Fig. 1 µCT reconstruction showing detail of the PEEK-SP construct.

Table 1. Measured pore size and strut spacing of PEEK-SP as measured by µCT and SEM. Values represent the average and one standard deviation.

Porogen Size	Pore Size (µm)	Strut Spacing (µm)
200-312 µm	280.0 ± 32.00	186.8 ± 55.5
312-425 µm	358.3 ± 52.39	250.2 ± 77.0
425-508 µm	478.3 ± 63.50	335.7 ± 98.4

Stress-strain behavior demonstrates that though the load-bearing capacity decreases when using A_T, this is mostly a geometrical effect as the strength of PEEK-SP approaches that of injection molded PEEK when calculated using A_{LB} (**Table 2**, **Fig. 2**). Furthermore, no significant difference was found in the modulus between the PEEK-SP samples and injection molded PEEK. However, failure strains were significantly decreased to below 50% of injection molded PEEK. The introduction of a surface porosity also decreases the fatigue strength of PEEK, with the difference becoming more pronounced at higher cycles. Furthermore, the fatigue resistance of PEEK-SP-450 appears to be lower than the 250 samples (Fig. 3). The average shear strength of smooth PEEK, PEEK-SP-250, PEEK-SP-350, and PEEK-SP-450 was 7.52±3.64, 23.96±2.26, 21.41±4.32, and 22.41±3.64 MPa, respectively. Different shear failure modes were apparent for smooth PEEK and PEEK-SP. Smooth PEEK failed at the glue layer interface and the PEEK-SP samples failed within the porous network and within the solid region on the edges of some samples.

Table 2. Measured strength, failure strain, and modulus for injection molded PEEK-SP-250, -350, and -450. Values represent the average ± one standard deviation. (*designates statistical difference between the respective sample and injection molded samples. $p<\alpha=0.05$)

Sample	Load-Bearing Stress (MPa)	Total Area Stress (MPa)	Strain (%)	Modulus, A_{LB} (GPa)	Modulus, A_T (GPa)
Injection Molded PEEK	97.7 ± 0.99	N/A	20.2 ± 2.43	3.34 ± 0.14	N/A
PEEK-SP-250	96.1 ± 2.61	71.1 ± 2.17*	7.79 ± 2.25*	3.36 ± 0.30	2.45 ± 0.31*
PEEK-SP-350	93.4 ± 1.49*	70.3 ± 3.44*	6.97 ± 0.86*	3.28 ± 0.21	2.49 ± 0.21*
PEEK-SP-450	94.5 ± 1.38*	66.9 ± 1.54*	8.14 ± 1.48*	3.12 ± 0.46	2.32 ± 0.22*

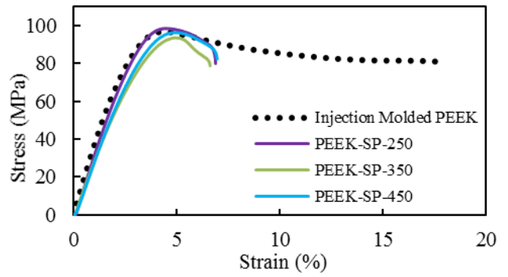

Fig. 2. Representative stress-strain curves of injection molded PEEK and surface porous PEEK with various pore sizes.

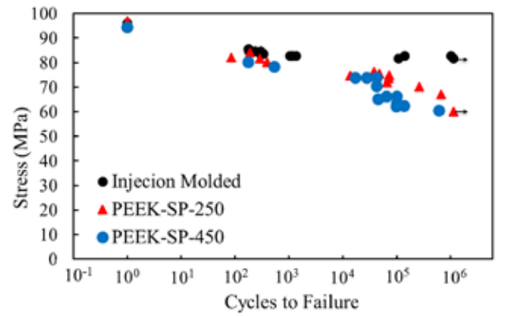

Fig. 3. S-N curve comparing the fatigue behavior of injection molded PEEK, PEEK-SP-250, and PEEK-SP-450. Arrows denote tests that were halted after reaching 10^6 cycles, which is defined as the runout stress.

Discussion: Using a melt extrusion and salt-leaching process, surface porous samples with a pore size (200-508µm) known to facilitate a more favorable osteogenic response and bone-ingrowth were created [8, 9]. Mechanical characterization showed that the main effect of the processing on the stress-related properties of PEEK-SP was a spreading out of the material as PEEK-SP retains its high specific strength (strength/density). However, the surface porosity had a notable effect on strain-related properties of PEEK-SP as the failure strain of each pore size was decreased by over 50%. The results also indicated that pore size had relatively little influence on the mechanical properties of PEEK-SP. Due to the cyclic loading experienced by orthopaedic implants and the often detrimental decrease in the fatigue resistance of polymers with surface flaws [10, 11], it was critical to evaluate the fatigue resistance of PEEK-SP. As shown, PEEK-SP demonstrated a high fatigue resistance though the surface porosity lowered the fatigue strength compared to injection molded PEEK. Finally, the inherent interfacial shear strength of the porous surface layer was tested as large shear stresses are experienced near bone-implant interfaces *in vivo* that can lead to micro-motion and implant loosening [12]. The significant increase in interfacial shear strength of PEEK-SP compared with smooth PEEK suggests that PEEK-SP will possess the advantage of a mechanical interlock and higher bonding strength between the implant biomaterial and the surrounding natural bone once ingrowth occurs, providing greater mechanical stability at this critical interface [13].

References:

[1] S. M. Kurtz, J. N. Devine, *Biomaterials* **2007**, 28, 4845.
[2] D. F. Williams, A. McNamara, R. M. Turner, *J Mater Sci Lett* **1987**, 6, 188.
[3] J. M. Toth, M. Wang, B. T. Estes, J. L. Scifert, H. B. Seim, 3rd, A. S. Turner, *Biomaterials* **2006**, 27, 324.
[4] J. D. Bobyn, G. J. Stackpool, S. A. Hacking, M. Tanzer, J. J. Krygier, *The Journal of bone and joint surgery. British volume* **1999**, 81, 907.
[5] V. Karageorgiou, D. Kaplan, *Biomaterials* **2005**, 26, 5474.
[6] J. Van der Stok, O. P. Van der Jagt, S. Amin Yavari, M. F. P. De Haas, J. H. Waarsing, H. Jahr, E. M. M. Van Lieshout, P. Patka, J. A. N. Verhaar, A. A. Zadpoor, H. Weinans, *Journal of Orthopaedic Research* **2013**, 31, 792.
[7] A. G. Mitsak, J. M. Kemppainen, M. T. Harris, S. J. Hollister, *Tissue engineering. Part A* **2011**, 17, 1831.
[8] B. D. Boyan, T. W. Hummert, D. D. Dean, Z. Schwartz, *Biomaterials* **1996**, 17, 137.
[9] K. H. Tan, C. K. Chua, K. F. Leong, M. W. Naing, C. M. Cheah, *Proceedings of the Institution of Mechanical Engineers, Part H: Journal of Engineering in Medicine* **2005**, 219, 183.
[10] J. A. Sauer, G. C. Richardson, *Int J Fract* **1980**, 16, 499.
[11] L. E. Nielsen, *Bulletin of the American Physical Society* **1975**, 20, 481.
[12] E. J. Cheal, M. Spector, W. C. Hayes, *Journal of orthopaedic research : official publication of the Orthopaedic Research Society* **1992**, 10, 405.
[13] J. D. Bobyn, R. M. Pilliar, H. U. Cameron, G. C. Weatherly, G. M. Kent, *Clinical orthopaedics and related research* **1980**, 291.

Acknowledgements: This work was supported by Solvay Advanced Polymers. N.T.E is supported by the National

Science Foundation Graduate Research Fellowship under Grant No. 2013162284. F.B.T. is supported by the TI:GER program at Georgia Institute of Technology. The technology disclosed in this manuscript has been licensed from Georgia Tech Research Corporation

Antithrombogenic Modification on PEEK with Bioinspired Phospholipid Polymer Grafting

Ishihara, K[1], Inoue, Y[1], Shiojima, T[1], Tateishi, T[1], Kyomoto, M[1,2], Tanaka, H[3], Munisso, M[4], Kakinoki, S[4], Kambe, Y[4], Yamaoka, T[4]
[1]Department of Materials Engineering, The University of Tokyo, Tokyo, Japan
[2]KYOCERA Medical Co., Osaka, Japan, [3]National Cerebral and Cardiovascular Center Hospital, Osaka, Japan, [4]National Cerebral and Cardiovascular Center Research Institute, Osaka, Japan
ishihara@mpc.t.u-tokyo.ac.jp

Introduction: We considered using PEEK in the cardiovascular devices, such as an artificial heart valve. The artificial heart valve requires high mechanical properties, antithrombogenicity and anti-infection. However, PEEK cannot satisfy those requirements. How to modify materials is changing bulk property and surface modification. In this study, we modified PEEK surface by "self-initiated photoinduced graft polymerization" for obtaining a super-functional PEEK [1]. The self-initiated photoinduced graft polymerization uses semi-benzopinacol radicals from benzophenone units in PEEK molecule structure under UV-irradiation. Advantages of this method are easy handling, well suited for application, and graft polymer chains strongly binding the substrate. 2-Methacryloyloxyethyl phosphorylcholine (MPC) polymers exhibit excellent biocompatibility, which is, antithrombogenicity, anti-infection due to reduced protein adsorption [2]. To evaluate fundamental blood compatibility on the poly(MPC)(PMPC)-graft-PEEK *in vitro*, the amount of protein, platelets and bacteria adhered on the surface was evaluated. Finally, we fabricated model artificial heart valve with PMPC-graft-PEEK to make *in vivo* antithrombogenic properties.

Methods and Materials: The surface of PEEK was ultrasonically cleaned in ethanol. The MPC was dissolved in degassed water and then adjusted to monomer concentration (0.25–1.0 mol/L) and temperature (25–60°C). PEEK was immersed in these solutions. Polymerization was carried out for 90 min on PEEK surface under UV irradiation (360 ± 50 nm, 2.5–9.0 mW/cm^2). After polymerization, the PMPC-graft-PEEK surface was washed with clean solvent to remove monomers and free polymers. PMPC-graft- PEEK was analyzed by XPS, FT-IR/ATR, water contact angle measurement, protein adsorption by micro BCA method and gold-colloid immune assay. Platelet and bacteria adhesion on the surface were evaluated with SEM after contact with suspension of these cells. Also, a PMPC-graft-PEEK artificial valve was prepared and aortic valve replacement was performed in a Gottingen miniature pig. Heparin anticoagulation was reversed after discontinuation of extracorporeal circulation circuitry by administrating protamine sulfate. After 24-h implantation, the surface of the artificial valve was observed with SEM. The longer implantation of the artificial valve for a few weeks was followed by echocardiography.

Results and Discussion: Photoinduced graft polymerization of MPC on the PEEK proceeded well. In the XPS and FT-IR/ATR spectra and water contact angle measurement showed that the hydrophilic PMPC layer formed on the PEEK substrate. Generally, in the radical polymerization, the molecular weight of polymer increases with increasing the monomer concentration. It seemed that the PMPC layer thickness increased with increasing MPC concentration. The density of the PMPC chains grafted on the PEEK surface increased with increasing UV intensity. For evaluating *in vitro* blood compatibility, the amount of adsorbed protein decreased on the PMPC-graft-PEEK significantly compared with that on PEEK even when human plasma was contact on the surface [3]. And this tendency indicated much more with increasing MPC concentration in feed solution during graft polymerization. This is corresponding to the increase hydrophilic nature of the surface. The MPC polymers can inhibit blood cell adhesion and activation. Thus, we can consider that the PMPC-graft-PEEK will show both excellent antithrombogenicity and mechanical property. We have implanted the artificial valve prepared with the PMPC-graft-PEEK for a few weeks. Some of the implants functioned well even it was *in vivo*. The surface observation on the PMPC-graft-PEEK after 24h-implantation revealed no blood cells adhered on the blood contacting part of the artificial heart (Fig.1).

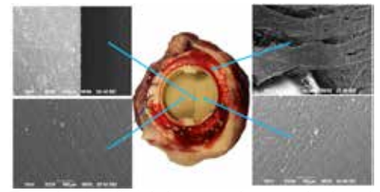

Fig. 1. Artificial heart valve made by the PMPC-graft-PEEK and SEM images at the surface after 24h-implantation.

Conclusions: The PMPC-graft-PEEK is candidate biomaterial for developing cardiovascular devices.

References:

1. Kyomoto M., Ishihara K., *Appl Mater Interfaces.* 2009:1;537-542.
2. Iwasaki Y., Ishihara K., *Sci Technol Adv Mater 2012*:13;064101(14p).
3. Tateishi T. *et al. J Biomed Mater Res* 2014: 102A;3012-3023.

Acknowledgments: This study was supported from Strategic Promotion of Innovative Research and Development (JST).

Enhanced PEEK *In Vivo* Osseointegration by Accelerated Neutral Atom Beam Processing

Joseph Khoury, Ph.D.[1]; Art Kurz[1]; James Bachand[1]; Richard C. Svrluga[1]; Michel Assad, Ph.D.[2]
[1]Exogenesis Corporation, Billerica, MA 01821; [2]AccelLAB Inc, Boisbriand, QC J7H 1N8
jkhoury@exogenesis.us

Introduction: Polyetheretherketone (PEEK) continues to gain popularity for many orthopedic applications but has significant limitations. PEEK is biocompatible, similar in elasticity to bone, and radiolucent; however, PEEK is inert and does not integrate well with bone [1]. Current efforts focus on increasing the bioactivity of PEEK with surface modifications, including coatings, to improve the bone-implant interface. We have developed a novel accelerated neutral atom beam technology (ANAB) that can modify the surface of an implantable medical device to a depth of no more than 2-3nm [2]. ANAB employs a directed beam of neutral gas atoms, which have average energies controlled over a range from a few electron volts (eV) to over 100eV per atom. ANAB leaves no residues in or on the material surface, therefore no coatings to delaminate. Initial *in vitro* studies showed significant increases in cell attachment, proliferation, and osteogenic differentiation of mesenchymal stem cells into osteoblasts growing on ANAB-treated PEEK as compared to controls [3]. In this study, we evaluated the *in vivo* osseointegration and bioactivity of ANAB-treated PEEK using an ovine femoral and tibial insertion model.

Methods: Medical grade PEEK rods (Solvay Plastics) were machined into 4 mm diameter cylindrical implantable rods measuring either 15 or 24mm in length (cancellous and cortical bone implantations, respectively). The PEEK implants were further modified with a series of macroscopic pores (1 mm^3 gaps or pits) as available void spaces created in order to fully demonstrate the extent of osteoid progression; implants used for biomechanics were not modified. Half of the devices were then treated by ANAB ($1x10^{17}$ argon atoms per cm^2), the remaining implants were kept as untreated controls. All surgical procedures and animal husbandry adhered to protocols approved by AccelLAB's IACUC, an AAALAC fully accredited institution. In order to evaluate new bone formation and implant-to-bone apposition, six adult female dorset sheep (≥ 12 months) underwent bilateral surgery on femurs and tibiae. Implants were placed in the cortical region of the mid-femur (n=2 per group/implantation time), the cancellous region of the distal femur (n=2), and the cancellous region of the proximal tibia (n=2). All implants were press-fitted with a 2 mm protrusion for alignment. Following surgical procedures, the animals were allowed to recover with full weight bearing and were then assigned to either a four-week or twelve-week implantation period with daily health checks. Following necropsy, PEEK explants and surrounding bone from the left hindlimbs were imaged by µCT (Skyscan 1172) and reconstructed into 3D images. The samples were then processed for non-decalcified bone histology using Exakt microgrinding and Goldner's Trichrome stain. The contralateral PEEK explants and surrounding bone from the right hindlimbs were assayed by a static push-out test using an Instron ElectroPuls E3000 in order to establish the stiffness (N/mm2), peak load (N), and interface strength (kPa).

Results: Following a 4-week implantation period, µCT reconstruction of the ANAB-treated implants showed excellent bone remodeling in absence of adjacent bone density differences. Following histology, the ANAB-treated implants (Figures 1B and F) also demonstrated a direct bone apposition and initiation of bone growth into the PEEK gaps/pits. In contrast, under µCT, the untreated PEEK controls revealed a thickened appearance of bone callous surrounding the implant that may be indicative of soft tissue and fibrosis; histological analysis later confirmed bone resorption and fibrous tissue presence around the control implants (Figure 1A and E). At the 12 week time-point, both histology and µCT imaging showed a clear osseointegration on ANAB-treated PEEK implants with an osteoid front colonizing the created voids, as opposed to the untreated-implants, which lacked any bony ingrowth (Figures 1 and 2). Moreover, histomorphometry results of ANAB-treated devices in cancellous bone at 12 weeks revealed a 3.09-fold increase of the percentage of bone apposition as compared with controls ($p<0.014$).

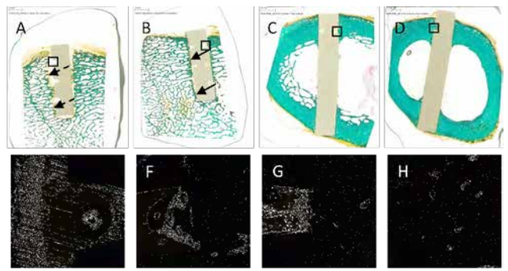

Figure 1. Goldner's Trichrome stain on distal femur cancellous and mid-shaft femoral cortical bone with PEEK implants. Four-week whole mount images show bone (green) resorption and fibrous tissue (yellow) invasion (dashed arrows) of cancellous control implants (A) and direct bone apposition (solid arrows) on ANAB-treated implants (B). Higher magnification images (boxed area in A and B) at the pits reveals fibrous tissue adjacent to the control implant (F) and bone ingrowth into pores of treated implants (F) also revealing new bone formation stained in orange. At 12 weeks, cortical bone shows little void fill on controls (C and G) while nearly complete void fill is seen on ANAB-treated implants (D and H).

For implants inserted in cancellous bone, biomechanic push-out testing carried out at 4 weeks revealed an enhanced bonding between ANAB-treated implants and adjacent bone resulting in a 2.14-fold stiffness versus untreated PEEK ($p<0.003$, Figure 3A). In addition, an increased implant-to-bone interface strength by 94.9% was observed ($p<0.04$, Figure 3B) when compared to controls. Similarly, following 12 weeks of implantation, ANAB-treated implants in cancellous bone demonstrated an increased bonding stiffness to 2.17 fold ($p<0.04$, Figure 3C) and improved implant-to-bone interface strength by 107.6% compared with controls (Figure 3D). In cortical implants, while no discernible differences were noted at 4 weeks post-implantation, the 12 week time-point revealed an increased stiffness of treated implants by 2.32 fold as compared to controls and improved implant-to-bone interface strength by 69.6% versus untreated PEEK.

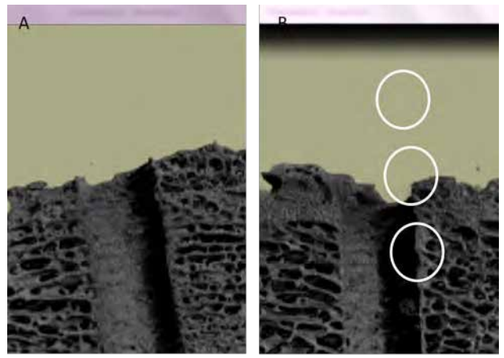

Figure 2. µCT reconstruction of radiolucent PEEK and surrounding bone, control (A) and ANAB-treated PEEK (B). Bone growing into the gaps are seen on the ANAB-treated implants indicated by the white circles (B), which is absent with controls (A).

Discussion: PEEK has become a material of choice for many orthopedic applications, however the strategies to promote osseointegration remains a challenge. Numerous research teams have attempted to modify PEEK surface properties using a variety of means including surface modifications such as plasmas, chemical modifications, surface coatings, including the addition of hydroxyapatite, as well as physical modifications such as porous PEEK. Most of these modifications have shown limited in vitro success [4]. In order to overcome the inert characteristics and to significantly improve the osseointegration of PEEK, this ovine model has shown an enhanced bone apposition and bone void ingrowth on ANAB-treated PEEK implants as compared with untreated PEEK devices. Both µCT and histology illustrated the limitations of untreated PEEK as an implant material with the presence of fibrous tissue with an impact on bone-to-implant strength, which may lead to potential implant failure. On the contrary, the ANAB-treated PEEK resulted in enhanced bone apposition from an early time point and lead to bone void ingrowth (Figure 1D, 2B). This bone apposition and integration were also reflected in significantly enhanced mechanical strength between the treated implant and the surrounding bone. Therefore, ANAB treatment of surfaces results in surface modifications which encourage osteoblast cell attachment, proliferation, and differentiation observed during the osseointegration process [3]. ANAB is not a coating and has nothing to delaminate from the surface. Because ANAB is less than 3-nm deep, the bulk properties of PEEK are not affected, leaving the overall strength, elasticity, and radiolucency unchanged. ANAB surface modification results in bioactive PEEK, which promotes osseointegration. In this study, we have demonstrated that surface modification of PEEK by ANAB results in a surface which encourages bone in vivo ongrowth and ingrowth without changing PEEK's desirable aspects.

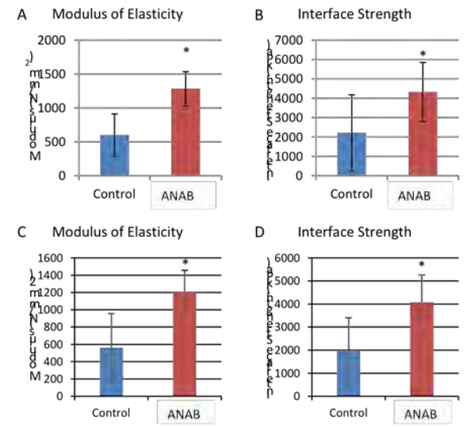

Figure 3. Biomechanical strength between implants and cancellous bone increases significantly on ANAB-treated implants as compared to controls. Significant changes (* $p<0.05$) were observed at both 4 week (A, B) and 12 week time-points (C, D): this is reflected by implant-to-bone stiffness (A, C) and bone-to-implant interface strength (B, D) on ANAB-treated implants as compared with controls.

Acknowledgments: We wish to thank Solvay for providing medical grade PEEK. Animal studies were conducted at AccelLAB, Inc., Boisbriand, QC. Biomechanical testing was performed at Pega Medical Inc., Laval, QC.

References: 1. Kurtz S.M. and Devine J.N. *Biomaterials.* 2007; 28:4845-4869.
2. Kirkpatrick A., et al. *Nucl. Instrum. Meth. B.* 2013; 307:281:289.
3. Khoury J., et al. *Nucl. Instrum. Meth B.* 2013; 307:630-634.
4. Ma R. and Tang T. *Int. J. Mol. Sci.* 2014; 15:5426-5445.

In vitro and *in vivo* evaluation of surface porous PEEK for orthopaedic applications

Torstrick FB[1], Evans NT[1], Dupont KM[2], Lee C[3], Safranski DL[2], Chang WA[3], Stevens HY[1], Lin A[1], Gall K[1], Guldberg RE[1]
[1]Georgia Institute of Technology, Atlanta, GA; [2]MedShape, Inc., Atlanta, GA; [3]Vertera, Inc., Atlanta, GA
brennan@gatech.edu

Introduction: Polyetheretherketone (PEEK) is an implant material used in spinal procedures, soft tissue reconstructions and various orthopaedic applications due to its strength, fatigue resistance and radiolucency. Although its use is widespread and its cytocompatibility is established[1], it is often associated with poor osseointegration. Introducing porosity is a common method to increase integration of orthopaedic implants by creating open space for bone ingrowth and implant fixation[2]. However, efforts to create porous PEEK (and other polymers) typically reduce its ability to bear load by creating bulk porosity throughout the implant[3, 4]. We have created a porous PEEK material that maintains high strength by limiting porosity to the surface of the implant while preserving the solid core to bear load. This study examines the *in vitro* and *in vivo* biological responses to these surface porous PEEK (PEEK-SP) constructs to predict their ability to facilitate cell growth and differentiation, and thereby enhance osseointegration.

Methods and Materials: Layer Creation: PEEK-SP was made using a polymer surface melt technique. PEEK (Zeniva® 500, Solvay Advanced Polymers) was extruded through the spacing of NaCl crystals (212-300µm) under heat and pressure. NaCl crystals were then leached in water, leaving behind a thin porous surface layer. Characterization: Porosity, layer thickness, and interconnectivity were evaluated using µCT (Scanco) (n=15). Surface porosity was determined by dividing the empty volume by the total volume of the porous layer. Average layer thickness was measured for each sample. Interconnectivity was calculated as the largest interconnected volume of empty space divided by the total volume. Pore size was measured from SEM images along the pore diagonal. Cell Differentiation: MC3T3-E1 cells (P10) were seeded onto 2 x Ø15 mm discs at 20,000 cells/cm^2. Materials included injection molded PEEK (PEEK-IM) and surface porous PEEK (PEEK-SP). Samples were cultured for 14 days in growth or osteogenic media, changing media every 3-4 days. ALP activity was determined by colorimetric intensity of cell lysates exposed to pNPP (n=8). ALP was normalized to DNA content using Picogreen

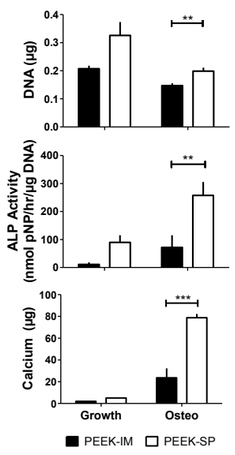

Figure 1: *In vitro* MC3T3 differentiation assays at 2 wk. ALP activity is normalized to DNA content. ** indicates P<0.01. *** indicates P<0.001. n=8.

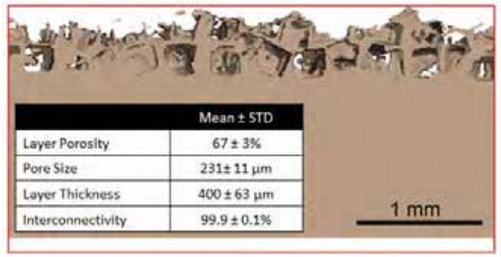

Figure 2: PEEK-SP characterization. Note cubic pore morphology due to cubic nature of NaCl crystals.

dsDNA (Invitrogen). Calcium content of parallel cultures was determined by a colorimetric Arsenazo III reagent assay (n=8). Osseointegration: The osseointegration of PEEK-SP implants was studied using an established bilateral rat femoral defect model[5] and evaluated using µCT and histology (n=6). 8 mm cylindrical PEEK implants with one porous (PEEK-SP) and one machined, smooth (PEEK-M) face were press fit into each defect and allowed to heal for 6 or 12 weeks (Figure 3). Statistics: Pore layer attributes are presented as mean ± SD. *In vitro* assay values are presented as mean ± SEM. *In vitro* data was analyzed using a two-way ANOVA with a Bonferroni post-test.

Results: Characterization of the porous surface revealed 67 ± 3% porosity, 99.9 ± 0.07% interconnectivity and thickness of 400 ± 63 µm (Figure 2).

DNA content, ALP activity and total calcium content of cells grown in osteogenic media were significantly greater for PEEK-SP compared to PEEK-IM (n=8). Similar patterns were evident in samples cultured in growth media, though not significant (Figure 1).

µCT reconstructions and plastic histological sections of undecalcified samples at 6 and 12 weeks confirmed bone growth into the porous PEEK surfaces (Figures 3 and 4).

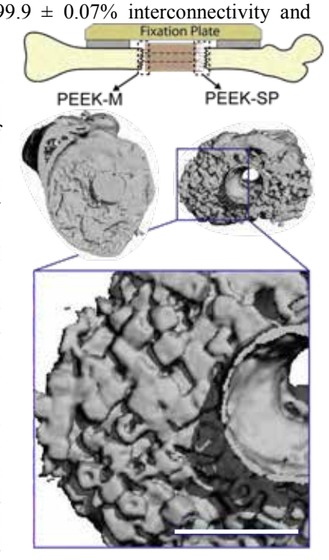

Figure 3: µCT 3D reconstructions of bone ingrowth at 12 weeks. Top cartoon depicts surgical implant configuration. PEEK-M indicates machined, smooth face. Note cubic morphology of ingrown bone that mimics cubic pores. Scale bar is 1 mm.

Cubic bone ingrowth was apparent at 4/6 porous interfaces with near mineralized tissue apposition to the pore walls (Figure 4b). As expected PEEK-M surfaces developed a substantial fibrous tissue layer between the bone and implant surface (Figure 4a). µCT data was in agreement with histological sections and provided further evidence that areas of ingrown bone had mineralized (Figure 4c).

Discussion: This work suggests that a surface porosity modification could enhance PEEK osseointegration through improved bone cell differentiation, bone ingrowth, and near mineralized tissue apposition to the implant surface. The surface porous network possessed a pore size, porosity and interconnectivity often chosen for porous orthopaedic biomaterials[2]. Cells grown on this surface possessed greater levels of ALP activity and greater amounts of calcium deposition, which are both markers of bone formation. Increased DNA from PEEK-SP samples implies the ability of the porous surface to support cell proliferation. Interestingly, both ALP activity and calcium deposition were increased (n.s.) in samples cultured in growth medium, suggesting that PEEK-SP may facilitate osteogenic differentiation in the absence of osteogenic factors in the media.

In vitro results were supported by the extent of bone ingrowth seen *in vivo*. µCT 3D reconstructions showed that ingrown bone possessed a cubic morphology similar to the cubic pore structure, indicating substantial invasion into the pore layer. Histological sections supported this finding, evidenced by the near apposition of mineralized tissue to the pore walls. Side-by-side comparison of histology and µCT data (Figure 4c) showed much of the ingrown tissue to be mineralized which could contribute enhanced interfacial strength between implant and bone – a vital requirement for stable implant fixation[6].

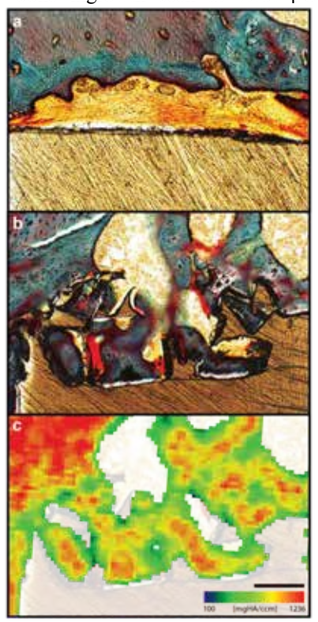

Figure 4: Histology of PEEK-M (a) and PEEK-SP (b) interface. Sections are ground MMA (20 µm) stained with Goldner's Trichrome. Mineralized bone appears greenish-blue, osteoid appears red, and PEEK is brown. (c) shows µCT mineral attenuation overlaid on (b). Blue represents less dense mineral and red represents denser mineral. Scale bar is 1 mm.

While current cell and animal data indicate that PEEK-SP may improve osseointegration, studies are being conducted with additional quantitative metrics to provide further evidence. The effects of pore size and layer thickness on osseointegration are currently being investigated *in vitro* and *in vivo*. Mechanical testing of the interface between PEEK-SP and bone will provide further functional information regarding the bone ingrowth seen in this study. Future work to enhance bone ingrowth will include augmentation of the pore layer with bioactive substances such as hydroxyapatite, lyophilized collagen or growth factor release from hydrogels.

Acknowledgments: This work was supported by Solvay Advanced Polymers. The technology disclosed in this abstract has been licensed from Georgia Tech Research Corporation. N.T.E is supported by the National Science Foundation Graduate Research Fellowship under Grant No. 2013162284. F.B.T. is supported by the TI:GER program at Georgia Institute of Technology.

References:

[1]Williams et al., *J Mater Sci Lett* 1987.
[2]Karageorgiou & Kaplan, *Biomaterials* 2005.
[3]Landy, et al., *J Appl Biomater Funct Mater* 2013.
[4]Converse, et al., *J Mech Behav Biomed Mater* 2009.
[5]Oest, et al., *J Orthop Res* 2007
[6]Gittens, et al., *Acta Biomater* 2014.

Silver Doped Titanium Oxide - PDMS Hybrid Coating Inhibits *Staphylococcus aureus* and *Staphylococcus epidermidis* Growth on PEEK

Nhiem Tran[a, b], Michael N. Kelley[a,b], Phong A. Tran[a, b], Dioscaris R. Garcia[a, b], Alan Daniels[a,b] John D. Jarrell[a, c], Roman A. Hayda[a, b] and Christopher T. Born[a, b, c]

[a] Department of Orthopaedic Surgery, Alpert Medical School, Brown University, Providence, RI, USA
[b] Weiss Center for Orthopaedic Trauma Research, Rhode Island Hospital, Providence, RI, USA
[c] BioIntraface Inc., North Kingstown, RI, USA

Introduction: Bacterial infection remains one of the most serious issues for treatments using orthopaedic implants. As many bacteria develop resistance to current antibiotics, there is a pressing need to develop antibiotic-independent coatings that use materials science-based approaches to prevent infections. In this study, a hybrid coating of titanium dioxide and polydimethylsiloxane (PDMS) was synthesized to regulate the release of antimicrobial silver to inhibit growth of *Staphyloccocus aureus* and *Staphyloccocus epidermidis*. Formulations with different titanium dioxide and PDMS ratios and different doping levels of silver were prepared using metal-organic chemistry. Three different coating concentrations of titanium dioxide were chosen to study the growth of *S. aureus* and *S. epidermidis* relative to the level of silver doping using spectrophotometry. The coatings were applied on the discs of polyether ether ketone (PEEK), a common spinal implant material and characterized using scanning electron microscope (SEM), X-ray photospectrometry and contact angle goniometry. Antibacterial property of these coatings was assessed via Kirby Bauer assay. The release of silver from the coatings was studied using graphite furnace atomic absorption spectrometry. Results showed that all silver doped coatings with different titanium dioxide – PDMS ratios effectively inhibit the attachment and growth of *S. aureus* and *S. epidermidis* in a dose-dependent manner. Importantly, the selected coatings were successfully applied on PEEK discs and completely inhibited biofilm formation. The release study demonstrated that the release rate of silver from the coating depended on doping levels and also the ratios of titanium dioxide and PDMS.

Methods and Materials: Silver doped titanium oxide/PDMS hybrid coating synthesis
Titanium oxide/PDMS hybrids doped with silver were prepared using a patented metal-organic synthesis method (BioIntraface®, North Kingstown, RI, USA). The titanium precursor and PDMS precursor were combined at three different volume ratios, and dope with Silver neodecanoate (25% in xylene, Gelest, Morrisville, PA, USA).

***S. aureus* and *S. epidermidis* culture**
Cultures of *S. aureus* and *S. epidermidis* were obtained from the American Type Culture Collection (ATCC 25923 and ATCC 35894 respectively, ATCC, Manassas, VA, USA). Bacteria were cultured overnight in TSB and diluted to working solution using a microplate reader (SPECTRAmax® PLUS 384, Molecular Devices Corp., Sunnyvale, CA, USA) at 562nm.

Adhesion and Growth on Silver Doped Hybrid Coated Surfaces
To determine silver concentration needed to inhibit *S. aureus* and *S. epidermidis* growth, silver doped hybrids coated 96-well plates were inoculated with bacterial solution at a density of 5x 10^6cfu/mL. The bacteria were allowed to adhere to the surface for 4 hours before being rinsed with PBS and replaced with new media. Bacterial solutions were then analyzed at 562nm using a spectrophotometer (SPECTRAmax® PLUS 384, Molecular Devices Corp., Sunnyvale, CA, USA).

Hybrid Coated PEEK Preparation and Characterization
Coating solutions with three titanium dioxide: PDMS ratios with two silver doping levels (38.4 µL and 384 µL) were prepared and named H50-38.4, H50-384, H75-38.4, H75-384, H95-38.4, and H95-384. The discs were dip coated, dried overnight, and heat treated on a hot plate at 95^{o}C for 1 hour. Scanning electron microscopy (SEM), X-ray photoelectron spectroscopy (XPS), and contact angle goniometry were used to examine the surface characteristics of the hybrid coated PEEK samples.

Kirby-Bauer Tests
To study antibacterial property of coated PEEK discs, *S. aureus* and *S. epidermidis* at 5 x 10^6 cfu/mL was streaked onto tryptic soy agar plates. Hybrid coated PEEK discs were placed onto the seeded agar plates and incubated for 24 hours at 37^{o}C. The halo of inhibition area around disks was photographed and analyzed using ImageJ software (NIH).

Biofilm Growth on Silver Doped Hybrid Coatings
To determine ability silver doped coatings to prevent bacterial biofilm formation, bacteria were allowed to adhere on coated PEEK disks as previously described. Samples were visualized by SEM (LEO 1530, LEO Electron Microscopy Ltd, England).

Release of Silver from Hybrid Coatings
To quantify the release of silver from the coatings, six coating conditions were applied to the bottom of glass scintillation vials. The silver concentration in the collected solutions was analyzed using a graphite furnace atomic absorption spectrometer (GFAAS).

Statistical Analysis
All statistical analysis was performed using Student's t-test to determine significance ($p<.05$) with at least 3 samples per test (N=3).

Results: Bacterial infections to implants have been one of the most serious issues for our community. The current study focused on hybrid silver-released coatings and the applicability of the coatings on a popular orthopaedic implant material, PEEK. The coating combined the bioactivity of titanium oxide, the flexibility of polymer PDMS, and the antibacterial property of silver. The results in this study suggested that accumulation and release rate of silver from the coatings depend on the ratio of titanium and PDMS of the coatings. The cumulative results provide evidence towards an effective antimicrobial coating with predictable and manageable pharmacokinetics against *S. aureus* and *S. epidermidis*. Previous studies also demonstrated that hybrid coatings enhanced cell growth and provided a more sustained release profile compared to pure metal oxide films or pure PDMS. Through optimization of metal oxide to PDMS ratios as well as level of silver doping, a bioactive orthopaedic coating which inhibits bacterial biofilm growth and at the same time promotes osseointegration can be achieved.

Discussion: In this study, novel titanium dioxide - PDMS hybrid coatings were formulated and doped with silver. The coatings showed the ability to inhibit the growth of both *S. aureus* and *S. epidermidis* in a dose-dependent manner with high potency. Moreover, the coatings were successfully applied on a commonly used orthopaedic material, PEEK. Coated PEEK doped with the higher level of silver showed large inhibition zones and completely prevented the formation of *S. aureus* biofilms indicating the successful release of ionic silver at bactericidal concentrations. The release study demonstrated that Ag was effectively eluted from the coatings. The amount and rate of release depended on the titanium to PDMS ratio and the doping level of Ag, which allows for customization of the pharmacokinetics of silver release. Since an anti-bacterial, anti-biofilm coating is highly desirable; these novel coatings will likely improve the treatments using implanted biomaterials.

Abstract 2nd PEEK meeting 2015

Title: Increased bone fusion on PEEK implants coated with nano-hydroxyapatite: A histomorphometric study in rabbit bone

Name of authors: Pär Johansson DDS, Ryo Jimbo DDS PhD, Ann Wennerberg, LDS PhD, Per Kjellin, PhD, Yusuke Kozai, DDS, PhD

Background: Polyetheretherketone (PEEK) is a material with excellent biomechanical properties due to its similarity to human bone. In orthopedic surgery PEEK has become an established alternative to metal implants for load-bearing applications. Metal implants can be insufficiently loaded due to a mechanical mismatch to bone, resulting in stress-shielding and eventually bone resorption. Due to the relative inertness of PEEK, it will not cause any foreign body reaction, nor will it osseointegrate very well in its pure form. Consequently, a variety of techniques have been employed to modify the PEEK interface ranging from bioactive bulk materials to surface modification. Most of the studies have shown improvements but the material modification resulted in reduced mechanical properties and coating failures.

Aim: The present study evaluates the osseointegration of hydroxyapatite (HA) coated PEEK implants with respect to histology and computed tomography. The study was conducted in a rabbit tibia and femur model.

Material and methods: Commercial PEEK substrates (Invibio Ltd. Lancashire, UK) with non-cutting screw shape and diameters of 3.5mm and length of 4mm were prepared for the study. The implants placed in femur were designed with a hole penetrating the apical part which permits evaluation of the osteoconductive properties. Half the implants (n = 24) were coated with HA^{nano} Surface (test, Promimic, Göteborg, Sweden) and the remaining (n = 24) were left uncoated (control). Onto the top of the test implants, 50 µl of coating solution was applied followed by rotation at 2700 RPM for 5 seconds. The implants were randomized inserted into the tibia and femur bone. The animals were euthanized after 3 and 12 weeks of subcutaneous, unloaded healing. Bone sections were retrieved, cut and stained with Masson-Trichrome and was evaluated with histomorphometry. The histomorphometric data was analyzed with Mann-Whitney test. Level of significance was 0.05.

Results: All implants were histologically osseointegrated with no clinical signs of infection. The tibia implants revealed a higher bone-to-implant contact for test after 3 weeks (p=0,016) and 12 weeks (p=0,042). The bone-area within the threads was significant higher for test after both healing times. In the femur the perforated hole in the femur implants showed significant higher area for test (3w: p= 0,000, 12w: p= 0,001)

Conclusions: Hydroxyapatite coated PEEK implants were found to outperform the uncoated PEEK in in the histomorphometric analysis. The finding of the larger bone-area in the penetrating hole for the HA-coated implant encourage this material compilation to be a competent alternative to metal implants in spinal applications, even in poor bone quality.

Plasma Treatment of Machined PEEK and CFRPEEK Implants: Wettability and Osteoblast Proliferation

Moon, PC[1], Jauregui, CE [2], Short, SJ[1], Pestov, DV [3], Madurantakam, PA[2]

1. General Practice Department, School of Dentistry, Virginia Commonwealth University, Richmond VA, USA
2. Philips Institute of Oral Health Research, School of Dentistry, Virginia Commonwealth University, Richmond VA, USA
3. Nanomaterials Characterization Center, School of Engineering, Virginia Commonwealth University, Richmond, VA, USA

pcmoon@vcu.edu

Introduction: Osseointegration of implants requires attachment and robust proliferation of bone cells on the implant surface. The effect of surface roughness and wettability of implants on cell proliferation was evaluated in this study.

Materials and Methods: Different types of plasma were generated from a mixture of gases (oxygen/nitrogen, hydrogen /nitrogen and carbon dioxide) under pressure using a Plasma Pen device (PVA TePla-America). Poly ether ether ketone (PEEK-OPTIMA) as well as carbon-fiber reinforced PEEK-OPTIMA (CFR-PEEK) was supplied by Invibio Ltd. The as-provided PEEK rods were machined to generate 2mm thick discs of varying roughness. Surface roughness was evaluated by digital light microscopy as well as scanning electron microscopy. The discs were mounted on a rotating mandrel and uniformly exposed to plasma. Wettability of treated PEEK discs with DI water was measured by sessile drop contact angle method using Rame – Hart digital goniometer. Changes in surface chemistry induced by plasma treatment were determined by XPS measurements. The discs were seeded with MG63 (osteoblast-like cells) following sterilization with 5000 ppm peracetic acid in 20% ethanol for 15 minutes (n=9). Cells were detached using trypsin after 3 days, counted and compared to initial seeding number to measure cell proliferation.

Results: XPS measurements revealed oxygen-nitrogen was the most oxidizing plasma tested. The contact angles of the PEEK changed from hydrophobic (~100 ^{o}) to very hydrophilic (~ 7^{o} to 15^{o}). The other plasmas lowered the contact angles to around 30^{o}. Rough machined surfaces produced grooves which were larger than the cells while a fine machined surface produced grooves a little smaller than the cells themselves (~30µm). We observed that carbon fibers aligned along the grooves produced during machining and the cells tended to align with the grooves. Cell proliferation was significant on both rough machined surfaces with no difference, regardless of plasma treatment. The lowest contact angles did not enhance cell proliferation. Experiments involving fine machined surfaces as well as carbon dioxide and hydrogen/nitrogen plasmas are ongoing and will be reported.

Discussion: From the results presented, we find that surface roughness is a more important factor in determining cell proliferation. Wettability at very low values may not be beneficial in promoting cell attachment as well.

Supported by: Academy of Osseointegration; VCU School of Dentistry; VCU VP for innovation Fund and Invibio Ltd.

The Effect of Processing Conditions on the Flexural Strength of Polyetheretherketone (PEEK) Used as Innovative Denture Base Material

S.A. MUHSIN[1], D.J. WOOD[1], P.V. HATTON[1], A. JOHNSON[1], and N. SERENO[2]
[1](School of Clinical Dentistry, Faculty of Medicine, Dentistry and Health, University of Sheffield)
[2](Juvora Ltd, Thornton Cleveleys, England)
smuhsin1@sheffield.ac.uk

Introduction: Despite the fact that material scientists and researchers have continued to improve the mechanical properties of denture base materials, none yet meet the ideal requirements. Currently used denture base materials have shortcomings related to biocompatibility and strength, and their components may fail for a variety of reasons. Flexural assessment is one of the most crucial basic factors in selecting material for dental uses. Polyetheretherketone (PEEK) is a new biomedical polymer which has been increasingly suggested to be used in dentistry. Nevertheless, no detailed studies have been published to assess PEEK as a denture base material in terms of flexural failure. Therefore, this studies aim is to evaluate the flexural behaviour of PEEK as a denture base material prepared by both thermo-pressing and machined techniques compared to the conventional base materials using a static 4-point bend test.

Methods and Materials: According to ISO standardization 1567: 2005, specimens (n=10) 65x10x2.5 mm were prepared from PEEK-Juvora™ discs using CAD/CAM technology; PEEK-Optima®NI1 (Invibio Ltd.) granules injected using denture injection method at 100, 150, 175, and 200˚C mould temperature to produce specimens; Polymethylmethacrylate (PMMA) specimens were prepared from both Heat-cured (Candulor, Switzerland) injected pellets (Brecrystal HP, Bredent, Germany); and cobalt chromium casting alloy (Co-Cr) (Wironit, Germany). The mould temperature for the injected technique was monitored using multi-sensitive thermocouples inserted inside the simulating RPD mould cavity during preheating. 400 Thermopress injection machine (Bredent, Germany) was used for injecting the material. According to the manufacturer recommendation, PEEK-OPTIMA®NI1 melt temperature was 380˚C while PMMA was 280˚C. The specimens were wet-polished using 600-grit waterproof abrasive paper, then stored in water at 37(±1)˚C for 50(±2) hours. Testing should ideally be conducted under humid conditions in order to simulate the oral environment, however, due to the limitation of the equipments, the tests were carried under normal room conditions immediately after water storage. The mechanical testing for the sample was established using a Lloyds tensile tester of 2.5 KN loading capacity (2000, England). However, 100 N was the maximum load applied to the specimens. The distance between the two supporting centers was 50(±0.1) mm, and a load crosshead speed of 5(±1) mm/min.

Results: All the tested materials resisted fracture under permanent deformation of 100 N. However, the results of the bend strength test are summarized in Table (1). PEEK-Juvora™ and PEEK-Optima®NI1 revealed significant flexural behaviour compared to PMMA ($P<0.001$), yet the resilience of injected PEEK was non-significant ($P>0.05$). The Co-Cr maximum deflection and resilience were extremely limited although the highest elastic modulus and flexural rigidity values measured up to thermoplastic materials.

Table (1)
Comparison of Four-Point Bending Test Results (N=10)

	EM (GPa)	FR (N/m²)	MD (mm)	R (J)
PEEK-Juvora™	5.57	7.5×10^{-2}	3.22	5.6×10^{-2}
PEEK-Optima® NI1				
100 ˚C	4.80	6.3×10^{-2}	3.97	3.8×10^{-2}
150 ˚C	4.85	6.4×10^{-2}	3.94	4.1×10^{-2}
175 ˚C	4.69	6.2×10^{-2}	3.95	3.4×10^{-2}
200 ˚C	4.91	6.6×10^{-2}	3.67	4.2×10^{-2}
PMMA				
Heat-cure	3.58	4.7×10^{-2}	5.49	3.1×10^{-2}
Injection	3.79	5×10^{-2}	5.51	3.2×10^{-2}
Co-Cr	206.33	276×10^{-2}	0.26	0.08×10^{-2}

EM: Elastic Modulus; FR: Flexural Rigidity; MD: Maximum Deflection; and R: Resilience.

Discussion: The flexural strength of denture base material is important for two reasons; firstly to prevent material deformation which is considered the primary mode of clinical failure, secondly to ensure a degree of elasticity and resilience to release the load applied to the mucosa under the denture due to occlusal force. Innovative base materials should not only equal the approved dominate market materials but also offer improved properties and advantages to be competitive. PEEK under static 4-point bend test revealed promising flexural properties, and PEEK-Juvora™ provides superior flexural behaviour with highest ability to spring back to its original shape after load removal. This is essential to utilize a strong and resilient fabricated prostheses to withstand impact loading. In conclusion, PEEK might be the new resource required for future denture material.

The Application of PEEK in Dental Implant Suprastructures: A Finite Element Analysis

Schwitalla, AD[1], Abou-Emara, M[2], Lackmann, J[2], Spintig, T[1],Müller, W-D[1]
[1]Charité University Medicine Berlin, Germany, [2]Beuth University for Applied Sciences, Berlin, Germany
andreas.schwitalla@charite.de

Introduction: Nowadays PEEK is frequently used as an alternative biomaterial to metallic implant components mainly in the fields of orthopedics (1,2) and traumatology (3,4). Additional to its distinguished biocompatibility, it combines many favorable material properties, e.g. its elastic modulus which is similar to that of bone.
Also its low density makes it an interesting biomaterial for dental applications.
In the field of implant dentistry the high elastic moduli of conventional titanium implants (~110 GPa) in combination with stiff materials for the according prosthesis (e.g. ceramics; 70-220 GPa) may cause high stresses in the bone-implant-interface during load transfer (5,6) due the lower elastic moduli of cortical (13.4 GPa) and cancellous bone (1.37 GPa). These stress peaks may cause peri-implant bone loss (7,8).
This problem leads to the assumption, that the use of PEEK for prosthetic components on dental implants generates bone protective effects as stress peaks at the bone-implant-interface could be reduced due to the higher elasticity of PEEK.
To evaluate the stress distribution at the bone-implant-interface in vitro, the finite element analysis (FEA) is a frequently used method (9,10).
The aim of the present FEA was to evaluate the bone's stresses and deformations during loading of a platform-switched dental implant modeled of titanium, which was completed with prosthetic components of PEEK.

Methods and Materials: A 3D section of a human mandible derived from a computer tomography scan was saved as *.stl data. The solid geometry of this section including both the cancellous and the cortical bone was rebuilt from the *stl data with Creo Parametric 2.0 (Creo Parametric 2.0, PTC, Needham, MA 02494, USA).
For reasons of simplification, a cylindrical platform-switched implant of 10 mm length and 4.5 mm width was designed. It was completed with an abutment with a conical implant-abutment-connection with an overall cone angle of 12°. The abutment was fixated on the implant with a central fixation screw. A porcelain crown of a lower left first molar was then cemented onto the abutment (Fig.1.1). Afterwards a commercial software (Ansys Workbench Version 14.0, ANSYS, Inc., Canonsburg, PA 15317, USA) was used to create a three-dimensional mesh of nodes and elements, including 498543 nodes and 137425 mainly hexahedral elements (Fig.1.2). The types of contacts between all parts were defined, whereas the contact between the implant and the bone allows micro-movements representing a more realistic approach (Table 1).
Regarding the material composition of the assembly three distinct types were evaluated via the finite element method (Table 2). The materials used were pure titanium, porcelain and a commercial medical grade PEEK (MC4420®, Evonik Industries, 45128 Essen, Germany) (Table 3). All materials were assumed to be isotropic and linear elastic.

Connected pairs			Type of the contact
Crown	+	Abutment	perfectly bonded
Screw	+	Abutment	perfectly bonded
Abutment	+	Implant	frictional (rough)
Implant	+	Bone	frictional (rough)
Screw	+	Implant	perfectly bonded
Cortical Bone	+	Cancellous Bone	perfectly bonded

Table 1: Summary of the contacts between all components.

Type	Implant	Screw	Abutment	Crown
1	titanium	titanium	titanium	porcelain
2	titanium	titanium	titanium	PEEK
3	titanium	titanium	PEEK	PEEK

Table 2: Overview of three different types of the assembly regarding the material composition.

Material	Elastic Modulus [MPa]	Poisson Ratio	Yield Strength [MPa]	Ref.
Titanium (Ti-6A1-4V)	110000	0,33	825	11
PEEK (MC4420®)	4100	0,4	95	Evonik Industries, 45128 Essen, Germany
Cortical Bone	13400	0,3	121[(12)]	10
Cancellous Bone	1370	0,31	-	9
Porcelain	68900	0,28	-	13

Table 3: Summary of the material properties used for the finite element analysis.

Nine occlusal contact points of 1 mm diameter were projected onto the occlusion surface of the crown (14; Fig.1.3). These points served as load areas for the applied force of 100 N, which was used vertically in the direction of the long axis of the implant (Load Case 1) and at an angle of 30° to the long axis of the implant coming from the buccal direction (Load Case 2) (Fig.1.4).
The peri-implant bone was analyzed regarding the Von-Mises stresses and surface contact pressures caused by the loading forces, whereas the yield strength of the bone was assumed at 121 MPa (12).

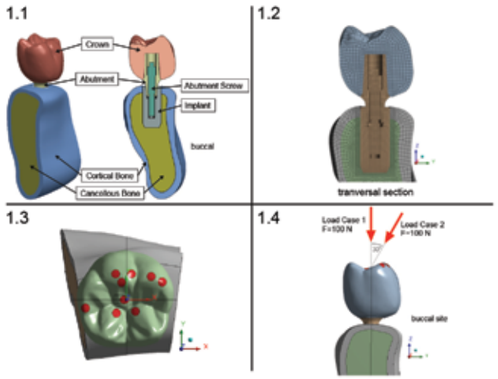

Fig.1: 1.1) Complete test set-up showing the implant-abutment crown-assembly within the mandibular bone;
1.2) 3D mesh with nodes and elements;
1.3) Occlusal aspect of the crown with nine occlusion points;
1.4) Demonstration of the load cases 1 and 2.

Results: The stress distribution of the FEA is exemplarily shown in Fig.2.

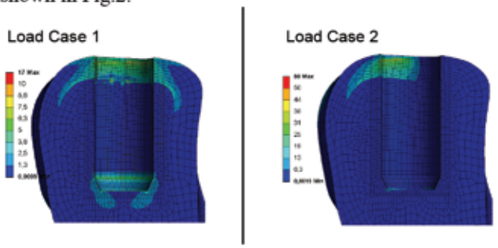

Fig.2: Distribution of the Von-Mises stresses within the peri-implant bone for the assembly of Type 1.

The maximum values of the evaluated values of the Von-Mises stresses and the surface contact pressures occurring within the peri-implant bone caused by loading are summarized in Table 4.

Type	Von-Mises stress [MPa]		Surface contact pressure [MPa]	
	Load case 1	Load case 2	Load case 1	Load case 2
1	17	59	5.7	39
2	17	59	4.6	36
3	17	66	4.8	20

Table 4: Summary of the maximum values resulting from the FEA within the peri-implant bone.

Discussion: Replacing prosthetic components of materials with a high elastic modulus like titanium by PEEK causes a reduction of the surface contact pressure within the implant-bone-interface, especially when an oblique load is applied. However, for load case 2 Type 3 showed the highest Von-Mises stresses and the lowest surface contact pressure at once. Probably using another 3D mesh with a different refinement algorithm could lead to more accurate values without high stress peaks.
For the current study a cylindrical implant shape was chosen for reasons of simplification. Yet, modeling implant threads can have a remarkable effect on the stress distribution (15). As commercial dental implants nowadays are generally screw shaped, this model might reflect a more realistic situation.

References:

1. Liao K. Performance characterization and modeling of a composite hip prosthesis. Exp Tech. 1994;18:33–38.
2. Maharaj GR, Jamison RD. Intraoperative impact: characterization and laboratory simulation on composite hip prostheses. In:Jamison RD, Gilbertson LN, ed. STP 1178: Composite Materials for Implant Applications in the Human Body: Characterization and Testing. Philadelphia, Pa: ASTM; 1993:98–108.
3. Corvelli AA, Biermann PJ, Roberts JC. Design, analysis and fabrication of a composite segmental bone replacement implant. J Adv Mater. 1997;28:2–8.
4. Kelsey DJ, Springer GS, Goodman SB. Composite implant for bone replacement. J Compos Mater. 1997;31:1593–1632.
5. Bougherara H, Bureau MN, Yahia L. Bone remodeling in a new biomimetic polymer composite hip stem. J Biomed Mater Res A. 2010;92:164-74.
6. Sarot JR, Contar CM, Cruz AC, de Souza Magini R. Evaluation of the stress distribution in CFR-PEEK dental implants by the three-dimensional finite element method. J Mater Sci Mater Med. 2010;21:2079-85.
7. Frost HM. Perspectives: bone's mechanical usage windows. Bone Miner 1992;19:257-71.
8. Huiskes R, Weinans H, van Rietbergen B. The relationship between stressshielding and bone resorption around total hip stems and the effect of flexible materials. Clin Orthop 1992; 274:124-34.
9. Borchers L, Reichart P. Three-dimensional stress distribution around a dental implant at different stages of interface development. J Dent Res 1983;62:155- 9.
10. Cook SD, Klawitter JJ, Weinstein AM. A model for the implant-bone interface characteristics of porous dental implants. J Dent Res 1982;61:1006-9.
11. Colling EW. The physical metallurgy of titanium alloys. Metals Park(OH): American Society for Metals; 1984.
12. Cowin SC, The Mechanical Properties of Cortical Bone Tissue, Bone Mechanics, S. C. Cowin, Boca Raton, CRC Press, Inc., pp. 97–128, 1989.
13. Lewinstein I, Banks-Sills L, Eliasi R. Finite element analysis of a new system (IL) for supporting an implant-retained cantilever prosthesis. Int J Oral Maxillofac Implants 1995;10:355-66.
14. Payne EV: Reproduction of the tooth form. New Techn Bull 1,36 (1961).
15. Winter W, Steinmann P, Holst S, Karl M. Effect of geometric parameters on finite element analysis of bone loading caused by nonpassively fitting implant-supported dental restorations. Quintessence Int. 2011 Jun;42(6):471-8.

Polyetheretherketon (PEEK) telescopic denture retained on implants and teeth for maxilla rehabilitation

Spintig, T[1]; Schwitalla, A[1]; Müller, W-D[1]
[1]Universitätsmedizin Charité Berlin, Departement of Dental Research, Berlin, Germany
tobias.spintig@charite.de

Introduction: Metal-free dental restorations are a rising patients' desire. Besides allergies and hypersensitivities towards metals or alloys, other materials becomes more and more in focus for dental prostheses.
Therefore Polyetheretherketon (PEEK) represents a valuable alternative to conventional dental materials. It has been approved by the FDA as implant material in the 1990s and has been implanted mainly in the fields of orthopedics and traumatology. Presently due to its outstanding properties it is also increasingly used for dental applications.

Patient, Methods and Results: In February 2013 a female patient (A.L.), 39 years old, came to the dental office complaining the slight loosening of tooth 11 (tooth mobility grade II). The general anamnesis was without pathological findings. After detailed oral investigation and evaluation of the panoramic radiography [Fig.1] the patient was explained that she required a complex oral rehabilitation. Different treatment plans were offered.

Fig.1 panoramic radiography February 2013

In a first step, the teeth 16, 15, 14, 12, 11, 21, 22, 25, 26 and 27 were extracted and a transitional prothesis was incorporated for two month. Afterwards 6 dental Implants (CAMLOG® Screw Line, Camlog Biotechnologies AG, Wimsheim, Germany) were inserted [Fig.2]. For the time of oral healing, osseointegration of the implants and as an anchorage for the transitional prothesis, tooth 13 was left until uncovering of the implants 6 month later.

Fig.2 panoramic radiography after insertation of 6 dental implants

Customizable abutments were used (CAMLOG® Titanium base CAD/CAM) to fabricate the individual zirconia implant abutments. Tooth 23 was served with a primary telescope made of zirconia [Fig.3]. Its outstanding properties allowed us to fabricate a CAD/CAM PEEK (JUVORA™, Ltd., Thornton Cleveleys, Lancashire, GB) supraconstruction without the need of any additional intermediate structures. Whereas the individual zirconia implant abutments (and tooth 23) served as primary telescopes, the PEEK supraconstruction similary act as secondary telescopes [Fig.3].

Fig.3 individual zirkonia abutments; PEEK supraconstruction

After veneering, the supraconstruction was incorporated. Teeth 37, 36, 44 and 45-47 were served with long-term provisorial crowns made of veneered PEEK [Fig.4].

Fig.4 finished PEEK-prosthesis

In function since about 9 month by now, the patient is still very satisfied and no failure of her prosthesis can be mentioned.

Inflammatory effects of different carbon-fiber reinforced PEEK particles *in vivo*

Utzschneider, S[1]; Paulus, AC[1]; Becker, F[1]; Lorber, V[1]; Buschmann, A[1]; Jansson, V[1]; Grupp, TM[1, 2];
[1]Department of Orthopaedic Surgery, University Hospital of Munich (LMU), Campus Großhadern, Marchioninistr. 15, 81377 Munich, Germany
[2]Aesculap AG Research & Development, Aesculap-Platz 1, 78532 Tuttlingen, Germany
sandra.utzschneider@med.uni-muenchen.de

Introduction: Today aseptic loosening is still one of the main reasons for revision of arthroplasty. This complex process due to wear particles still is not understood in detail. So far, Ultra-high-molecular-weight-polyethylene (UHMWPE) is the bearing material of choice in knee arthroplasty, but there is a growing demand for alternative bearing materials with improved wear properties. Lately, increasing interest developed in the use of natural and carbon-fiber-reinforced-poly-ether-ether-ketones (CFR-PEEK). Considering the use of CFR-PEEK as a potential alternative bearing material to UHMWPE in uni- and bicompartmental knee arthroplasty, the biological reaction to CFR-PEEK wear particles has to be analyzed.
The aim of this study was to analyze the biological activity of wear particles of two different (pitch and PAN) carbon-fiber-reinforced- (CFR-) PEEK varieties in comparison to ultra-high-molecular-weight-polyethylene (UHMWPE) *in vivo*. The authors hypothesized no difference between the used biomaterials analyzing synovial tissue, adjacent bone and articular cartilage. Considering the use of materials for unicompartmental knee replacement, the analysis of cartilage is particularly important, as intact remaining cartilage is mainly responsible for the long term success of the arthroplasty.
Methods and Materials: The tibial inserts were made from UHMWPE (GUR 1020) and PEEK (PEEK-Optima LT1, Invibio Ltd. Thornton-Cleveleys, UK) with either a carbon-fiber reinforcement of 30% pitch (PITCH) or 30% polyacrylonitrile (PAN) based carbon fibers. The experimental inserts were implanted in 24 knee prostheses (UnivationF®, Aesculap, Germany) on a four station knee simulator (EndoLab GmbH Thansau, Germany) for over 5 million cycles according to ISO 14243-1 (2002). After separation of the particles by acid digestion, they were imaged by scanning electron microscopy (SEM). Based on the determined particle size and shape parameters, sterile polymer particles were generated using the above described cryo-pulverization process avoiding side effects, e.g. a contamination with lipopolysaccharides. Particle size and shape distribution were similar with those from knee simulator testing. Then, 50 µl of a particle containing suspension in phosphate buffered saline (PBS) was injected in the left knee joints of female BALB/c mice under sterile conditions. For the control group, only PBS was used. After seven days an intravital fluorescence microscopy and a histological evaluation of the synovial layer were performed to investigate the synovial inflammation and microcirculation. For a validation of the results, the cytokine expression (IL-1b, IL-6, TNF-a) was measured in the synovial layer, the adjacent bone and the articular cartilage using immunohistochemistry.
Results: All tested biomaterials showed enhanced leukocyte-endothelial cell interactions, an increase of functional capillary density and a histological increased inflammatory reaction compared to the control animals, but without any significant difference between tested biomaterials. In contrast, elevated cytokine secretions were detectable. CFR-PEEK pitch caused a significantly higher level of cytokine expression in the articular cartilage compared to the other groups. In addition, in the adjacent bone of the two CFR-PEEK varieties significantly increased cytokine expressions compared to UHMWPE and control group were detected.
Discussion: CFR-PEEK pitch wear particles might provoke a degeneration of the remaining cartilage, which might limit the use of that biomaterial especially for unicondylar arthroplasty. However, further investigation is needed.
Elevated levels of IL-1β and TNF-α found in the adjacent bone indicate that wear particles had to migrate or were actively being transported into the bone, since the wear particles were injected intraarticularly. Compared to the UHMWPE group, the CFR-PEEK pitch and the CFR-PEEK PAN group showed a higher degree of inflammation in the adjacent bone. Whereas the reason for this is unclear, it is important to take note of the proinflammatory effect of PEEK wear particles.
The used *in vivo* model was introduced to measure leucocyte-endothelial-cell interactions in respect of inflammatory reactions to wear particles. Direct effects on the bone metabolism cannot be measured which is a major limitation of the study. All drawn conclusions are based on the measured inflammatory cytokine expressions as key factors in aseptic loosening.

PEEK Femoral Component in TKA: Bone Remodeling and Device Performance during Gait and Squatting

de Ruiter, L[1], Janssen, D[1], Briscoe, A[2], Verdonschot, NJJ[1,3]
[1]Orthopaedic Research Lab, Radboud University Medical Centre, Nijmegen, The Netherlands; [2]Invibio Ltd, Lancashire, UK;
[3]Institute of Biomedical Technology, University of Twente, Enschede, The Netherlands
Lennert.deRuiter@radboudumc.nl

Introduction: The mechanical performance of an all-polymer femoral implant in total knee arthroplasty (TKA) has been described by Moore et al. in 1998 after a clinical trial with a 10-year follow-up period[1]. Although they reported a proper performance from their polyacetal-on-polyethylene device, e.g. reduced wear, absence of implant fractures and similar survival to cobalt-chrome (CoCr) parts, significant improvements were not found. Since then no real considerations for an all-polymer TKA device have been reported. In this study we return to a polymer-on-polymer bearing couple by replacing the conventional CoCr femoral component by PEEK-OPTIMA® (a polyetheretherketone (PEEK) from Invibio ltd, UK). We wanted to investigate its use during both a highly frequent exercise (gait) and a high-demanding task (deep squat). It is hypothesized that a more compliant implant could reduce the periprosthetic stress shielding and, hence, decrease the loss of bone stock. However, a polymer could also increase the risk of implant fracture or failure of the underlying cement mantle. We evaluated these determinants with the finite element (FE) method.

Methods and Materials: In this study a cemented cruciate retaining implant was used according to an existing TKA design. The FE method can predict stresses and strains, but is less reliable in determining a factor of safety. However, the clinical performance of the established CoCr device is known and can, by comparison, be used to determine a factor of safety for the PEEK device. Hence, each model was run for both materials. The deep squat model was based on the Oxford Knee Rig and ranges between 40 and 155 degrees of flexion. It was used to evaluate the structural integrity of the femoral component and the cement mantle as squatting puts a high demand on the reconstructed knee. Analyses were performed for compression and tension and related to the material's respective yield stress (Table 1) for assessment of safety. The second model mimicked gait according to the ISO 14243-1 standard and was used to analyze bone remodeling, as that is determined by the most frequent type of loading. To this extent a third, 'intact' version of the gait model provided the comparison with a healthy knee. The strain energy was used as a measure for bone remodeling and analyzed in 2 mm thick segments from the distal bone cut to 30 mm proximally.

Results: The maximum tibiofemoral contact forces were found at 145 degrees of flexion. This was the moment at which both thigh-calf contact and condylar bone-implant load sharing were activated. Around this flexion angle the loads on the implant and cement were most critical and were therefore analyzed and described in more detail. In both compression and tension the CoCr femoral component showed stress intensities at the intercondylar notch, which were absent in the PEEK implant. The highest loads were found at the tibiofemoral contact site at the bearing surface (compression) and internal surface at the posterior chamfer (tension). Lower level stress patterns were found at the anterior flange at the bearing surface. Under compression the CoCr and PEEK implants were loaded similarly, with a maximum of 120 MPa and 110 MPa, respectively (Figure 1). The compressive loads in the CoCr implant were distributed over a larger area than for PEEK. Relative to the yield stress, PEEK (95 percent) scored substantially worse than CoCr (10 percent). In tension stresses amounted up to 250 MPa for CoCr and 98 MPa for PEEK (Figure 1). Normalized to yield stress CoCr reaches 43 percent, PEEK 90 percent.
The bone cement showed more similarity between both configurations. Under compression this was 60 and 70 MPa peak stress for CoCr and PEEK respectively. Tension was even more similar with 16 and 17 MPa peak stress (Figure 2). However, the stress patterns were distinctly different for both configurations. Where for CoCr stresses accumulated in the proximal transitions into the bone (pegs anterior flange and cement pocket edges), the PEEK stresses were distributed more over locations similar to the implant's contact site.
The bone strain energy patterns during gait showed markedly different patterns between constructs. At all distal-to-proximal sections the total strain energy was higher for PEEK. Both the pattern and the magnitude of the PEEK configuration were more similar to the 'intact' reference, with a slight increase in strain energy over the entire gait cycle (Figure 3).

Discussion: For the implant itself, normalized loads were higher for PEEK than for CoCr, reducing the factor of safety for that reconstruction. However, indications are present that could explain such high stresses to have been caused by non-physiological sources, such as computational (contact) artifacts. Additionally, analyses also show that only a small section of the implant is at risk. Therefore, it is not possible to say whether the entire reconstruction would fail. The similarity of cement mantle stresses in the CoCr and PEEK configurations do not necessarily mean equivalence in safety. The success of CoCr implants might be partially explained by the stress protection of the underlying cement, which should be studied for its contribution. On bone remodeling the coarse nature of the 'intact' model requires caution when interpreting the results. A more sophisticated model could provide a more detailed assessment, but it appears that in the PEEK construct bone strains are more similar to an intact knee joint than for conventional CoCr, indicating a reduced post-operative bone remodeling stimulus.

References:

1. DJ Moore, MA Freeman, PA Revell, GW Bradley, M Tuke. Can a total knee replacement prosthesis be made entirely of polymers? J Arthroplasty, Jun;13(4):388-95 (1998).

Table 1. Material properties

Material	Young's modulus (MPa)	Yield strength (MPa) *
PEEK-Optima®	3700	117/90
CoCr	210000	1200/600
PMMA	2866	97/40
Femur	200-20000	n/a

* Compressive/Tensile strength

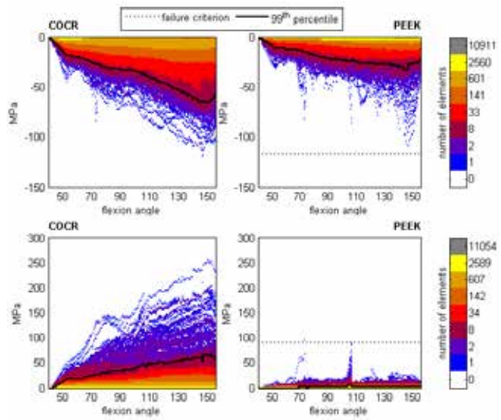

Figure 1. Femoral component. Compression (top), tension (bottom)

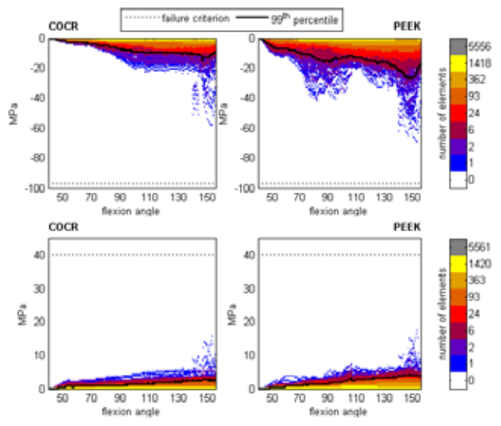

Figure 2. Cement mantle. Compression (top), tension (bottom)

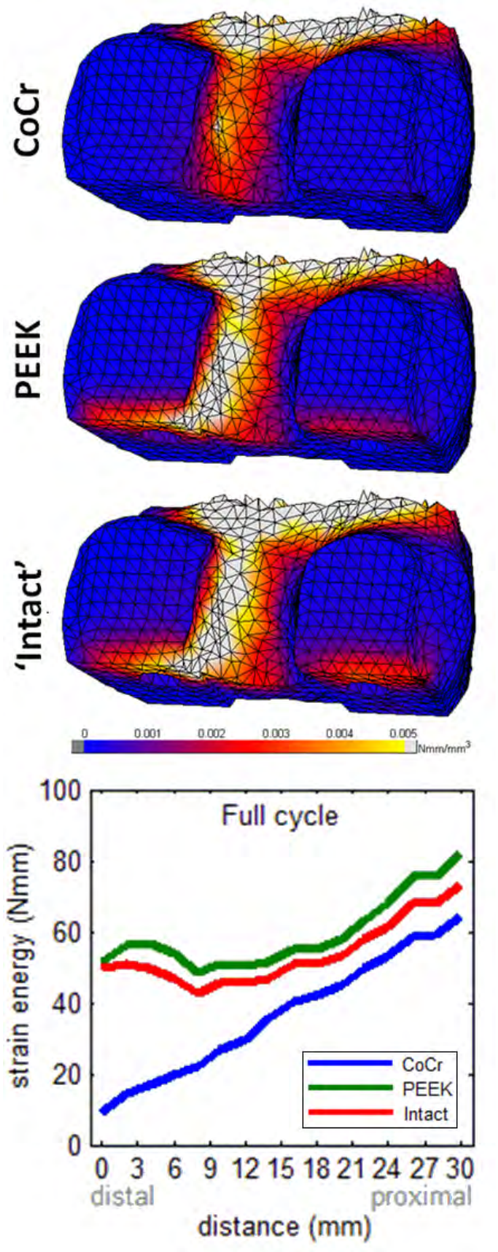

Figure 3. Periprosthetic femur. In view are the cut posterior condyles and intercondylar notch

Early Results of a New Rotating Hinge Knee Implant

Alexander Giurea[1], Hans.-Joachim Neuhaus[2], Rolf Miehlke[3], Reinhard Schuh[1],

Richard Lass[1], Bernd Kubista[1], Reinhard Windhager[1]

[1]Dept. of Orthopaedics, Medical University of Vienna,Waehringer Guertel 18-20, A-1090 Vienna, Austria

[2]Dept. of Traumatology and Orthopaedics, St. Vincenz Hospital Am Stein 24, D-58706 Menden, Germany

[3] Joint-CenterRhein-Main, Wilhelmstr. 30, D- 65183 Wiesbaden, Germany

a.giurea@gmx.at

Introduction:
Indication for rotating hinge (RH) total knee arthroplasty (TKA) includes primary and revision cases, with contradictory results. The aim of this study was to report prospective early results of a new modular rotating hinge TKA (EnduRo®).
For this implant several new design features and a new bearing material (carbon-fiber reinforced poly-ether-ether-ketone, CRF-PEEK) have been developed. Furthermore, we tried to establish a new classification of failure modes for revision TKA.

Methods and Materials:
152 EnduRo® rotating-hinge prostheses were implanted in two centers. In 90 patients a primary implantation has been performed and 62 patients were revision cases. Knee Society Score (KSS), Western Ontario and McMaster Osteoarthritis Index (WOMAC), Oxford Knee Score (OKS) and Range of motion (ROM) were assessed before surgery, 3 months postoperatively, 12 months postoperatively and anually thereafter.
We defined 3 types of complications:
Type 1 : Infection Type 2: periprosthetic complications and Type 3: implant failures.

Results:
KSS, WOMAC, OKS, and ROM revealed significant improvements between the preoperative and the follow-up investigations.
There were 14 complications (9.2%) leading to revision surgery, predominantly type 2. The overall survivorship with revision for any reason as endpoint was 85.4% (CI: 75.6–91.5) at 2 years. The implant associated survivorship was 92.1% (CI:81.5–96.8)
Revision cases revealed statistically significant inferior outcome compared to primary cases.

Discussion:
Our study shows excellent clinical results of the EnduRo® TKA. Furthermore, no premature material failure or unusual biological response to the new bearing material could be detected.

Carbon-Fiber-Reinforced PEEK as an alternative bearing material in artificial knee arthroplasty

Grupp TM[1,2], Pfaff A[1], Fritz B[1], Schroeder C[2], Schwiesau J[1], Giurea A[3], Utzschneider S[2]
[1]Aesculap AG Research & Development, Tuttlingen, Germany
[2]Ludwig Maximilians University, Clinic for Orthopaedic Surgery, Munich, Germany
[3]AKH Department of Orthopaedics, Medical College University of Vienna, Austria

thomas.grupp@aesculap.de

Introduction:
For the evaluation of carbon-fibre-reinforced (CFR) PEEK as alternative bearing material in knee arthroplasty two challenging design areas have been examined – fixed bearing unicompartmental knee arthroplasty (UKA) and a rotating hinge knee (RHK) design.

Unicompartmental knee arthroplasty has become a successful clinical treatment for isolated medial gonarthrosis in young and active patients with relief of pain, fast recovery and restoration of function. Fixed bearing UKA designs are mostly based on a low congruent tibio-femoral articulation to accommodate on the individual patient kinematics. The low congruency leads to a high stress concentration in the polyethylene inlay and bears the risk for enhanced abrasive wear, delamination and structural fatigue failure. The first sector of our study was to evaluate the suitability of two different CFR-PEEK materials for fixed bearing unicompartmental knee articulations with low congruency.
Total knee arthroplasty with a rotating hinge knee prosthesis has become an important clinical treatment option for knee revisions and primary patients with severe varus or valgus deformities and instable ligaments. The rotational axle constraints the anterior-posterior (AP) shear and varus-valgus moments but currently used polyethylene bushings may fail in the midterm due to insufficient creep resistance of the material. The second direction of our study was to develop appropriate test setups for the in vitro evaluation of CFR-PEEK as an alternativ bushing material with enhanced creep and fatigue behaviour an a RHK design.

Methods and Materials:
An in vitro wear simulation was performed for 5 million cycles according to ISO 14243-1 on 12 fixed bearing unicompartmental knee devices (Univation® F Aesculap Tuttlingen, Germany) on a EndoLab knee simulator. For the tibio-femoral articulation the material combination UHMWPE versus CoCr29Mo6 was used as a reference with broad clinical experience. Two alternative gliding surface materials based on CFR-PEEK with 30% PAN or pitch fiber content were examined.
For the RHK design a series of specific biomechanical tests were developed based on clinical failure mechanism and in vivo loading data for anterior-posterior (AP) compression shear, varus-valgus bending and hyperextension moment test conditions.
In vitro wear simulation was performed on 4 rotating hinge knee devices (EnduRo® Aesculap, Germany) for 5 million cycles. The mobile gliding surfaces were made out of polyethylene (GUR 1020, β-irradiated 30 ± 2 kGy). For the bushings of the rotational and flexion axles and the flanges a new bearing material based on carbon fiber reinforced (CFR-PEEK) with 30% PAN fiber content was used. The amount of wear was measured gravimetrically and a particle analysis out of the serum has been undergone according to Affatato et al. 2001.
The in vitro failure modes and wear pattern of the RHK design were compared to retrieved devices with a focus on the CFR-PEEK components.

Results:
The volumetric wear rate of the UKA polyethylene gliding surfaces as reference was 8.6 ± 2.17 mm^3/million cycles, compared to 5.1 ± 2.29 mm^3/million cycles for CFR-PEEK pitch and 5.2 ± 6.92 mm^3/million cycles for CFR-PEEK PAN but without statistically significant differences between the test groups.

For the rotating hinge knee design with the gliding surface made out of UHMWPE and the bushings and flanges made out of CFR-PEEK PAN a cumulative amount of wear of 13.1 ± 4.1 mm^3 with an average wear rate of 2.4 mm^3/ million cycles was measured including all polymer components. The UHMWPE and CFR-PEEK particles were comparable in size and morphology and predominantly in submicron size.

The in vitro failure mechanism and surface articulation pattern of the AP compression shear, varus-valgus, hyperextension and wear tests are comparable to findings on retrieved CFR-PEEK components.

Discussion:
From our observations, we conclude that CFR-PEEK is obviously unsuitable as bearing material for fixed bearing knee articulations with low congruency and it cannot be recommended as it remains doubtful wether it reduces wear compared to polyethylene. In the fixed bearing UKA examined, application threshold conditions for the biotribological behaviour of CFR-PEEK bearing materials have been established.
In contrast to the UKA results the biomechanical and biotribological findings for the rotating hinge knee design demonstrate the high potential of CFR-PEEK as a suitable material for high congruency articulations, such as RHK bushings and flanges.

Investigation of Fretting-Corrosion Behavior of PEEK-Metal Interfaces and Comparison with Metal-Metal Interfaces

Sevi B. Kocagöz, BS [1]; Eric S. Ouellette, BS [2]; Sachin A. Mali, MS [2]; Jeremy L. Gilbert, PhD [2]; Steven M. Kurtz, PhD [1,3]

[1] Implant Research Center, Drexel University, Philadelphia, PA
[2] Biomaterials Institute, Syracuse University, Syracuse, NY
[3] Exponent, Inc., Philadelphia, PA

Introduction: Release of metallic particles and degradation products from modular junctions in orthopedic devices is a clinical concern [1-3]. In a previous study it is shown that the use of ceramic femoral heads, an alternative to CoCr alloy heads, may mitigate corrosion at the modular head-neck interface in hip joint arthroplasties [4]. Using biochemically inert materials may mitigate or eliminate mechanically assisted crevice corrosion (MACC), the mechanism of material release at the modular junctions [5,6]. Previous finite element analysis studies warrant the investigation of poly(ether-ether ketone) (PEEK) for orthopedic applications [7]. PEEK has excellent biocompatibility and is widely used in biomedical applications; yet, its tribochemical properties for modular applications are unknown [8,9]. Swaminathan et al. [10], present a triboelectrochemical test set-up designed to simulate MACC in vitro. Their model accounts for all the mechanical and electrochemical parameters involved in fretting-corrosion and allows for testing any material combination. The purpose of this study was to use the electrochemical set-up presented [10] to test the tribochemical properties of PEEK-CoCr alloy and PEEK-Ti alloy interfaces.
Methods and Materials: The previously described fretting corrosion test system [10] induces sliding contact between a flat circular disk (diameter 35mm) and a cone shaped flat bottom cylindrical pin (cylinder top diameter 8mm, cone shaped flat bottom diameter 0.5-1mm). The pins and disks used for this study were made from PEEK (Invibio Ltd., Lancashire, UK), Ti6Al4V alloy (ASTM-F1472) and CoCrMo alloy (ASTM- F1537) with the following test combinations: CoCrMo pin-CoCrMo disk, PEEK pin-CoCrMo disk, PEEK pin-Ti6Al4V disk, Ti6Al4V pin –CoCrMo disk. Prior to testing, the pin tips and disks are polished to 600 grit and covered with acrylic coating material for a controlled test area. Only the pin tip and a small area surrounding the contact region of the pin tip on the disk (approx. diameter 2.5mm) were exposed. Experiments were performed at room temperature in phosphate buffered saline solution (pH 7.4). The pins were attached beneath the multi-axial load cell in the vertical orientation. A differential variable reluctance transducer (DVRT, Microstrain Inc., USA) is used to record the motion of the pin relative to the disk. Disks are placed horizontally in a chamber attached to the piezoelectric actuator, which is used to simulate fretting motion displacement of 50µm at 3Hz frequency. Variable-load, fretting corrosion tests were performed on all material combinations and each combination was tested in triplicate. Normal loads were varied from 0.5N to 50N or until a load is reached where there is no longer any translational motion of the pin but only pivoting due to "sticking" to the surface of the disk. Sticking is confirmed by a customized LabView software (National Instruments, Austin, TX) used to display multi-axial loads and coefficient of friction. At each load, fretting motion is induced for 120 seconds with a 300 second break in between to allow baseline current to restabilize. CoreView (CoreView Systems Private Limited, Maharashtra, India) is used to record and monitor electrochemical data and confirm stability of baseline current. Post testing, pin tips and contact locations on disks were inspected using scanning electron microscopy (SEM, JEOL JSM-5600) and an optical microscope (KH-8700, HIROX) for quantification of contact area.
Results: Average current density is calculated by taking the difference between the fretting current at each applied normal load and subsequent baseline current. Nominal stresses are calculated by dividing the applied normal load by the contact area identified by microscopy. Work done per fretting cycle at each load is calculated by multiplying the applied normal load with the DVRT displacement data at the given cycle. The difference in current density response between the PEEK material couples and the metal-metal material couples were statistically significant ($p<0.05$). Average fretting current densities for the CoCr pin on disk tests and the Ti pin on CoCr disks were 1.01mA and 1.03mA respectively. The average fretting current densities for the PEEK pin on CoCr disk and PEEK pin on Ti disks were 4.2µA and 3.2 µA respectively. The average fretting current density is always higher for the former metal-metal couples compared to the latter PEEK-metal couples for all normal loads applied during the tests (Figure 1). The bell shaped behavior of increase then decrease in work with increasing stress is seen in all couples (Figure 2) due to the beginning of sticking at a certain level of stress. PEEK-metal couples show earlier sticking and lower work. There was no significant difference between the resulting coefficient of friction values for the various couples, which was approximately 0.2.
Discussion: There is significant difference between the fretting-current response between the material couples that use a PEEK interface and between those that do not. This indicates that there was less disruption to the passivation film on the surface of the metal disks when they are coupled with a PEEK pin. SEM and optical microscopy also did not reveal any visible disruption to the metal surface in the tests using PEEK pins confirming the lower fretting currents generated during these tests. These preliminary results indicate that PEEK may be a promising biomaterial for use in orthopedic applications to mitigate fretting-corrosion.

References:

[1] Chana R, Esposito C, Campbell PA, Walter WK, Walter WL. Mixing and matching causing taper wear: corrosion associated with pseudotumour formation. J Bone Jt Surg Br 2012;94:281–6.
[2] Gill IP, Webb J, Sloan K, Beaver RJ. Corrosion at the neck-stem junction as a cause of metal ion release and pseudotumour formation. J Bone Jt Surg Br 2012;94:895–900.
[3] Meyer H, Mueller T, Goldau G, Chamaon K, Ruetschi M, Lohmann CH. Corrosion at the cone/taper interface leads to failure of large-diameter metal-on-metal total hip arthroplasties. Clin Orthop Relat Res 2012;470:3101–8.
[4] Kurtz SM, Kocagoz SB, Hanzlik JA, Underwood RJ, Gilbert JL, Macdonald DW, et al. Do Ceramic Femoral Heads Reduce Taper Fretting Corrosion in Hip Arthroplasty? A Retrieval Study. Clin Orthop Relat Res 2013;471:3270–82.
[5] Urban RM, Gilbert JL, Jacobs JJ. Corrosion of modular titanium alloy stems in cementless hip replacement. J ASTM Int 2005;2(10):1e10.
[6] Rodrigues DC, Urban RM, Jacobs JJ, Gilbert JL. In vivo severe corrosion and hydrogen embrittlement of retrieved modular body titanium alloy hip-implants. J Biomed Mater Res B Appl Biomater 2009;88(1):206e19.
[7] Ruiter, Lennert, Dennis Jansen, Adam Briscoe, and Nico Verdonschot. *A Biomechanical Analysis of a PEK-Optima® Femoral Component on Implant Fixation, Construct Integrity and Bone Remodeling Opportunities in Total Knee Arthroplasty*. Proc. of Orthopedic Research Society Annual Meeting, New Orleans. 2014.
[8] Kurtz, S.M. and J.N. Devine, PEEK biomaterials in trauma, orthopedic, and spinal implants. Biomaterials, 2007. 28(32): p. 4845-69.
[9] Kurtz, S., PEEK Biomaterials Handbook2012: Elsevier.
[10] Swaminathan, Viswanathan, and Jeremy L. Gilbert. "Fretting Corrosion of CoCrMo and Ti6Al4V Interfaces." *Biomaterials* 33.22 (2012): 5487-503. Web.

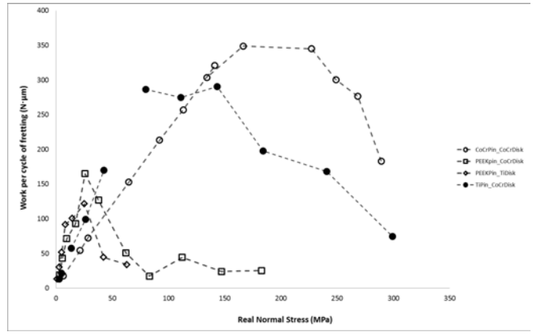

Figure 2: Work per cycle of fretting vs. real normal stress is reported for all material couples. Sticking of the pin on the disk begins at the peak work value. Average values obtained from triplicate tests for each material couple is compiled.

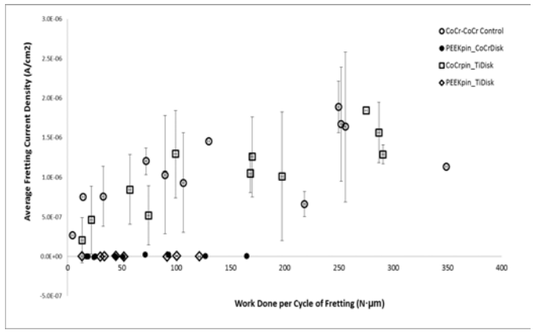

Figure 1: Average fretting current density vs. work done per cycle of fretting for all four material couples. Work done is significantly higher for metal-metal couples compared to PEEK-metal. Average values obtained from triplicate tests for each material couple is compiled.

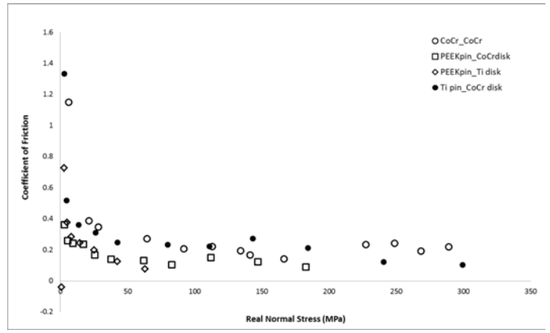

Figure 3: Coefficient of friction (COF) values vs. real normal stress for all material couples. Irrespective of material couple, COF values start higher and decreases quickly in a small range of applied stress and reaches a plateau value. Average values obtained from triplicate tests for each material couple is compiled.

Improved Bone Remodelling Stimulus with a Novel PEEK Implant for Total Knee Replacement

Rankin, K. E.[1], Dickinson, A. S.[1], Briscoe, A.[2], Browne, M.[1]
[1]University of Southampton, SO17 1BJ, UK, [2]Invibio Ltd, Thornton Cleveleys, FY5 4QD, UK
k.rankin@soton.ac.uk

Introduction: Total knee replacement (TKR) is an increasingly common procedure for the treatment of degenerated articular joint surfaces. However, survivorship is limited and a 4% revision rate remains at 9 years [1]. Periprosthetic bone remodelling after TKR may be attributed to local changes in the mechanical strain field of the bone as a result of the stiffness mismatch between traditional high modulus metallic implant materials (~220GPa) and the supporting bone. This can lead to significant loss of periprosthetic bone density, which may promote implant loosening, and complicate revision surgery. Strain-adaptive bone remodelling theory suggests that bone cells react to local deviations in strain, and predicts that below a certain threshold of strain, bone will be resorbed [2]. A novel polyetheretherketone (PEEK) implant with a modulus of 4 GPa, within the range of that of bone (1-20 GPa), has the potential to reduce stress shielding whilst eliminating metal ion release. Digital Image Correlation (DIC) is increasingly used in biomechanics for strain measurement on complex, heterogeneous anisotropic material structures. In this study, DIC was used following a previously validated technique [3] to compare bone strain distribution after implantation with a novel PEEK implant to that induced by a contemporary metallic implant.

Methods and Materials: The distal third of three anatomical femur models (Sawbone AB, Sweden) were sectioned and potted in PMMA resin, aligned to represent standing stance, such that the anatomical axis was 6 degrees adducted from the mechanical axis, 3 degrees to the vertical axis [4]. One distal femur was implanted with a mid-size metallic (Cobalt-Chromium, CoCr) femoral component from a commercial implant system and another was implanted with a PEEK-OPTIMA® (PEEK) (Invibio Ltd, UK) femoral component of the same size and geometry. Both components were fixed in place using Palacos R acrylic bone cement (Heraeus Medical GmbH) mixed under vacuum. The final femur section was left intact as a reference model. To allow surface strain measurement, a speckle pattern was applied to the surface of each bone and dual 2 MP cameras (Limess GmbH, Germany) were used to acquire speckle images of the lateral bone surface in 3D. All models were subjected to standing loads on the corresponding UHMWPE tibial component using an axial Instron 5569 electromechanical test machine (ITW Inc, USA). Six repeat loaded tests were performed for each femur to assess measurement variability and tibial component positioning. Six repeat unloaded cases were conducted to assess measurement sensitivity. Vic-3D software (Correlated Solutions Inc, USA) was used to calculate the displacement and strain fields under loading. The strain was then averaged within sixteen 5 mm^2 strain gauge areas across the lateral surface of each bone for quantitative comparison.

Results: The sensitivity of DIC strain measurements to noise (mean + 3 standard deviations) was $<\pm$130 με and the experimental error ($\pm$ 3 standard deviations) was $\pm$197 με, or 8.2% of the peak strain magnitude in the region of interest, 2400 με. Relatively low bone strains were measured on the lateral surface of the bone implanted with CoCr compared to the intact bone. Quantitatively, a greater deviation was observed between the intact-vs-CoCr datasets (R^2: 0.618, regression slope = 0.4314). A closer agreement was shown between the intact-vs-PEEK datasets (R^2: 0.797, regression slope = 0.939).

Discussion: Low strain measurements in the central metaphyseal region of the bone implanted with CoCr compared to the intact bone indicated stress shielding which may lead to resorption, a theory corroborated by bone density scans of implanted metallic TKRs [5,6]. High bone strain in regions close to the CoCr implant can be attributed to the high stiffness mismatch between implant and bone, where the bone is constrained to the implant with cement. High strain gradients near the stiff CoCr could potentially compromise implant fixation, leading to loosening. The compressive strains in the PEEK implanted model were similar to those in the intact case, suggesting that PEEK may transfer more physiological bone strains with reduced stress shielding effects, promoting bone maintenance in these regions. A shift in strain path was observed in both implanted bone models, which can be attributed to the change in articular surface geometry.

In conclusion, DIC has been developed and successfully employed for evaluation of a novel PEEK TKR implant in comparison to a contemporary metallic implant. The PEEK-OPTIMA® implant produced a strain distribution closer to that of the physiological intact bone case, and therefore would be expected to have less of a stress shielding effect, improving long term bone preservation. To confirm this, the methodology will be applied to cadaveric samples in subsequent work.

References

[1] NJR for England, Wales, NI, 2013, *10th Annual Report*
[2] G H Van Lenthe et al, 1997. *JBJS (Br)* 79B(1):117-122
[3] A S Dickinson et al, 2010. *JBiomechEng* 133.
[4] S Pickering et al, 2013. *JBJS. Knee*
[5] T A Soininvaara et al, 2004. *Knee* 11:297-302
[6] R B Abu-Rajab et al, 2006. *JBJS Br* 88B:606-13

Intracorporeal Ultrasonic Welding of PEEK Implants

Dr Peter Bonutti, Justin Beyers, Matt Cremens
OsteoWeld, Effingham, IL
info@osteoweld.com

Introduction: Previous investigations of the use of high frequency ultrasound for intracorporeal welding have focused on the use of FDA approved poly-L-lactic acid in an arthroscopic environment. In order to improve the strength, longevity, and biocompatibility of the implant, the use of Polyether ether ketone (PEEK) has been evaluated as a potential option for intracorporeal welding. In this investigation, a variety of implant configurations were evaluated in a laboratory setting to determine if welding in both arthroscopic and endoscopic environments could be consistently accomplished.

Methods and Materials: The OsteoWeld Ultrasonic Fixation System (OsteoWeld, Effingham, Illinois) was used to weld two PEEK implant configurations in a laboratory setting. The OsteoWeld Ultrasonic Fixation System comprises a generator which uses digital signal processing to consistently create an ultrasonic waveform that automatically compensates the drive signal for use in arthroscopic and endoscopic environments, a footswitch to activate the system, and an autoclave safe hand piece used to convert the ultrasonic waveform into vibratory energy to weld the implant.

The first implant design (Configuration 1) that was evaluated comprised of two components, a threaded anchor to be implanted in bone and a tack that would pierce tissue and secure it back to the bone surface. Both components were machined from implant grade PEEK, and were attached by the distal tip of the tack welding to a central pocket in the anchor.

The second implant design (Configuration 2) was also comprised of two machined components also machined from implant grade PEEK, a 4.8 mm solid rod and a tack similar in size to those evaluated in Configuration 1. The rod had a small 1.9 mm diameter drilled hole for receiving the tacks for welding.

Results:

Time Testing

The weld times for both Configuration 1 and Configuration 2 were completed in less than 500 milliseconds.

Mechanical Testing

After welding, the Configuration 1 samples were evaluated by a tensile test to separate the tack from the anchor by pulling on the tack head. The mean failure load of the 10 tested samples was 103.2 lbs. and in only one case was the weld breaking the cause of failure.

After welding, the Configuration 2 samples were also evaluated by a tensile test to separate the tack from the rod by pulling on the tack head. The mean failure load of these 10 tested samples was 31.5 lbs. and in only one case was the weld breaking the cause of failure

Thermal Testing

For both Configuration 1 and Configuration 2, temperature measurements on the surface of the samples showed little fluctuation with welding.

Weld Control

For both weld configurations additional testing was done in both fluid and air environments to evaluate the ability of the system to operate in diverse conditions. For both implant configurations the system was able to consistently drive and maintain the drive frequency in dry, moist, and wet environments.

Discussion: PEEK implants of both configurations that were ultrasonically welded with the OsteoWeld Ultrasonic Fixation System were evaluated in a laboratory setting. Due to the strength of the welded implants, safe temperature levels, similar modulus to cortical bone and limited debris we concluded PEEK is a viable polymer for ultrasonically welding to create, modular constructs in the body.

The Role of Thermal History on the Semicrystalline Morphology and Impact Strength of PEEK

Bellare, A[1], Kozak, A.[2] and Spiegelberg, S[2]
[1]Brigham & Women's Hospital, Harvard Medical School, Boston, MA; [2]Cambridge Polymer Group, Boston, MA
anuj@alum.mit.edu

Introduction: Poly (ether ether ketone) (PEEK) is a high performance biocompatible thermoplastic that is finding increasing use in trauma, spine and orthopedic implant applications due to its high modulus and tensile strength combined with biocompatibility. PEEK has a high glass transition temperature (Tg) of approximately 143ºC and a melting temperature of approximately 345ºC. Like most semicrystalline polymers with a high glass transition temperature, thin films of PEEK can be rapidly cooled (quenched) from the melt to form amorphous films, but quenching of PEEK prevents bulk components to be completely amorphous, and they consequently remain semicrystalline. It is well known that the crystalline morphology of semicrystalline polymers affect their macroscopic properties, such as tensile properties, impact strength, fracture toughness and fatigue strength. In this study, we utilized several crystallization routes to investigate their effect on the nanoscale lamellar morphology and on macroscopic mechanical properties, specifically impact strength. Such a methodology, combining processing, morphological and macroscopic property measurement has the potential to guide in developing PEEK components with enhanced properties.

Methods and Materials: PEEK pellets (Ketaspire-820, Solvay Specialty Polymers) were compression molded using a hydraulic press (Carver Inc, Wabash, IN) into plaques of 12.5 mm thickness. During molding, the pellets were heated to a temperature of 400ºC and cooled using the following protocols: (1) Slow cooled (SC) at a rate of 3ºC/min (2) Quenching (Q) at a rate of 15ºC/min (3) Quenched and annealed at 250ºC for 16 hours (QA), (4) Quenched, remelted at 380ºC and quenched again to maximize nucleation and (5) Isothermally crystallized at 330ºC for 16 hours. A TA Q2000 differential scanning calorimeter (DSC) was utilized to measure the crystallinity for all groups [n=3] using a heating rate of 20ºC/min and a heat of fusion of 130 J/g. Small angle x-ray scattering (SAXS) data was collected from 2mm thick PEEK sheets using a CuKα x-ray source (Rigaku S-Max3000) with an scattering range of q_{min}=0.05 [1/nm] and q_{max}=1.0 [1/nm], where the scattering vector, q, is defined as: $q = (4\pi/\lambda)\sin\theta$, λ is the wavelength of the x-ray (=0.154 nm) and θ is one-half the scattering angle. Izod impact testing was conducted according to ASTM D256 using an Instron CEAST 9050 impact tester (n=3).

Results: A combination of DSC and SAXS (see Figure 1) showed that PEEK-IC had a significantly ($P<0.05$, ANOVA) higher crystallinity and lamellar thickness over the PEEKs with other crystallization routes (see Table 1) whose crystallinity and lamellar thickness was not significantly different from each other ($p>0.05$), except for PEEK-SC which had a significantly higher lamellar thickness over that of PEEK-Q and PEEK-QA. The impact strength of PEEK-QA and PEEK-QQ was generally lower than that of PEEK-SC, PEEK-Q and PEEK-IC ($p<0.05$, ANOVA) except for the pair PEEK-QQ and PEEK-SC which were not significantly different ($p=0.136$) (see Figure 2). There was also no statistically significant difference in the impact strength of PEEK-SC, PEEK-IC and PEEK-Q ($p<0.05$).

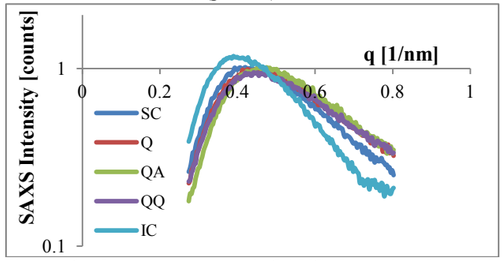

Figure 1. Lorentz corrected SAXS Intensity [counts] versus scattering vector, q [1/nm] for various PEEKs.

Sample ID	X [%]	D [nm]
PEEK-SC	49.0 ± 3.3	6.2 ± 0.4
PEEK-Q	46.5 ± 1.9	5.7 ± 0.2
PEEK-QA	47.3 ± 1.5	5.7 ± 0.2
PEEK-QQ	47.7 ± 0.9	5.9 ± 0.1
PEEK-IC	53.9 ± 2.2	7.2 ± 0.3

Table 1. Crystallinity [%] (X) and lamellar thickness [nm] (D) from DSC and SAXS respectively

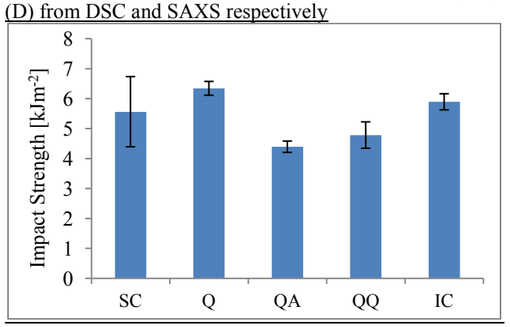

Figure 2. Impact strength [kJm-2] (mean ± standard deviation) for various groups of PEEKs.

Discussion: This study showed that the impact strength of PEEK was not affected whether it was slowly crystallized, quenched or isothermally crystallized. This result is likely due to its high rate of crystallization, which dominates the formation of lamellar nanostructure of PEEK. The impact strength of quenched and then reheated PEEKs were found to be lower, probably due to residual stresses induced by repeat quenching. Isothermal crystallization was the most effective in increasing crystallinity but again did not significantly affect impact strength. In summary, this study showed that PEEK Ketaspire 820 is a robust polymer whose impact strength is not strongly dependent on thermal history.

PEEK OPTIMA® LT1 for High Temperature Laser Sintering (HT-LS)

Berretta, SI[1], Ghita, OR[1], Evans, KE[1] and Anderson, AN[2]
[1]College of Engineering, Mathematics and Physical Sciences, University of Exeter, Exeter, UK
[2] Invibio Biomaterial polymer solutions, Thornton Cleveleys, UK
sb508@exeter.ac.uk

Introduction: High Temperature Laser Sintering (HT-LS) is an additive manufacturing technology that allows production of complex and highly customized components using powdered high temperature polymers such as PolyEtherEtherKetones (PEEK). During the process a laser induces the sintering of the material particles layer upon layer until a part is completed. Absence of tooling, high freedom of design without additional cost on the single item and the possibility to utilize high temperature biocompatible materials, make use of HT-LS an ideal candidate for the fabrication of medical devices. EOSINT P800 system is the only commercial equipment able to sinter high temperature polymeric powders. The system currently works with Polyetherketone (PEK) powder, a polymer belonging to the chemical family of Polyetherarylketones (PEAK), but having a melting point (mp) of approximately 30°C higher than PEEK (PEEK mp=343˚C, PEK mp=373˚C). While investigation on laser sintering of PEK components has been recently provided [1-3], research into new high temperature powders has not been considered. This work represents the first study on the medical grade PEEK OPTIMA LT1® (Invibio Biomaterials Solutions, UK [4]) for laser sintering. This paper presents results of the analysis into the particle morphology of PEEK powders, the optimization of the manufacturing parameters and an early stage application product.

Methods and Materials: The material used for the manufacture of PEEK components was OPTIMA LT1®, supplied by Invibio Biomaterials solutions [4]. PEEK presents a glass transition temperature of 143˚C and a melting temperature of 343˚C. The material was thermally treated for 24 hours at an annealing temperature of 250 ˚C and sieved before use in the EOSINT P800. Performance of PEEK have been compared with the properties of the PEK material ("EOS HP3" [5]) currently used in the P800 system. Both raw and treated PEEK powders have been studied in terms of flow behavior and particle morphology, using the Angle Of Repose (AOR) test and Scanning Electron Microscopy (SEM), respectively. AOR test (ASTM C144 standard) is a measurement of the angle that a cone of bulk material forms when poured over a flat surface. The test is based on the assumption that every material has its own specific angle of repose. The smaller the angle of repose is, the higher the flowability. The test was repeated six times on each material. SEM examination of the powder materials was carried out by using a Hitachi S-3200N scanning electron microscope. The samples were coated with 4nm of gold coating in order to reduce the surface charging and the electron secondary imaging was set with an accelerating voltage of 25kV. The images were then analyzed with the image processing program Image J [6], software capable of evaluating shape descriptors on particle specimen images. Roundness and circularity parameters were calculated. More than a thousand particles were analyzed for each grade. Tensile samples of treated PEEK, built at different laser energy inputs, were manufactured in the P800 system. Each set included 30 tensile samples fabricated with ISO 527-2-1A geometries along the x direction of the building chamber. The tensile testing experiments were carried out using the LLOYD instrument EZ20 mechanical testing machine at room temperature (20˚C). The testing speed was equal to 2mm/min, the breaking speed was 15mm/min and the gauge length was 85mm. Seven cranial implants were manufactured using the optimum manufacturing settings. Main dimensions (x,y,z) of the seven units were measured using Mitutoyo digital vernier caliper and compared with the CAD file model. The size of a central cavity was also measured in all the parts and reported in the results. The percentage differences between nominal and real values were then evaluated.

Results:
The results of the angle of repose tests for the powder materials are reported in table 1.

Material	AOR [˚]
OPTIMA LT1®(PEEK)	53 ± 1
OPTIMA LT1® TREATED	46 ± 1
HP3 (PEK)	42 ± 1

Table 1. AOR results [7]

Although HP3 PEK showed the highest flow behavior, PEEK exhibited a similar flow performance when treated. Images of HP3 PEK, PEEK and treated PEEK particles are reported in figures 1-3, respectively.

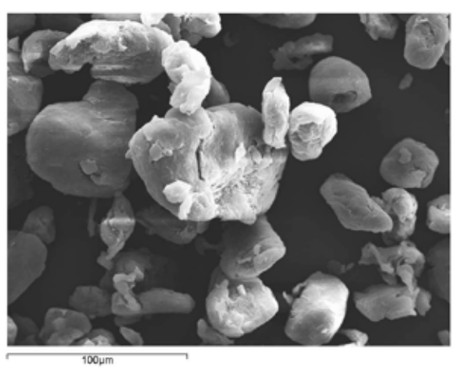

Figure 1. HP3 PEK particles

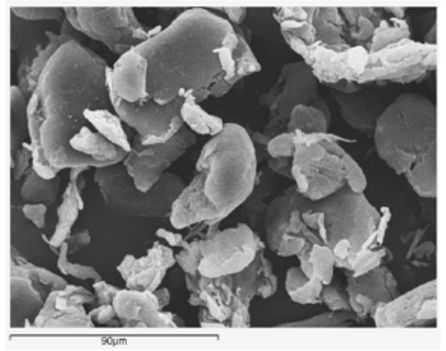

Figure 2. OPTIMA LT1® particles

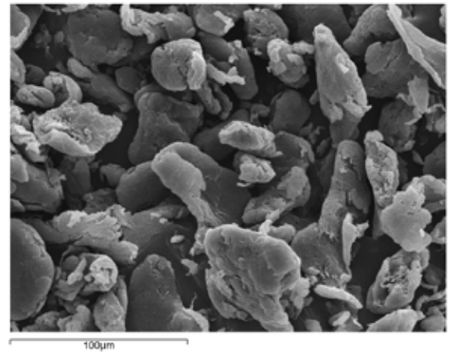

Figure 3. Treated OPTIMA LT1® particles

HP3 PEK particles appeared fairly round with smooth surfaces, while OPTIMA LT1® particles exhibited more irregular shapes and sharp elements. The treating of OPTIMA LT1® improved the results overall, outcome confirmed also by the AOR measurements. The results of the shape descriptors Roundness and Circularity are reported in figure 4, utilizing the Mahalanobis distance within the software package MATLAB[8].

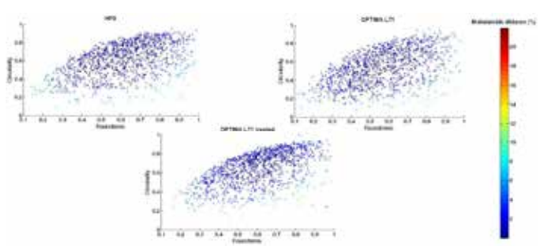

Figure 4. Particle Shape results for HP3, OPTIMA LT1® and OPTIMA LT1® treated

HP3 PEK and treated OPTIMA LT1® seemed to include particles that exhibited a fairly high level of circularity and roundness at the same time. OPTIMA LT1® particles appeared more spread out along low values of circularity and roundness, confirming the presence of sharper and more elongated elements.
The Ultimate Tensile Strength (UTS) of HP3 PEK [2] and treated OPTIMA LT1® are reported in figure 5.

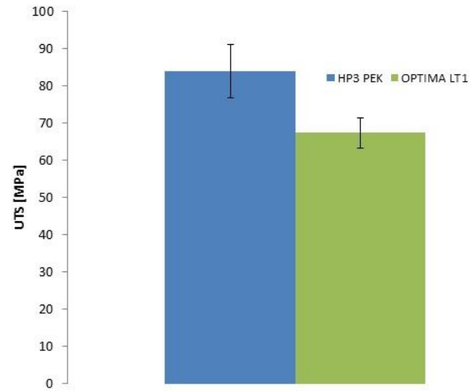

Figure 5. UTS of the laser sintered samples with deviation standard bars

HP3 PEK exhibited a UTS value of 84 ± 7 MPa, while OPTIMA LT1® samples presented UTS values of 67 ± 4 MPa. Although OPTIMA LT1® gave slightly lower values than HP3 PEK, it still meets the mechanical performances required for the fabrication of medical implants and even other engineering applications[9, 10]. One of the seven cranial implants is shown in figure 6, while the nominal dimensions on the CAD file are illustrated in figure 7.

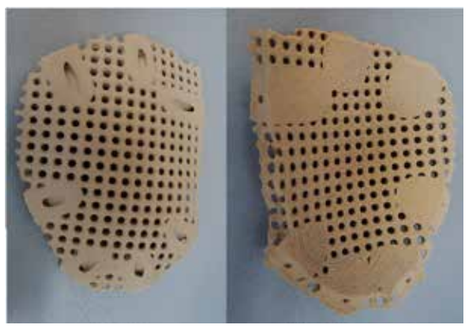

Figure 6. Cranial implant in PEEK OPTIMA® LT1

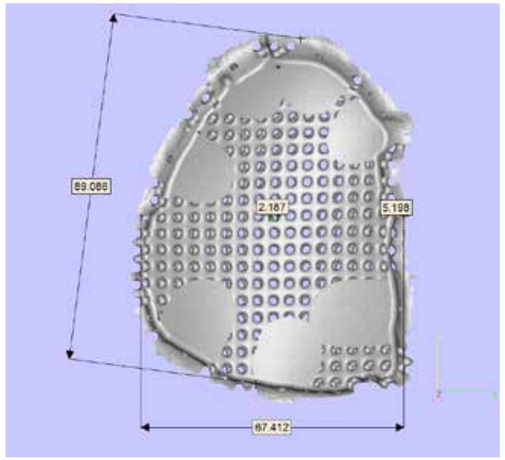

Figure 7. CAD design of the cranial implant

The results of the % difference between real and nominal values of the seven implants are provided in table 2. The implants showed higher deviation along the z axis. Measurements were taken with an accuracy of 0.02mm. A more accurate study could be carried out at a later date using a CMM laser scanning system.

Sample	x [%]	y[%]	z[%]	Circular cavity[%]
1	0.5	0.6	7.5	5.6
2	0.3	0.5	5.0	0.6
3	0.6	0.5	5.0	0.6
4	0.2	0.6	5.6	3.3
5	0.5	0.6	5.8	1.1
6	0.5	0.6	6.6	0.3
7	0.3	0.4	6.0	0.6

Table 2. % Variations of the 7 cranial implants from the CAD design

Discussion: The AOR values of HP3 PEK and treated OPTIMA LT1 ® appeared comparable and both indicated good flow behavior. The particle shape analysis outlined some differences between untreated PEEK and the other two grades (HP3 PEK and treated PEEK), thus explaining the variation found in the flow results. The good mechanical performance obtained from the laser sintered PEEK samples open the way to the use of PEEK in HT-LS for the fabrication of medical components. Lastly, early stage measurements of geometrical tolerances of seven laser sintered cranial implants are for the first time here reported. Depending on the geometry and application requirements, further work on topology optimization of part shrinkage will be able to address tolerances issues.

1. Beard, M.A., et al., *Material characterisation of Additive Manufacturing components made from a polyetherketone (PEK) high temperature thermoplastic polymer*, in *Innovative Developments in Virtual and Physical Prototyping*2011, CRC Press. p. 329-332.
2. Ghita, O., et al., *High Temperature Laser Sintering (HT-LS): An investigation into mechanical properties and shrinkage characteristics of Poly (Ether Ketone) (PEK) structures.* Materials & Design, 2014. **61**(0): p. 124-132.
3. Ghita, O.R., et al., *Physico-chemical behaviour of Poly (Ether Ketone) (PEK) in High Temperature Laser Sintering (HT-LS).* Journal of Materials Processing Technology, 2013.
4. Invibio. *http://www.invibio.com/*.
5. EOS, *http://www.eos.info/en/home.html*.
6. NHS. *Image J.* Available from: http://rsbweb.nih.gov/ij/.
7. Berretta, S., O. Ghita, and K.E. Evans, *Morphology of polymeric powders in Laser Sintering (LS): From Polyamide to new PEEK powders.* European Polymer Journal, 2014. **59**: p. 218-229.
8. MATLAB. *http://www.mathworks.co.uk/products/matlab/*.
9. Lethaus, B., et al., *Cranioplasty with customized titanium and PEEK implants in a mechanical stress model.* J Neurotrauma, 2012. **29**(6): p. 1077-83.
10. Thomas, S. and V.P. M, *Handbook of Engineering and Specialty Thermoplastics: Volume 3: Polyethers and Polyesters* 2011: Wiley.

Correlation between crystallinity and mechanical properties of PEEK for orthopaedic applications

Regis, M[1, 2]; Bracco, P[2], Zanetti, M[2], Mercuri, D[1]
[1]R&D department, Limacorporate S.p.A., IT
[2]Chemistry department, University of Torino, IT
marco.regis@limacorporate.com

Introduction: PEEK is becoming one of the most interesting biopolymers for orthopedic applications: in fact, its chemical stability, tribological properties, and the possibility to add carbon fibers, are of great interest [1]. However, there is controversial information on in vivo reaction to PEEK wear debris, and on its mechanical properties evolution [2, 3]. This limits its application to spine and trauma devices only. In order to better understand PEEK and CFR PEEK final properties, investigating the polymer structure and morphology is a key factor. According to the findings reported in the literature, PEEK exhibits a double melting peak behavior that has to be fully understood and addressed in order to have a stable crystal structure, and consequently, well determined mechanical properties [4].
The aim of this study is therefore to investigate the structure-properties relationship of PEEK and to provide information on the evolution of its processing-dependent properties, with the aim to extend the use of PEEK in orthopaedics.
Methods and Materials: samples at disposal for this study were two carbon fiber reinforced PEEK formulations, which differed for the fibre chemical nature, supplied in form of granules (Invibio Ltd, UK). The fibre used was PAN based (ni1ca30) or Pitch based (Motis), and both materials had the same fibre content (30%wt). Granules were pre-heated at 70°C to remove the residual moisture and injection moulded into 127x12.7x3.7mm rectangular-shaped platelets. Nozzle temperature was 400°C, above the PEEK matrix melting temperature Tm (343°C), to ensure a proper material flow in the moulds. After equilibrating the mould temperature at 250°C, the extracted specimens were cooled in air. In order to differentiate the crystal structure of the polymer, part of the samples were subjected to different annealing treatments (200, 225, 250, 275, and 300°C for 5h, air cooling, constant heating rate 5°C/min).
The evolution of the crystal structure was assessed by DSC (DSCQ20, TA instruments, US), FT-IR spectroscopy (Spotlight 400, Perkin-Elmer, US) and density measurements (XSE205DU, Mettler-Toledo, CH). DSC and density measurements were carried out according to reference standards [5, 6]. The crystallinity percentage (X%) was calculated either from the DSC data by the formula [7]

$$X\% = \frac{melting\ peak\ Area}{130} \cdot \nu_m \cdot 100$$

which takes into account the amount of reinforcement ν_m, or from the density measurements by considering the hydrostatic shift of the specimen. IR analyses were performed in specular reflectance mode on the smooth, flat surfaces of the specimens (100x100µm spot dimension, 4cm^{-1} resolution, 16 scans per spectra, investigated range 700-4000cm^{-1}). The spectra were then treated with Kramers-Kronig algorithm, and crystallnity was evaluated by considering the 1280/1305cm^{-1} band ratio [8]. In order to evaluate the resulting mechanical properties, all samples were subjected to mechanical test in flexion, according to ASTM D790 [9]. The samples were tested at a 5mm/min rate with a 100KN class 0.5 certified load cell equipped apparatus (MTS, Mini Bionix II 858, US).
Results: DSC thermograms for ni1ca30 and Motis are illustrated in Figure 1. The annealing treatment results in the formation of a double melting peak, whose position and intensity showed a strong dependence on the annealing temperature.

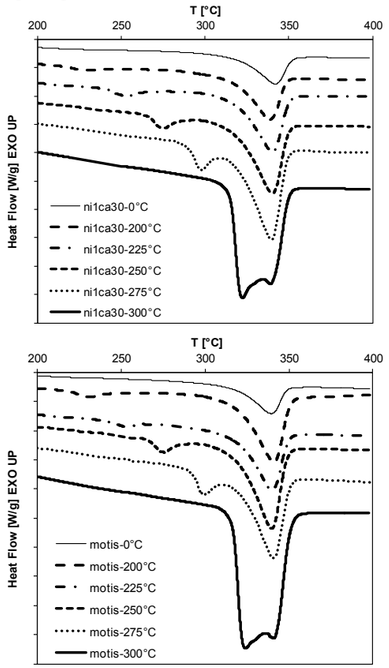

Figure 1. DSC thermograms for annealed and as moulded ni1ca30 (up) and Motis (down) CFR PEEK.

As a result, the amount of crystallinity, calculated by the above mentioned formula, was found to raise accordingly to the heat treatment temperature, ranging from 32.3% to 42.1% for ni1ca30 CFR PEEK, and from 31.5% to 39.6% for Motis CFR PEEK for the "as moulded" samples and the 300°C annealed samples, respectively.
FTIR band ratio and density measurements are reported in Table I, together with crystallinity calculation. The

correlation between DSC resulting crystallinity and FTIR band ratio (Figure 2) showed accordance between the two methods. In addition, even if density changes were within 0.02g/cm^3, data dispersion was narrow and the trend was in accordance to DSC and IR analysis.

Table I. FTIR band ratio and measured density in ni1ca30 and Motis in different annealing conditions.

Sample	anneal. T[°C]	X[%]	1280/1305cm^{-1}	ρ[g/cm^3]
ni1ca30	-	32.3	1.17	1.388
	200	33.8	1.19	1.402
	225	35.4	1.18	1.405
	250	36.7	1.23	1.409
	275	39.2	1.31	1.411
	300	42.1	1.44	1.415
Motis	-	31.5	1.17	1.424
	200	31.9	1.20	1.429
	225	33.8	1.25	1.432
	250	34.9	1.27	1.434
	275	38.0	1.36	1.437
	300	39.6	1.50	1.440

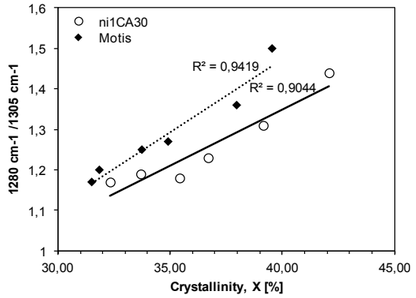

Figure 2. correlation between DSC and IR measurements.

Mechanical properties varied accordingly to polymer crystallinity as well. A significant rise of flexural load was observed for annealed specimens compared to the material in "as moulded" conditions (Figure 3, $p<0.02$).

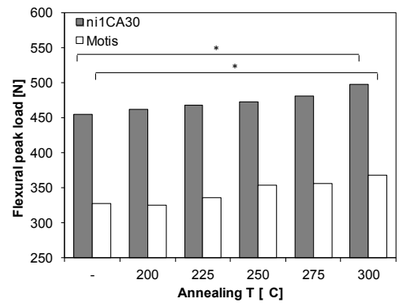

Figure 3. flexural peak load for both ni1ca30 and Motis in different annealing conditions.

For both ni1ca30 and Motis CFR PEEK, a 10% increase in strength could be reached.

Peak load varied from 455N to 498N, and from 328N to 367N, respectively.

Discussion: DSC thermograms of annealed samples showed the appearance of a secondary melting peak for both the materials considered. This phenomenon can be due to a melting and re-crystallization phenomena which has been supposed to occur during the heating stage of the DSC analysis [10]. However, there is no literature consensus on this aspect, and both FT-IR and density measurements performed in this study indicate that the overall crystallinity was enhanced by the annealing treatment: band ratio and density (Table I) are increasingly higher for higher annealing temperatures, demonstrating the existence of a crystallinity growth regardless to the interpretation of the DSC thermograms peaks. Therefore, it can be concluded that data obtained from DSC, FTIR and density measurements confirm that thermal history plays a significant role in the enhancement of the crystal phase within the polymer structure. Differences between PAN based and Pitch based CFR PEEK materials have been observed, indicating that the chemical nature of the fibre may influence the overall crystallinity. According to DSC results, it seems that the overall crystallinity increase after the annealing treatments is lower for Motis PEEK compared to ni1ca30 PEEK. Also in this case, FTIR and density measurements seem to be in accordance with the above mentioned interpretation. This may indicate that the different carbon fibres can influence the crystal growth in the polymer matrix. More adequate characterization techniques such as X-ray diffraction or SEM are needed to draw appropriate conclusions on crystal structure, though. The resulting mechanical properties were affected by thermal treatments as well, indicating that there is a strict correlation with the crystalline content. Differences in mechanical properties between ni1ca30 and Motis are due to the different mechanical performance of the reinforcement fibre. This result is considered to be particularly encouraging, since the mechanical properties improvement in a polymer matrix composite material is largely due to the reinforcement addition [11]. It is therefore believed that maximizing the polymer crystal growth will have a beneficial effect in terms of material structure stability, giving the possibility to expand the use of PEEK and CFR PEEK in the orthopaedic field.

References:

1. Kurtz SM, *et al.*, Biomaterials 28, 2007
2. Meyer MR, *et al.,* JBMR 28, 1994
3. Chivers RA, *et al.*, Polymer 35, 1994
4. Wei CL, *et al.*, Polymer 44, 2003
5. ASTM F2026, ASTM international, 2007
6. ISO 1183-1, International Standard Organisation, 2012
7. Kuo MC, *et al.*, Materials chemistry and physics, 2010
8. Chalmers JM, *et al.*, Micron, 27, 1996
9. ASTM D790, ASTM international, 2010
10. Lee Y, Porter RS, Macromolecules, 20, 1987
11. Harris B, Maney Materials Science ed., 1999

MECHANICAL AND STRUCTURAL ANALYSES OF TIO_2 AND HA COATED PEEK BIOMATERIAL

SARGIN, F. [1,a], TURK, A. [1,b], CELİK, E. [2,c]

[1]Celal Bayar University, Manisa, TURKEY

[2]Dokuz Eylul University, İzmir, TURKEY

[a] fatih.sargin@cbu.edu.tr [b] ahmet.turk@cbu.edu.tr [c] erdal.celik@deu.edu.tr

The importance of synthetic thermoplastic polymer polyetheretherketone (PEEK) in clinic applications has been increasing lately. PEEK is replacing metal implants because it is superior qualifications such as biocompatibility, being chemically stable, being transparent to X-rays and having an elastic modulus similar to human bone. However PEEK is a bioinert material and this property of its, prevents PEEK forming good integration with bone tissues after implantation. In this study it was aimed to enhance bioactivity and mechanical properties of PEEK by depositing TiO2 on PEEK substrate using PVD and coating hydroxyapatite using atmospheric plasma spray method. Elemental analysis performed by XRD and microstructural analysis performed with SEM and optical microscope to uncoated PEEK, TiO_2 coated PEEK and HA+ TiO_2 coated PEEK samples. Samples were also subjected to mechanical tests such as hardness test, roughness test and scratch test.

Morphology and Impact Strength of PEEK containing Hydroxyapatite Micro- and Nano-fillers

Spiegelberg, S[1], Kozak, A[1] and Bellare, A[2]
[1]Cambridge Polymer Group, Boston, MA; [2]Brigham & Women's Hospital, Harvard Medical School, Boston, MA
Stephen.Spiegelberg@campoly.com

Introduction: Polyether ether ketone (PEEK) is a commonly used biomaterial due to its strength, chemical inertness, and processability. High melt flow PEEK is desirable for injection molding processes, but the lower molecular weight necessary to achieve a lower melt viscosity can result in reduced mechanical properties. Incorporation of fillers such as hydroxyapatite (HA) can potentially improve mechanical properties, such as tensile and compressive modulus, and simultaneously provide enhanced biocompatibility. In this study, we blend two forms of HA into PEEK and measured their dispersion and impact strength. We hypothesized that the lower particle size HA would have a less deleterious effect on the toughness of PEEK than the higher particle size HA since the larger particles would act as larger size defects, which are known to have a greater effect on the toughness and strength of semicrystalline polymers.

Methods and Materials: PEEK pellets (Ketaspire-880, Solvay Specialty Polymers), micrometer size conventional HA (Sigma-Aldrich) and nanometer size HA (< 200nm per Sigma Aldrich) were dried in an oven at 150ºC for two hours. The PEEK pellets were thereafter mixed with 3 vol% HA fillers (referred to as PEEK-microHA and PEEK-nanoHA, respectively) and blended at a temperature of 420ºC using a high speed mixer (Eurostar power control-visc, IKA Works GmbH, Staufen, Germany) operating at 300 rpm. Following blending with the PEEK, the samples were compression molded using a hydraulic press (Carver Inc, Wabash, IN) into plaques of 12.5 mm thickness. Unblended PEEK, subjected to the same thermal history as PEEK with fillers, was used as the control. Dynamic light scattering (DLS) provided the particle size distributions of the hydroxyapatite particles. The HA particles were suspended in isopropanol and sonicated for 30 minutes. After they were allowed to settle for >12 hrs, they were analyzed in a Malvern Zetasizer Nano ZS90. Scanning electron microscopy was conducted on fractured surfaces of the three molded samples with a Zeiss EVO LS15 SEM equipped with an energy dispersive spectroscopy detector. Images were collected in backscattered mode, in which higher atomic number materials appear brighter against the background PEEK. Izod impact testing was conducted according to ASTM D256 on an Instron CEAST 9050 impact tester with n=3 per sample group.

Results: The DLS showed that the nanoHA had a peak particle size of 92 nm, while the microHA had a peak particle size of 672 nm. SEM micrographs showed that the HA particles were uniformly distributed in the PEEK with no large agglomerates present (Figure 1); EDS confirmed that the particles were HA. The particle spacing in the PEEK-microHA blend was approximately 10 µm, and approximately 2 µm for the PEEK-nanoHA blend. Impact strength tests showed that the impact toughness of PEEK-microHA was 45% lower than that of PEEK-control (p=0.001, ANOVA) while the impact toughness of PEEK-nanoHA decreased by 29% (p=0.011) although there was no statistically significant difference between the impact strength of PEEK-microHA and PEEK-nanoHA (p=0.096) (see Figure 2).

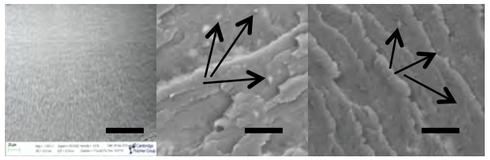

Figure 1: SEM micrograph of control, unfilled PEEK (left), PEEK-microHA (middle) and PEEK-nanoHA (right). [Scale bar = 20 µm].

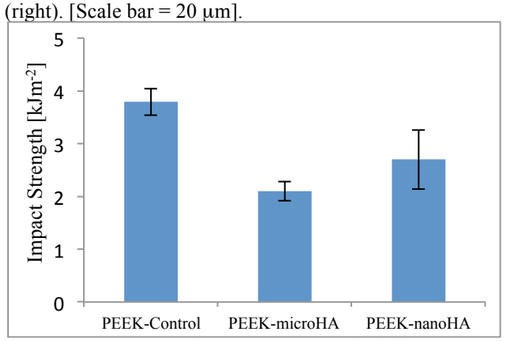

Figure 2: Histogram of Impact strength of PEEK-control, PEEK-microHA and PEEK-nanoHA.

Discussion: This study showed that HA filler blended into Ketaspire-880 PEEK at 3 vol % decreased its impact strength regardless of particle size. A likely reason for the decrease is the weak interfacial strength between the dispersed filler particles and PEEK. When the PEEK containing filler particles in the melt state is crystallized as it is cooled to room temperature, the increase in density due to crystallization likely shrinks the polymer away from the particles thus providing weak adhesion between filler and the matrix PEEK polymer. Thus the filler particles merely act as defects loosely embedded in the PEEK matrix. Larger defects are known to affect the toughness of the matrix polymer more strongly, which is likely why the microHA lowered the toughness of PEEK-control to a greater extent than nanoHA. A limitation of this study is that we only investigated the effect of a single volume fraction of filler on the impact strength of PEEK. A more comprehensive study is required with various volume fractions of fillers to determine the optimum particle size and volume fraction that would provide PEEK-filler composites with the highest toughness and impact strength, which are important for their application as load bearing implants.

Thin Film Self-Reinforced Composite PEEK: Characterization and Evaluation as a Potential Orthopedic Biomaterial

Eric S. Ouellette[1,2], Jeremy L. Gilbert[1,2]
1. Department of Biomedical and Chemical Engineering, Syracuse University, Syracuse, NY, 13244
2. Syracuse Biomaterials Institute, Syracuse, NY, 13244

Background: Fretting crevice corrosion of metallic biomaterials is a paramount concern in the orthopedic community. Evidence of fretting corrosion has been increasingly reported since the inception of modular design, particularly in total hip prostheses[1–3]. With the understanding that modularity introduces anatomical and surgical benefits, it is important to look toward methods of preventing fretting corrosion that do not include elimination of modular design. Self-reinforced polymer composites are a class of materials that could potentially act as a barrier to fretting corrosion. Their strength, wear resistance, and ability to be fabricated from a single (potentially biocompatible) material are attractive attributes when considering an insulating barrier between two metallic surfaces[4,5]. The goal of this work, therefore, is to describe the process of hot compaction of melt-spun Poly (Ether Ether Ketone) fibers into uni-axially oriented thin film self-reinforced composite PEEK (SRC-PEEK), explore thermal, structural, and material properties, and evaluate their potential as a barrier to corrosion through pin-on-disk fretting corrosion experiments.

Experimental: SRC-PEEK was fabricated by uni-axially arranging melt-spun PEEK fibers (spun in-house) in a lay-up approximately 2-3 fiber diameters in thickness in a stainless steel channel mold. The fibers were compacted on a Carver hydraulic press in a temperature range of 340-344 ^{0}C, for 10 minutes at a pressure of 2.6 MPa. Resulting films were imaged with digital optical microscopy (DOM)(Hirox, Hackensack, NJ), and evaluated with DSC from 60-380 ^{0}C, 10 ^{0}C/min (TA instruments, New Castle, DE), WAXS (Rigaku, Japan), and tensile testing at 2 mm/min displacement rate (Test Resources, Shakopee, MN). Samples were also subjected to pin-on-disk fretting corrosion experiments with a thin film SRC-PEEK sample seated between a CoCrMo pin and Ti6Al4V disk at a constant load of 14 N and held at -50 mV vs. Ag/AgCl in phosphate buffered saline (pH=7.4), with a displacement and rate of 50 µm and 2.5 Hz, respectively for approximately 12,500 cycles. Micromechanical (tangential force vs. pin displacement, coefficient of friction vs. total cycles) and electrochemical data were collected for the length of the test. Thin film samples were analyzed post-test in SEM (JEOL 5600, Japan) with energy dispersive spectroscopy (EDS) (Princeton Gamma Tech, Princeton, NJ) and in 3D DOM.

Results: DSC indicated an increase in T_m from the PEEK fiber used to fabricate the SRC-PEEK as well as for isotropic PEEK. The T_g became more subtle than the fiber and bulk suggesting a higher crystalline fraction. Figure 1 shows that crystallinity by WAXS was found to be higher for SRC-PEEK than for PEEK fibers (44% vs. 28%, $p < 0.05$). Crystal size was larger for SRC-PEEK than PEEK fiber (156 Å vs. 69 Å, $p < 0.05$), and Hermanns orientation parameter was found to be comparable (0.71 vs. 0.76), indicating similar degrees of crystalline orientation. Modulus, ultimate tensile strength, and yield stress were higher for SRC-PEEK than PEEK fiber (2.8 GPa vs. 2.3 GPa, 245 MPa vs. 195 MPa, and 95.7 MPa vs. 50.3 MPa, respectively, $p < 0.05$), while strain-to-failure in SRC-PEEK was comparable to PEEK fiber (75.7% vs. 67%, p=0.494) (Figure 2). From figure 3, SRC-PEEK performed better than control metallic couples in pin on disk testing, as evaluated by average current at 12,000 cycles (.003 µA vs. 3.241 µA, $p < 0.05$). Coefficient of friction at 12,000 cycles showed no difference between SRC-PEEK and control groups (p=0.156). Post-test analysis of SRC-PEEK samples showed clear areas of wear induced by the pin, but 3D optical profiling showed indentation into the SRC-PEEK surface of only about 8 µm. EDS revealed transfer of some particles of CoCrMo alloy to the SRC-PEEK surface, but instances were localized to the edges of the pin's wear patterns. The particles did not appear to have been embedded into the surface or engaged in third-body wear of the polymer surface.

Discussion: This work was aimed at evaluating a new material, SRC-PEEK, for its potential as an orthopedic biomaterial to be used in the modular head-neck junction of THA devices. The materials properties of SRC-PEEK are better than the PEEK fibers that they are comprised of, and the strength and strain-to-failure are higher than typical ranges for bulk isotropic PEEK. In processing the fibers into SRC-PEEK, the microstructure increased in crystalline fraction, owing to the melting and re-crystallization of the fiber surface. Crystal size was found to be significantly larger due to the nature of the processing; the slow cooling rate of the compaction mold allowed for nucleation and a long period of growth before cooling below T_g. Cold crystallization of the remaining fiber phase is also likely a factor playing into the increased crystallinity and crystal size. Crystalline orientation remained the same between fibers and SRC-PEEK, suggesting that the extent of the isotropic crystalline phase grown during cooling was not significantly affecting the preferred crystalline orientation. Electrochemical results from pin on disk testing showed that the SRC-PEEK could effectively insulate

the alloy surfaces, preventing the development of fretting currents. Importantly, coefficient of friction was found to be the same for the CoCrMo-SRC-PEEK-Ti6Al4V surface as the CoCrMo-Ti6Al4V control. This could be an important factor in seating mechanics of heads utilizing SRC-PEEK films in the future. Minor transfer of material to polymer surfaces is not yet a concern, pending further testing and electrochemical analysis. SRC-PEEK shows promise for use as a novel orthopedic biomaterial.

1. Gilbert, J. L., Buckley, C. A. & Jacobs, J. J., *J. Biomed. Mater. Res.* **27,** 1533 (1993).

2. Rodrigues, D. C., Urban, R. M., Jacobs, J. J. & Gilbert, J. L., *J. Biomed. Mater. Res. - Part B Appl. Biomater.* **88,** 206–219 (2009).

3. Gilbert, J. L., Mehta, M. & Pinder, B. *J Biomed. Mater. Res. - Part B Appl. Biomater.* **88,** 162–173 (2009).

4. Ward, I. M. & Hine, P. J., Polymer, **45,** 1413–1427 (2004).

5. Matabola, K. P., Vries, a. R., Moolman, F. S. & Luyt, a. S., *J. Mater. Sci.* **44,** 6213–6222 (2009).

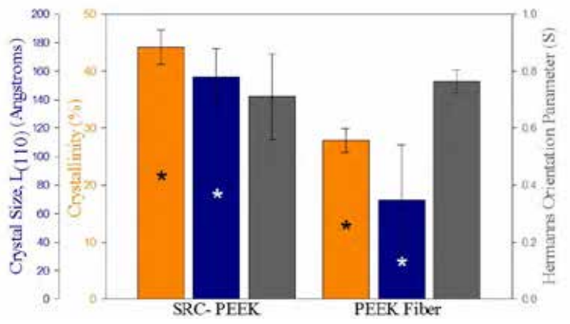

Figure 1: Structural parameters for SRC-PEEK and PEEK fiber as calculated from WAXS. Crystallinity is represented by orange bars, crystal size by blue, and hermanns orientation parameter by grey. * denotes significant differences ($p < 0.05$).

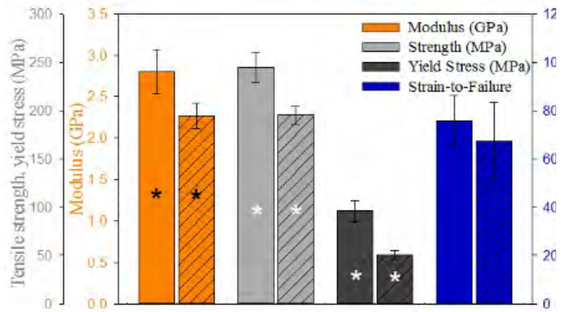

Figure 2: Mechanical properties of SRC-PEEK (solid bars) and PEEK Fibers (hashed bars). * denotes significant differences in properties between SRC-PEEK and PEEK Fibers ($p < 0.05$).

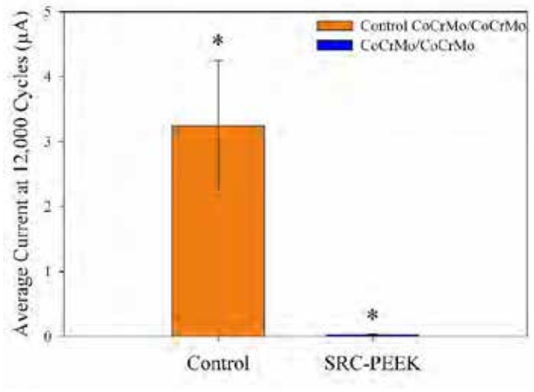

Figure 3: Electrochemical performance of SRC-PEEK compared to CoCrMo-Ti6Al4V control. Currents at 12,000 cycles are significantly lower in SRC-PEEK lined samples than controls.

Development of a Peek-Ceramic Cervical Disc

Hovda, DC[1]
[1]Simplify Medical, Inc., Mountain View, CA, USA
dhovda@simplifymedical.com

Introduction: The Simplify™ Disc is a cervical artificial disc manufactured from PEEK endplates and a mobile alumina matrix composite core that is indicated in skeletally mature patients for spinal arthroplasty for cervical degenerative disc disease with related pain at one level from C3-C7. The PEEK endplates have a plasma-sprayed titanium coating. The articulating surfaces on the endplates have a concave surface and the core has two convex surfaces. These components assemble in such a way as to allow physiological rotation as well as translation in both anteroposterior and lateral directions. Superior and inferior endplates are available in multiple footprints, thicknesses, and lordoses to accommodate anatomical variation, but the articulating features are identical and all assemblies use a universal core. In addition to providing motion and height restoration, the Simplify Disc permits subsequent visualization of the anatomy using magnetic resonance imaging (MRI) without the significant radiographic artifact produced by current commercially available discs with metal endplates.

An overview of preclinical and clinical experiences with the Simplify Disc will be presented.

Methods and Materials: To demonstrate structural integrity under expected physiologic loads, ASTM F2346 static and dynamic axial compression and shear compression tests were conducted. A worst-case combination of ASTM F2423 and ISO 18192-1 parameters was used to characterize *in vitro* wear representative of the thinnest endplates under Mode I conditions. Impingement characteristics were also investigated using a combination of solid modeling, finite element analysis, and *in vitro* wear testing. MR safety tests per ASTM F2052, F2213, F2119, and F2182 were also conducted.

The Simplify Disc has been implanted internationally since January 2013. Early implants with minor design differences related to the bone-contacting features were implanted initially.

Results: The results of strength, stability, wear, and impingement tests are summarized in the table below. Preliminary results for dynamic shear compression and Mode I wear studies are presented since these tests are still on-going. Note that the ≤4 mm MRI artifact represents a non-optimized scan, so that minimal artifact is likely under clinical conditions.

Axial compressive strength, static	≥ 10,000 N
Axial compressive strength, fatigue	≥ 1,000 N
Shear compressive strength, static	491 N
Shear compressive strength, fatigue	≥ 123N
Wear (Mode I)	0.9 mg/MC
Impingement (Mode IV)	1.9 mg/MC
Displacement force due to MRI	< gravity
Torque due to MRI	None
Heating due to MRI	< 3°C
Artifact due to MRI in 3.0T field	≤4 mm

Between January 2013 and July 2014, 84 single-level Simplify Discs, Generation 1, were implanted by 18 spinal surgeons internationally. Thirty-one of these patients have passed their one year follow-up, with no explants or re-operations at the index level. An update will be provided on the clinical experience. No adverse safety events related to either disc have been reported. The surgeons reported satisfaction with the ease of implantation, MRI compatibility of the discs, and absence of metal-on-metal wear.

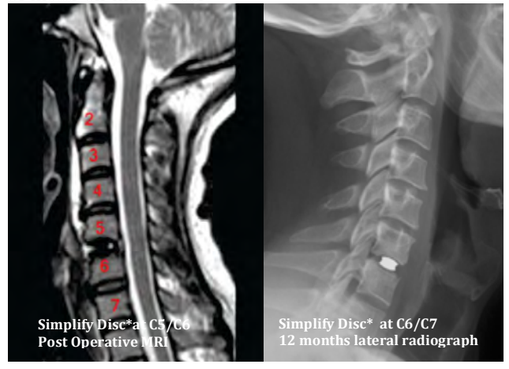

Discussion: The preclinical and clinical results to date for the Simplify Disc are promising. An IDE clinical trial is anticipated in 2015.

*Note: Simplify Disc Generation 1

Evaluation of viscoelastic properties of an oblong PEEK rod construct in a spondylolisthesis reduction model

Julien P, Daniel W, Sasi V
Medtronic Spinal and Biologics, Memphis, TN, USA
sasi.vadapalli@medtronic.com

Introduction: Viscoelasticity is a natural phenomenon occurring in materials and the human body when the stress or strain changes with time to a constant mechanical condition. In the body, this has been observed when the spine slowly shrinks throughout the day under the influence of upper-body weight[1] and disc hydration. In a material, viscoelastic effects are tied to the molecular and chemical structure of the material and is a common property of biological tissues and polymers such as PEEK. Posterior lumbar fusion using pedicle screws and rods is widely used as a treatment for back pain that is unresponsive to conservative management. Since 2006, Oblong PEEK rods (CD HORIZON® LEGACY™, Medtronic, Memphis, TN) have been available to treat patients requiring spinal fusion. Current clinical evidence suggests that when PEEK rods are used as an adjunct to fusion, they offer acceptable clinical outcomes with adequate fusion rates compared to traditional instrumentation.[2] Surgical intervention could cause strain on a patient's bony and muscular structures while instrumenting with pedicle screws and rods. The goal of this bench study was to assess the viscoelastic properties of pedicle screw-rod constructs in a spondylolisthesis reduction model (Fig. 1) to evaluate their short-term response to stress (load) or strain (displacement) from a surgical procedure.

Methods and Materials: Static Creep testing in a simulated Spondylolisthesis reduction model (Fig. 1) was devised following ASTM D2990.[3] Shear load (anterior-posterior, A/P) was applied with a servo hydraulic test frame. The test construct was set in a saline solution maintained at 37 ± 2°C. Literature review indicates that the shear load the lumbar spine experiences in daily living activities is in the ranges of 100N to 2000N. Creep loading testing was carried out with four A/P load levels at 2000 N, 1500N, 1000 N, and 500 N for the Oblong PEEK rod and 1500 N for the 5.5 mm titanium Rod (CD HORIZON® LEGACY™). Relaxation testing was also carried out with displacement levels associated with their respective initial A/P loads at 2000 N, 1500 N, 1000 N, 500 N, and 250 N for the Oblong PEEK rod and at the extremes (1500 N and 250N) for the Titanium rod.

Figure 1: Spondylolisthesis reduction model with PEEK Rod

Results: Figures 2 and 3 provide the responses of the Oblong PEEK rod and Titanium constructs for the various load (creep) and displacement settings (relaxation).

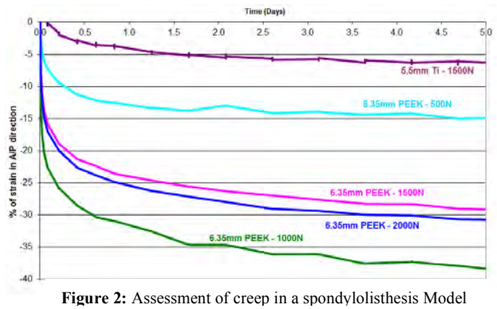

Figure 2: Assessment of creep in a spondylolisthesis Model

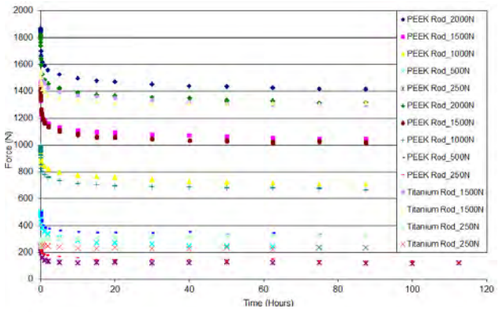

Figure 3: Assessment of relaxation in a spondylolisthesis Model

Discussion: At the various load (creep) and displacement settings (relaxation), the Spondylolisthesis reduction model for both Oblong PEEK rod and Ti Rod constructs reached a new steady state between 2 – 4 days after the initial loading condition. PEEK rods demonstrated the highest change in strain (15%- 39%) for any applied load when compared to titanium rods. The proposed test method captures the viscoelastic behavior of PEEK rods and indicates that PEEK rods adapt to the loading environment.

References: [1]. Eklund JA et al: Shrinkage as a measure of the effect of load on the spine. Spine. 1984 Mar;9(2):189-94.[2]. Mavrogenis AF et al: PEEK rod systems for the spine. Eur J Orthop Surg Traumatol. 2014 Jul;24. [3]. ASTM F2990-09, "Standard Test Methods for Tensile, Compressive, and Flexural Creep and Creep Rupture of Plastics".

Antibiotic Drug Release PEEK Clip to Combat Surgical Site Infection in Spinal Fusion Surgery

A. Sevit,[1] N. Hickok,[2] F. Forsberg,[3] J.R. Eisenbrey,[3] C. Kepler,[2] S. Kurtz,[1]
[1]School of Biomedical Engineering, Science and Health Systems, Drexel University, Philadelphia, PA 19104, USA.
[2]Department of Orthopedic Surgery, Thomas Jefferson University, Philadelphia, PA 19107, USA, and
[3]Department of Radiology, Thomas Jefferson University, Philadelphia, PA 19107, USA
Email: as3437@drexel.edu

Introduction: Surgical Site Infection (SSI) is a devastating outcome of spinal fusion surgery, arising in 8.5% of primary surgeries and 12% of revision procedures [1]. Often SSI is marked by biofilm formation on the implant surface, which because of its antibiotic insensitivity, decreases the success of systemic antibiotics. If possible, the most effective treatment option is a secondary surgery—where the currently infected device is removed and another device is implanted [2].

To eradicate pathogens before adherence to the implant aggressive prophylaxis is critical. By maintaining supra-therapeutic antibiotic levels at the hardware site during the peri-operative period, contaminating bacteria may be eradicated before they progress to a full-blown infection. Currently surgeons pack wound sites with up to 1 g of powdered vancomycin (VAN) prior to suturing. However, the efficacy of this practice is currently unclear. Our goal is to prolong the aggressive prophylaxis, post removal of suture drains, by ultrasound-mediated drug release from an antibiotic containing vessel.

Because of its known biocompatibility the vessel will be manufactured in selective laser sintered (SLS) poly(ether ether ketone) PEEK. Within the clip will be a single reservoir containing VAN. Channels into the reservoir will be sealed with a thin poly(lactic acid) membrane. Once the suture drains have been removed, ultrasound will be applied to the wound site using a standard clinical probe.

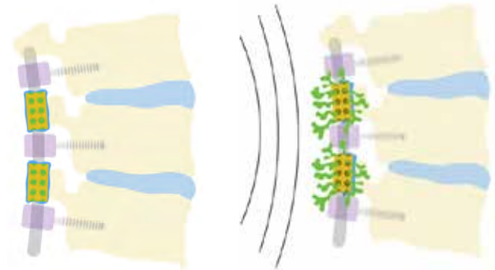

Fig 1. Clips attach posteriorly to the fusion rod, loaded with drug and coated in a PLA membrane. Seven days after surgery, ultrasound is applied to the wound site, rupturing the PLA membrane and releasing the antibiotic to bathe the implant.

As the application of ultrasound is completely non-invasive (unlike injection), it does not contribute to patient suffering. Not only will the application of ultrasound rupture the PLA membrane, releasing the drug into the wound site, sonication will also mobilize adherent bacteria making them more susceptible to antibiotics [3]. This two-pronged attack makes ultrasound an ideal tool for drug-delivery to combat SSI.

Methods and Materials: The device under development is a single-well clip, which interfaces with a standard 5.5 mm spinal fusion rod. Design of the device was done in Solidworks (Dassault Systémes, Waltham, MA). The devices were manufactured in selective laser sintered (SLS) PEEK by Invibio Biomaterial Solutions (Lancastershire, UK).

The manufactured clips were analyzed via µCT (Scanco µCT 80) to verify the accuracy of the dimensions. Four samples were scanned at medium resolution (voxel dimension = 0.02 mm^3) and the dimensions of six critical design aspects were investigated. Data was imported into Analyze 9.0 (Mayo Clinic, Phoenix, AZ) and measurement was performed with the line measure tool. Each measurement was performed three times to mitigate inconsistency in the technique. Measured dimensions were compared to dimensions specified in Solidworks using a single value t-test ($\alpha<0.05$).

Clips were loaded with a mixture of 50 mg of powdered VAN and 5 mg Methylene Blue (MeB) for visualization of release. PLA (MW 60 kDa) was dissolved in Chloroform ($CHCl_3$) at a concentration of 25 mg PLA per mL $CHCl_3$. Two clips were coated in the mixture and left for 24 hours for solvent evaporation. Clips were attached to stainless steel rods (medical grade 316L) and submerged in saline at 22^0 C. After an initial incubation period for 15 minutes ultrasound was applied to one of the coated clips for 15 minutes using a Sonix RP scanner with an L4-9 probe (Analogic Ultrasound, Richmond, BC, Canada) transmitted at 5 MHz and 3 MPa (peak-to-peak) acoustic output pressure. The other was left undisturbed as a control. Release was monitored for 76 hours with aloquats taken at regular intervals. The UV absorption of the mixture at 285 nm was measured via spectrophotometry (Tecan M1000 Pro, Männedorf, Switzerland) to determine the concentration of VAN in solution.

Results: The clip was successfully manufactured in selective laser sintered PEEK. We verified the size of the rod interface by clipping the device onto a retrieved 5.5 mm spinal fusion rod. The device attached easily to the rod with minimal effort, however, it also gripped tightly with no visible gap between the rod and the clip. Ease of attachment is an important feature of the clip so it is easy for the surgeon to use and does not prolong surgery time. On the other hand, while the clip will not bear any load, the fusion rods are known to flex slightly *in vivo*, so it is important that the clip fits securely.

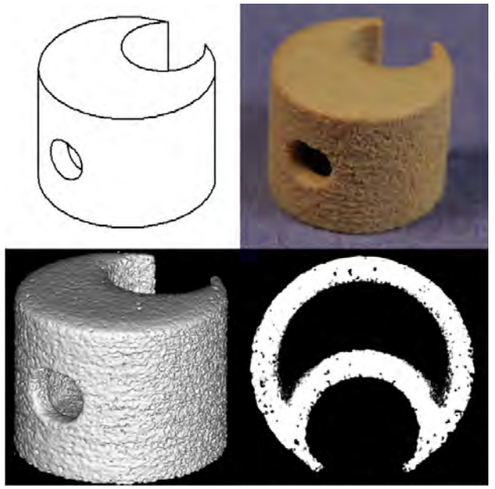

Fig 2. (Clockwise starting from top left) solidworks drawing of the clip, actual device before drug loading and application of PLA membrane, µCT cross section of the clip showing the porosity of the material, µCT rendering of clip.

µCT measurements verified the accuracy of the manufacturing with most critical dimensions measuring within 0.2 mm of their specification. The width of the clip was the least accurate design aspect, measuring 0.32 mm less than the specified dimension. In general the SLS technique generated more accurate vertical dimensions than horizontal dimensions. This is particularly apparent in the drug-delivery hole, which, despite being specified as perfect circle, has a significantly larger diameter measured along the horizontal axis (3.16 mm) than along the vertical axis (3.00 mm).

Design Aspect	Designed (mm)	Measured (mm)
Height	9.00	9.07
Width	12.00	11.68
Wall Thickness	1.50	1.46
Interface Radius	5.70	5.89
Horizontal Hole D.	3.00	3.16
Vertical Hole D.	3.00	3.00

Table 1. Selective Laser Sintering of the device was generally accurate, however, dimensions along the horizontal axis tended to be less accurate than those along the vertical.

Cross sections also revealed the porosity of the SLS PEEK material, which allowed for the diffusion of water across the clip walls. While this makes controlled drug delivery problematic, the solution was to coat the entire device in the PLA membrane.

During the initial incubation period (first 15 minutes) 11 mg of drug leached out of the experimental clip while 3 mg leached out of the control. This was probably drug that mixed with the membrane while it was in a liquid state. Post sonication, a burst release was observed in the experimental clip resulting in 15 mg of drug release over the first hour and 20 mg of drug release over the 76 hour period. The control clip showed only minor release past the initial incubation and a total release of 3-4 mg of drug.

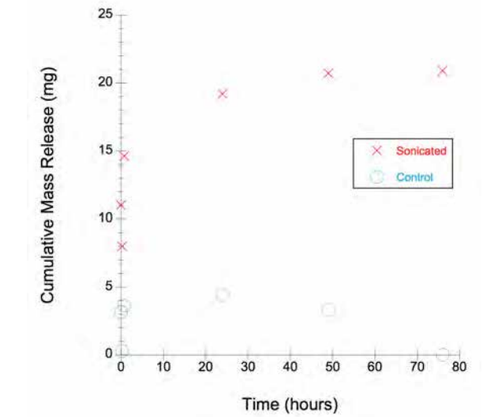

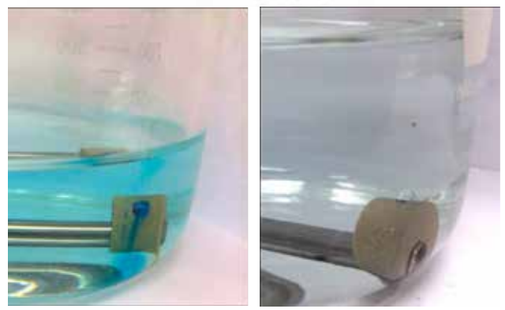

Fig 3. (Top) Release profile of the sonicated an unsonicated clips over a 76-hour release period. (Bottom left) Release of drug from the sonicated clip turns the media blue. (Bottom right) Unsonicated clip showing no release of drug.

Discussion: A PEEK antibiotic delivery vessel has been designed which interfaces with a standard 5.5 mm spinal fusion rod. Although pores were observed in the samples that allow for the passage of water through the clip wall, the PLA membrane held for 48 hours in the unsonicated control, demonstrating completeness of coating. Moreover, response to ultrasound was observed in the experimental clip with greater than 40% release of drug after 76 hours. In future work we will optimize the PLA membrane by coating clips with varying concentrations of PLA. We will also reduce the clip size and wall thickness to optimize the response to sonication.

References:

1. S. Kurtz, et. al. The Spine J., vol. 11, iss. 10, pp. S22-S22, August 2011.
2. M. Ishii, et. al. Glbl. Spn. J., vol. 3, iss. 2, pp 95-101, April 2013.
3. A. Trampuz, et. al., N Engl J Med, vol. 16, pp 654-663, August 2007.

Tribological Studies of PEEK on PEEK Facet Resurfacing Devices

[1,2]Siskey, R; [1]Baykal, D, [3]Dahl, M
[1]Exponent Inc., Philadelphia, PA, [2]Drexel University, Philadelphia, PA, [3]Zyga Technology Inc., Minnetonka, MN
Corresponding author rsiskey@exponent.com

Introduction

The zygapophyseal, or facet, joints are a commonly treated source of back pain, and rates of percutaneous facet joint procedures in older adults have quadrupled since 2002 [1]. Osteoarthritis of the facet is a common cause of pain, and when conservative treatments fail, patients are left with few options for treatment. The facet is a synovial joint and can be resurfaced or augmented with articulating prostheses similar to other orthopedic devices. Devices for this application may require considering alternate biomedical materials which provide durability and compliance under the activities of daily living. Therefore, a tribological study of a facet resurfacing device made from polyetheretherketone (PEEK) was developed and carried out.

Several standards were considered in the development of this protocol. ASTM F2694 and ASTM F2790 provide methods for testing lumbar total facet prostheses. However, total facet prostheses completely remove the pedicles and totally replace the facet joints. Therefore there was no standard test that directly applied to this device. A device-specific test was developed based on these standards that used facet joint-specific load and motion patterns to test the Glyder® Facet Restoration System.

Materials and Methods

Facet loads and motions were identified from published data in literature [2,3]. The facet joint has an average displacement of 4 mm (2 mm standard deviation) at full flexion [2]. To accurately represent a lifetime of motion during the activities of daily living, an eliptical displacement motion of 4 mm by 2 mm has been identified to be representative of the wear path [2, 3]. This wear path is similar to the “circularly translating pin-on-disk” wear path described in Saikko, 1997, which produces a continually changing velocity vector, therefore producing cross shear [4]. According to published data on the normal in vivo forces applied to the facet joint, loads may reach 150 N, but typical loading during normal daily activity is approximately 50 N [5]. A normal load of 68 N was selected to reach a contact pressure of 0.5 MPa.

Test samples were manufactured from PEEK used in the Glyder® system (PEEK OPTIMA™ LT1). The samples were elliptical in shape and had a major axis of 14 mm and a minor axis of 12 mm. The samples were mounted on both the inferior and superior fixtures of an AMTI OrthoPOD and tested for 10 million cycles (Fig. 1). Testing was conducted at approximately 1.0 Hz, and the test was stopped every 0.5 million cycles for fluid exchange and interval analysis. The interval analysis consisted of mass measurement and photo documentation. The bovine serum, with a protein content of 20 g/L, was also subjected to particle analysis per ASTM F1877. Two sets of load soak samples were subjected to only axial load and used to correct for fluid absorption throughout the test.

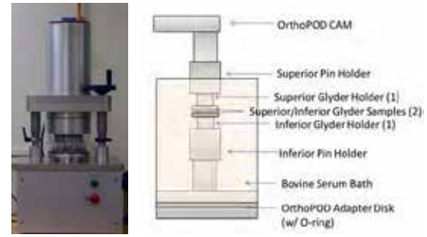

Figure 1. AMTI OrthoPOD (left) and schematics of a single test station schematic (right).

Results

The average mass loss for the Glyder® samples was 2.8 ± 0.9 mg, which represents 1.4 ± 0.4% of the untested samples. Overall, the superior and inferior sample couples, by station, demonstrated an average total mass loss rate of 0.57 ± 0.22 mg/MC. This mass wear rate corresponds to a volumetric wear rate of 0.44 ± 0.17 mm^3/MC (Fig. 2). One device demonstrated an increased wear rate from 5.0 to 5.5 MC. Further inspection of this sample found some increased scratching on the articulating surface, however, it appeared consistent with the wear mechanisms taking place for the entire group of samples. At the end of 10.0 million cycles, no functional failures were observed. The articulating surfaces of the device demonstrated a mild burnished appearance along with linear and elliptical scratches indicative of abrasive and third body wear mechanisms, respectively (Fig 3.). The particle analysis found the particles to range between 0.10 and 19.85 µm. The ASTM F1877 parameters were consistent with the spheroidal smooth particles observed under SEM. EDS confirmed the majority of these particles to be polymeric in nature.

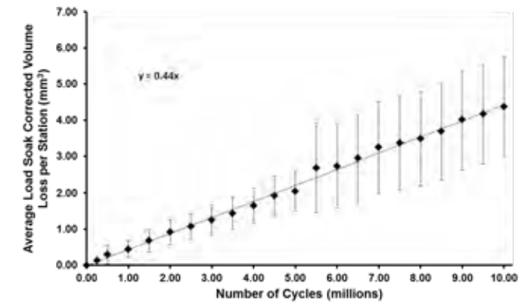

Figure 2. - Average total volumetric loss (mm^3) of six wear stations. Error bars represent ± one standard deviation. Average volumetric wear rate is 0.44 ± 0.17 mm^3/MC.

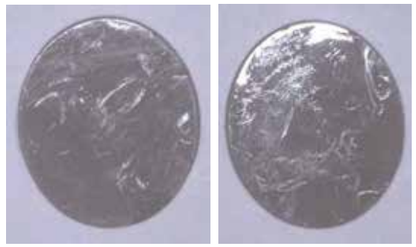

Figure 3. – Photodocumentation of a superior (left) and inferior (right) Glyder test coupons after 10 MC of Mode I testing.

Discussion

Testing revealed the Glyder® samples exhibited burnishing when subjected to loads and motions expected at the facet joint. The PEEK material demonstrated a wear performance consistent with other previously published PEEK tribological studies for spinal devices [6,7]. Grupp, et al. report a wear rate of 1.4 ± 0.4 mg/MC or 1.1 ± 0.3 mm^3/MC for a PEEK-on-PEEK cervical disc. Brown, et al. reported wear rates ranging from 0.27 ± 0.01 to 0.96 ± 0.07 mg/MC or 0.21 ± 0.01 to 0.74 ± 0.05 mm^3/MC for the PEEK on PEEK NUBAC device. Further investigation and standardized protocols for investigating facet resurfacing devices are warranted under both clean (Mode I) and adverse (Mode III) tribological conditions.

Acknowledgements

This research was support by Zyga Technology Inc.

References

1. Manchikanti, et al., Explosive growth of facet joint interventions in the medicare population in the United States: a comparative evaluation of 1997, 2002, and 2006 data, 2010.
2. Kozanek, et al. Range of motion and orientation of the lumbar facet joints in vivo, 2009.
3. Jegapragasan et al. Characterization of articulation of the lumbar facets in the human cadaveric spine using a facet-based coordinate system, 2011.
4. Saikko V. A multidirectional motion pin-on-disk wear test method for prosthetic joint materials, 1998.
5. Niosi et al. The effect of dynamic posterior stabilization on facet contact forces: an in vitro investigation, 2008.
6. Grupp, et al. Alternative bearing materials for intervertebral disc arthroplasty, 2010.
7. Brown, et al. An In Vitro Assessment of Wear Particulate Generated From NUBAC: A PEEK-on-PEEK Articulating Nucleus Replacement Device, 2011.

Evaluation of HA/PEEK material in an ovine cervical fusion model: a pilot study

Walsh, WR[1], Pelletier, M[1], Bertollo, N[1], Christou, C[1], Brady, M[2]
[1]Surgical & Orthopaedic Research Laboratories, Prince of Wales Clinical School, University of New South Wales, Prince of Wales Hospital, Sydney, Australia
[2]Invibio Limited, Hillhouse International, Thornton-Cleveleys, Lancashire, FY5 4QD, UK
W.Walsh@unsw.edu.au

Introduction: For nearly 15 years, PEEK-OPTIMA® Natural, has been utilized in spinal fusion surgeries, predominantly in the form of load-bearing cages. Clinical studies continue to suggest that PEEK-OPTIMA performs as well as, or better than, equivalent interbody fusion devices made of metals or allograft, while providing some distinct clinical advantages[1-3]. This includes mechanical strength, a modulus similar to cortical bone, imaging compatibility, and biocompatibility. In recent years efforts have been concentrated on increasing the osseointegration of PEEK-based devices, leading to the introduction of a number of technologies aimed at controlling the surface interactions at the bone-implant interface. A potential limitation of some technologies, especially titanium plasma spray coatings, is the inability to coat all surfaces of an interbody device, including the walls surrounding the graft space; thereby limiting the available area for bone on growth. Bulk incorporation of osteoconductive materials including hydroxyapatite (HA) into the PEEK matrix is one potential solution to this problem, and ensures all machined surfaces of a final device have the potential for enhanced bone on-growth. PEEK-OPTIMA® HA Enhanced is one such material in which HA has been fully dispersed in the PEEK matrix. This HA-PEEK biomaterial has previously demonstrated enhanced bone apposition within 4 weeks compared with PEEK-OPTIMA Natural in a long bone sheep model[4].
The current pilot study aims to compare the *in vivo* response to PEEK-OPTIMA HA Enhanced, PEEK-OPTIMA Natural and allograft interbody spacers in a more challenging ovine cervical fusion model.

Methods and Materials: Cervical interbody fusion devices of identical design were machined from PEEK-OPTIMA Natural, PEEK-OPTIMA HA Enhanced or allograft bone. Twenty-five fully mature female sheep were randomly assigned to three test groups to undergo cervical fusion at two non-adjacent spinal levels (C2-C3 and C4-C5): PEEK-OPTIMA HA Enhanced vs. allograft, PEEK-OPTIMA Natural vs. allograft, or PEEK-OPTIMA HA Enhanced vs. PEEK-OPTIMA Natural. Locally harvested bone saturated with autogenous bone marrow aspirate was used to fill the central cavity of the interbody fusion devices, and supplemental anterior plate fixation was also applied. The outcome measures, including micro computed tomography (micro CT) and histological assessment of the operated levels were evaluated at 6, 12, and 26 weeks following surgery. A semi-quantitative grading scale was used to assess new bone formation in the fusion as well as the device surfaces, the quality of new bone formation bridging in the fusion as well as the device surfaces, and the degree of direct bone-device contact.

Results: The biocompatibility of PEEK-OPTIMA HA Enhanced was supported by this study, and all of the implant materials were well tolerated. Both PEEK-OPTIMA Natural and PEEK-OPTIMA HA Enhanced devices remained structurally intact throughout the implantation periods. In contrast, there was significant resorption of the allograft implants, and fracture of the devices was evident as early as the six-week time point. In total, 6 of the 13 (46%) allograft implants fractured during the implantation period.
Allograft devices showed a high degree of new bone formation and incorporation into the surrounding bone. This was countered however, by the high degree of resorption and mechanical instability, leading to fracture.
Upon histological examination, the local bone inside the PEEK-OPTIMA HA Enhanced devices appeared to be more robust at 6 and 12 weeks compared to the local bone inside the PEEK-OPTIMA Natural devices at the same time points. These differences were less evident at 26 weeks, but remained suggestive of a superior result for graft in the PEEK-OPTIMA HA Enhanced devices compared to PEEK-OPTIMA Natural (Figure 1).

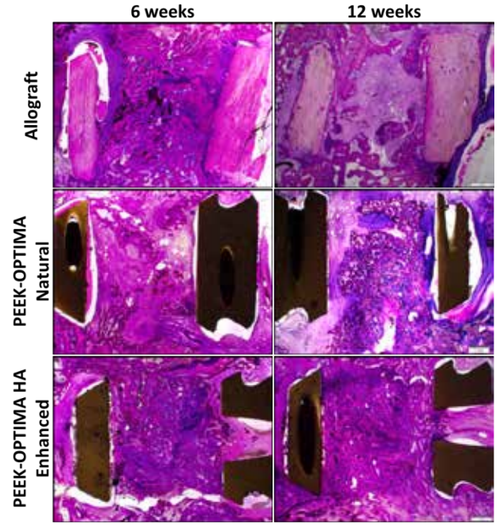

Figure 1: *Histological comparison between allograft, PEEK-OPTIMA Natural and PEEK-OPTIMA HA Enhanced demonstrates the status of the graft material inside the devices over time.*

Micro CT analysis did demonstrate that new bone formation was greater with the PEEK-OPTIMA HA Enhanced devices compared with PEEK-OPTIMA Natural at six weeks. The quality of new bone bridging between the vertebral bodies and contributing towards fusion also appeared to be superior in the PEEK-OPTIMA HA Enhanced group compared with PEEK-OPTIMA Natural, at both the 6 and 12 week time points (Figure 2). Finally, from the micro CT analysis, there was a trend towards greater direct bone contact with the PEEK-OPTIMA HA Enhanced devices compared with PEEK-OPTIMA Natural, and this was more evident at the early time points.

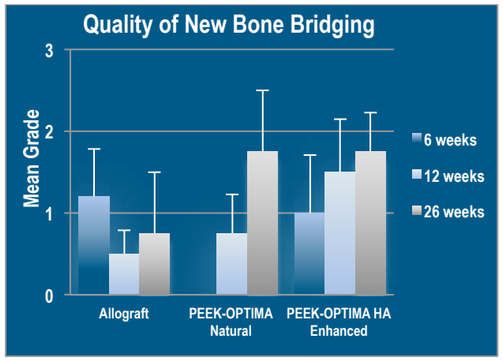

Figure 2: *Micro CT analysis of the quality of new bone formation bridging in the fusion.*

Discussion: Histological comparison between allograft, PEEK-OPTIMA Natural and PEEK-OPTIMA HA Enhanced demonstrates the status of the graft material inside the devices over time. This cervical interbody fusion model represents a complex and challenging setting for the evaluation of new materials. The previous long bone study was the first step in demonstrating the potential of PEEK-OPTIMA HA Enhanced in enhancing bone ongrowth, and providing a more favourable local environment for bone compared with PEEK-OPTIMA Natural[4]. The long bone model is limited by the fact that there is no movement between the bone and the implant surface, and the implants are not under load. In contrast, the cervical fusion model is a more demanding and dynamic environment, with implants under load and motion between the vertebral bodies and the device endplates.

The current study builds on the findings of the long bone model, in which enhanced bone on-growth was demonstrated, and supports the notion that PEEK-OPTIMA HA Enhanced provides a more favourable environment than PEEK-OPTIMA Natural or allograft bone in a cervical fusion setting, providing an osteoconductive surface on all faces of a device.

References:

[1] Chou, Y.C., *et al*. J Clin Neurosci, 2008.
[2] Lied, B., *et al*. BMC Surg, 2010.
[3] Chen, Y., *et al*. Eur Spine J, 2013.
[4] Pre-clinical study in an ovine bone defect model. Data on file at Invibio. This has not been correlated with human clinical experience

A Novel PEEK Titanium Structural Composite for Spinal Devices

Fang, S[1]
[1]Orthofix Inc, Lewisville, TX, USA
samfang@orthofix.com

Introduction: Thermoplastic PolyEtherEtherKetone (PEEK) is a commonly used material for spinal devices due to its excellent chemical and mechanical properties such as biocompatibility, radiolucency and low elastic modulus. However, as a bio-inert material, PEEK also prevents bony integration with adjacent bone tissues upon implantation, a hindrance when used for spinal fusion surgery. To overcome this shortcoming, a novel PEEK Titanium Structural Composite (PTSC) was developed. Utilizing both emerging additive manufacturing technology (3D printing) and traditional plastic injection molding method, the PTSC is manufactured by combining porous titanium and PEEK material together to improve bioactivity of PEEK while maintaining its biocompatibility, radiolucency and low elastic modulus. In this paper, the structure and manufacturing method of PTSC were introduced. In addition, the results of the imaging and mechanical characterization of PTSC and its applications in spinal device were also presented.

Methods and Materials: PTSC has a four layered structure as illustrated in Fig 1. The porous titanium layer has a designed 3D porous microstructure that has potential for bone ingrowth and also provides a rough surface to increase initial implant stability. The PEEK/Titanium inter-digitation layer has an array of dove tail groves locking PEEK and porous titanium layer together. A thin solid titanium membrane layer also exists between porous titanium layer and PEEK/titanium inter-digitation layer to prevent PEEK overflowing into the porous titanium layer during injection molding process.

Fig 1. Schematic of PTSC four-layered structure

The manufacturing of PTSC starts with manufacturing of titanium plate containing porous titanium layer, solid membrane and the layer with dove tail grooves using an additive manufacturing method (selective laser melting). This emerging additive manufacturing method is capable of creating complex macro (overall) geometry as well as micro structure such as pores and dove tails, making it ideal for manufacturing PTSC titanium plate. Once the titanium plate is finished, the plate is then injection molded with PEEK to form PTSC.

To characterize the PTSC, a cervical interbody device (Orthofix CONSTRUX Mini PTC™) utilizing PTSC was developed. As shown in Fig 2, it has a PEEK core with two PTSC end plates on its inferior and superior surfaces.

To understand PTSC's performance under medical imaging, the device was implanted in a cadaver and a serious of images was taken under both X-ray and CT machines. In addition, a battery of mechanical testing was also conducted to investigate the mechanical performance of the device with PTSC and the results were compared with that of PEEK device. The testing was conducted following ASTM F2077 standard and FDA's guidance.

Fig 2. Spinal interbody utilizing PTSC (left) and detailed view of its PEEK/Titanium inter-digitation layer (right)

Results: The following pictures show typical imaging performance of PTSC. It can be seen that the device with PTSC is radiolucent at its PEEK core while its titanium end plates are visible which is necessary for evaluation of the device location and also eliminate the need for tantalum makers commonly used in PEEK devices.

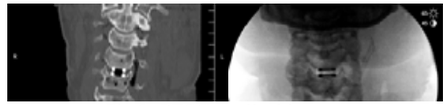

Fig 3. PTSC medical images

Fig 4 shows the comparison of the normalized yield loads between device made of PEEK and that made of PTSC. All data indicated that the PTSC device performers significant better than the PEEK device.

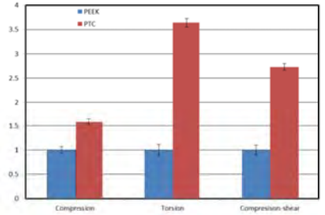

Fig 4. Mechanical testing results comparison

Discussion: Comparing with traditional monolithic PEEK material, PTSC is bioactive and it maintains PEEK's advantages such as radiolucency. Unlike commonly used plasma sprayed titanium coating used for PEEK devices, the PTSC is a composite structure that has a much thicker porous titanium layer with designed 3D porous microstructure which may be beneficial for clinical applications in which bony ingrowth is needed.

A computational investigation into the use of carbon fibre reinforced PEEK laminates for orthopaedic applications

E.A Gallagher[1], C.M. Ó Brádaigh[2], J.P. McGarry[1]

[1]Dept. of Biomedical Engineering, National University of Ireland Galway, Ireland
[2]School of Engineering, University College Cork, Ireland

Introduction

Stress shielding is a well-documented side effect of stiff metallic orthopaedic implants; they can also cause artefacts with MRI and CT imaging [1&2]. Polyetheretherketone (PEEK) is now broadly accepted as a suitable alternative to metal for spinal implants [3]. The addition of continuous unidirectional carbon fibres (CFs) to PEEK allows laminates to be designed with customised anisotropic properties, providing mechanical advantages over homogenous metal osteosynthesis implants (e.g. potentially decreasing stress shielding). In this study finite element models are developed to analyses the mechanical performance of CF/PEEK laminated fracture fixation plates for the distal radius under multi-axial physiological loading. Traditional titanium plates and unreinforced PEEK plates are also analysed for comparison. .

Reliable design of CF/PEEK implants requires a fundamental understanding of micro-scale failure mechanisms. A multi-scale modelling strategy is used to determine device failure due to micro-scale debonding of CFs from the surrounding PEEK matrix under physiological loading. A coupled cohesive zone model (CZM) is used to simulate mixed-mode fracture at the fibre-matrix interface [4].

Methods

Macro-scale analyses

Laminated composite plate designs are developed using a variety of different layups and ply orientations. Finite element models of distal radius fixation plate geometries are subjected to the physiological loading experienced in the radius, i.e. combined bending (4.9Nm) and torsion (0.68Nm) [5, 6] (Fig. 1A). In this study results are presented for two laminated plate designs:

Laminate 1 [0°/0°/90°/0°/90°/0°/90°/-45°/45°]s
Laminate 2 [90°/0°/90°/45°/90°/0°/-45°/0°/0°]s

Simulations are also performed for a homogeneous unreinforced PEEK fracture plate and for a homogeneous titanium fracture plate.

Micro-scale analyses

Representative volume elements (RVEs) with varying fibre volume fractions (20%, 40% and 60%) were modelled in the commercial FE code ABAQUS 6.10. A python script was developed, which disperses the fibres randomly throughout the polymer matrix. Periodic boundary conditions were applied to the RVE. The CZM is implemented via a user defined interface (UINTER) subroutine to capture the fibre-matrix interface debonding.

Results

The strain distributions in the four material configurations are shown in Fig. 1B. The deformation of the PEEK plate (34% strain) is considerably higher than the other three plates (~2% strain). The maximum computed strains in the laminate plate designs exceed the longitudinal tensile failure strain of CF/PEEK (1.58%), with maximum strains of 2.2% and 2.7% being computed for laminate 1 and laminate 2, respectively.

Micro-scale models reveal distinctive shear bands for microstructures with 60% fibre volume fraction. Significant stress localisation is computed in regions of highly clustered fibres. Such stress localisation leads to the initiation of fibre debonding, even at low levels of applied strain (Fig. 1C).

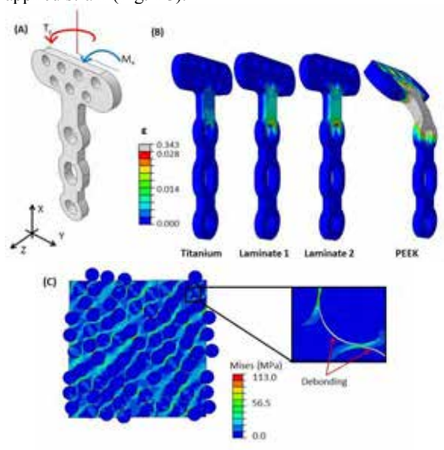

***Fig. 1: A)** Plate geometry and applied loading; **B)** Strain distributions in the titanium plate, laminate 1, laminate 2 and the homogeneous PEEK plate; **C)** 60% RVE model under transverse shear illustrating the fibre-matrix debonding*

Discussion

Simulations demonstrate the significant challenge in the design and optimisation of fibre reinforced laminated composites for orthopaedic applications. Macro-scale models of distal radius fixation plates reveal that unreinforced neat PEEK implants are excessively compliant. In contrast CF/PEEK laminated implants, if correctly designed, can support physiological multi-axial loading without excessive deformation. Careful laminate design will limit the stress concentrations around the screw holes, minimizing the possibility of screw pull out. The elimination of material failure in the region of the screw holes is critically important if CF/PEEK laminates are to be considered as an alternative to metal fixation plates.

Micro-mechanical analyses suggest that a high fibre density may result in significant micro-structural stress localisation and fibre-matrix debonding, reducing the effective strength and stiffness of the implant.

References

[1] Li, C., *et al*, Biomaterials, 23: 2002. **[2]** Rohner, B., *et al*, Vet Comp Orthopaed, 18: 2005. **[3]** Kurtz, S.M., *et al*, Biomaterials, 28: 2007. **[4]** McGarry, P., *et al,* J Mech Phys Solids, 63: 2014. **[5]** Christen, P., *et al*, J Biomech, 46: 2013. **[6]** Hirahara, H., *et al*, J Hand Surg-Am, 28: 2003.

Acknowledgements: The Irish Research Council

Seeing Is Believing: Treatment Of Proximal Humerus Fractures Using A Novel Radiolucent Implant And Its Effect On Reduction Accuracy, Healing Rate, And Functional Outcome

David J. Hak[1], Cyril Mauffrey[1], Todd Oliver[2]
1. Denver Health / University of Colorado, Denver, United States
2. Columbia Orthopedic Group, Columbia, United States
david.hak@dhha.org

Introduction: The development of locked implants has markedly improved our ability to obtain fixation in proximal humerus fractures, however complication rates remain substantial. Recently, a radiolucent carbon fiber plate with a low modulus of elasticity has become commercially available for management of proximal humerus fractures. The purpose of this study was to review the reduction accuracy, healing rate, functional outcome, and complications of a series of patients treated with a novel radiolucent carbon fiber plate.

Methods and Materials: We retrospectively reviewed 17 displaced proximal humerus fractures in 16 patients treated by ORIF using a novel radiolucent carbon fiber proximal humerus plate. The average patient age was 57 years (range 25 – 96 years). The injury mechanism was low-energy (fall from standing) in 8 patients, and high-energy in 8 patients (3 motorcycle collisions, 2 motor vehicle collisions, 2 struck pedestrians, and 1 fall from 25 feet). Two high-energy fractures were type II open while the remainder were closed fractures. There were seven 2-part fractures, eight 3-part fractures, and two 4-part fractures. Three cases were lost to follow-up. The average follow-up of the remaining patients was 6 months. Radiographs, operative data, and post-operative data were analyzed.

Results: The average total operative time was 117 minutes and the average total fluoroscopic imaging time was 81 seconds. A deltopectoral approach was used in 15 cases, while 2 were fixed using a deltoid split. The average number of screws inserted into the humeral head was 7 (range 6 – 9) and all but one plate was secured to the shaft with 3 bicortical screws. Adjunctive calcium phosphate cement was injected into the humeral head in 4 cases. Reduction accuracy was assessed as anatomic or near-anatomic in 14 cases, while in 3 cases there was either a varus or extension malreduction. The radiolucent plate permitted excellent intra-operative reduction visualization, but the deforming forces precluded an anatomic reduction in these cases. There was no loss of fixation or implant failure. Humeral head settling with secondary screw penetration was seen in only 1 case, a 65 woman with known osteoporosis in whom the humeral head fixation was supplemented with calcium phosphate cement. All fractures united. The progression of fracture healing could be easily observed on the lateral radiographs, since the plate did not obscure the ability to see the anterior and/or posterior cortex. There were no post-operative infections. One patient, who suffered a loss of tuberosity fixation, failed to recover satisfactory range of motion.

Discussion: The radiolucent carbon fiber plate offers advantages in fixation of proximal humerus fractures. It's radiolucent property permits more accurate assessment of fracture reduction and healing. The plates low modulus of elasticity may be beneficial in achieving fracture union and minimizing settling with secondary screw penetration. Our preliminary experience with this novel implant is very favorable for the management of displaced proximal humerus fractures.

PEEK Bone Plate Structures for Mandibular Fracture Fixation

Lovald, ST[1], Jaekel, D[1], Kurtz?
[1]Exponent, Inc., Menlo Park, CA, USA
slovald@exponent.com
djaekel@exponent.com

Introduction: Rigid internal fixation allows an early return to form and function for human mandible fractures. Although generally accepted as successful, plate removal rates associated with complications have been reported in up to 30% of treated patients.[1-3] For any form of rigid internal fixation, metallic bone plates can create an environment which the patient is susceptible to stress shielding and refracture, infection, thermal sensitivity, and artifacts during radiographic evaluation. Another problem which is less reported is the issue of asymmetric fixation due to the stiff bone plate being applied to a single side of the bone surface. This may cause splaying of the fracture on the unsupported lingual side.[4] Bone plates made of PEEK could provide an alternative fixation option which may mitigate some of these risks. In particular, PEEK bone plates could potentially reduce stress shielding effects, allow a more even stress distribution through the fracture callus, as well as provide enhanced radiographic visualization during implantation and at post-operative evaluation.

The use of polymer based materials for fracture fixation has been limited due to a belief that polymer materials do not provide adequate stiffness during the early postoperative period. For any bone fracture, if fracture callus deformation exceeds a small tolerance, new tissue cannot form to bridge and calcify the fracture.[5] Historically, the thickness of the bone plate could be increased to make up for lost stiffness, though there are drawbacks to thicker bone plates, including increasing risks for palpability, as well as hindering the ability of the surgeon to contour the plate to the patient bone surface. PEEK is an ideal polymer candidate material due to the greater strength (on a per mass basis) than many metals and an elastic modulus (4-20 GPa) that can be tailored to that of cortical bone.[6] The purpose of the current study is to use a mandibular finite element (FE) model to determine a safe and feasible PEEK fracture fixation system which provides the same amount of fixation stability as that of commonly used titanium plate.

Methods and Materials: An FE model of a human mandible was created for the purpose of designing and optimizing a PEEK bone plate to fixate fractures of the mandibular body region. Mandibular geometry was segmented from computed tomography data from a 22-year-old man with full dentition and normal occlusion (Mimics, version 7.3, Materialise, Ann Arbor, MI). Boundary conditions were applied representing bite forces for a unilateral molar clench, an incisal load, and a unilateral canine load.[8,9] The fracture was created as a 1-mm-thick bony callus region in the body region. The material properties of initial connective tissue were used for the bony callus fracture region (E=3 MPa,v=0.4)[7]. An x-shaped truss-style bone plate was used to fix the fracture using 8 solid cylinder screws embedded and perfectly bonded in the bone (Figure 1). The bone plate was designed material properties for 30% (w/w) chopped carbon fiber reinforced PEEK (E=20 GPa).

An alternate model with the same conditions was created substituting the PEEK plate for a titanium strut-style matrix miniplate.

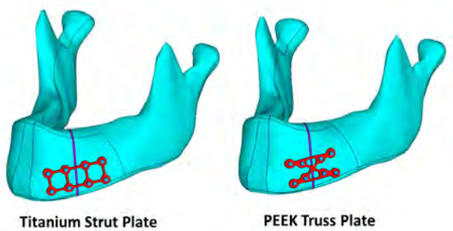

Figure 1. FE analysis compared a traditional strut style plate

The performance of the PEEK plate was tailored to be equal to the titanium strut plate. The methodology used a novel design process comprised of the following stages: *1*) shape optimization, *2*) design parameter optimization analyses, and *3*) biomechanical comparison to standard bone plates. Results of interest in the model included the principal strains in the callus region and peak stresses in the fixation plates. ANSYS 11.0 (ANSYS, Canonsburg, PA) was used for all FE analyses.

Results: The ideal structure which can provide maximum fixation stiffness with a minimum amount of implanted materials was determined in a previous study using a topological optimization routine (Figure 2).[6] An x-shaped truss-style bone plate has been reported to provide superior fixation strength during incisal, canine, and molar loading compared to similarly sized tension bands and strut-style matrix plates which have been used for decades.

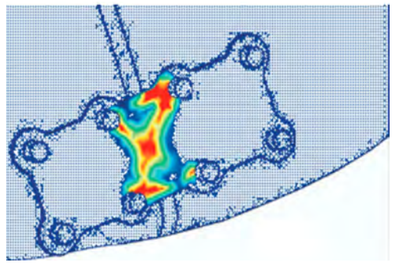

Figure 2. Density plot output from a topological optimization analysis for a mandibular body fracture. The density plot shows the ideal structure (in red, density=1) to stabilize this particular fracture.

Under the common bite loads the model determined that a PEEK bone plate with a thickness of less than 1.35 mm and a similar footprint could provide the same amount of fixation stability as a currently marketed strut-style titanium miniplate (1.0 mm thickness).

Discussion: This study optimized a truss-style mandibular body fracture plate manufactured from carbon fiber reinforced PEEK to provide the same functional mechanical properties of a currently marketed titanium strut miniplate. For years, mandibular bone plate designs have been tested and compared according to simple in-plane and out-of-plane bending models, which has encouraged the use of basic linear reconstruction and band plate designs. Recent work[4,6] has shown that mandibular fracture biomechanics are more complex than has been represented in traditional testing methodologies; in particular, there is a significant amount of shearing in the fracture plane which is not adequately captured using historical bending tests. The use of complex numerical models provides an opportunity to alter and optimize the structure of bone plate designs for specific anatomical regions.

The increase in thickness of the PEEK plate was within 35% of its titanium counterpart and is well within the normal ranges of available plate thicknesses. This is a promising outcome, considering the PEEK formulation considered has less than 20% the stiffness of titanium. The results suggest that bone plates comprised entirely of PEEK materials can provide a safe environment for fracture healing in the mandibular body. Smarter design processes which incorporate the techniques presented here could usher in the use of softer polymer materials as the primary material of fixation constructs. The methods developed in this study may be adapted for other trauma applications.

[1. Bhatt V, Langford RJ. Removal of miniplates in maxillofacial surgery: University Hospital Birmingham experience. *Journal of oral and maxillofacial surgery : official journal of the American Association of Oral and Maxillofacial Surgeons.* May 2003;61(5):553-556.

2. Murthy AS, Lehman JA, Jr. Symptomatic plate removal in maxillofacial trauma: a review of 76 cases. *Annals of plastic surgery.* Dec 2005;55(6):603-607.

3. Lamphier J, Ziccardi V, Ruvo A, Janel M. Complications of mandibular fractures in an urban teaching center. *Journal of oral and maxillofacial surgery : official journal of the American Association of Oral and Maxillofacial Surgeons.* Jul 2003;61(7):745-749; discussion 749-750.

4. Lovald S, Baack B, Gaball C, Olson G, Hoard A. Biomechanical optimization of bone plates used in rigid fixation of mandibular symphysis fractures. *Journal of oral and maxillofacial surgery : official journal of the American Association of Oral and Maxillofacial Surgeons.* Aug 2010;68(8):1833-1841.

5. Prein J. Anatomic Approaches. In: Prein J, ed. *Manual of Internal Fixation in the Cranio-Facial Skeleton*. Berlin: Springer Verlag; 1998:51-56.

6. Lovald ST, Wagner JD, Baack B. Biomechanical optimization of bone plates used in rigid fixation of mandibular fractures. *Journal of oral and maxillofacial surgery : official journal of the American Association of Oral and Maxillofacial Surgeons.* May 2009;67(5):973-985.

Biomechanical Performance of Shape-Memory PEEK Soft Tissue Fixation Devices

Smith, KE[1], Safranski, DL[1], Griffis, JC[1], Gall, K[2]
[1]MedShape, Inc., Atlanta, GA, [2]Georgia Institute of Technology, Atlanta, GA
ken.gall@mse.gatech.edu

Introduction: Over 2 million soft tissue repair procedures are performed each year, including 400,000 anterior cruciate ligament (ACL) reconstructions and 50,000 biceps tenodesis procedures[1,2]. In over 50% of ACL reconstructions, soft-tissue grafts replace the torn ACL[1]. Securing soft tissue to bone is necessary for proper healing and joint stability. Interference devices are used to create a friction fit between soft tissue, bone, and effectively compress soft tissue by generating a radial force during insertion. Shape-memory polymers are mechanically active materials that change shape in response to a stimulus, such as heat, water, or mechanical force[3]. Shape-memory PEEK Altera® allows for the creation of medical devices that can expand *in situ*. The objective of this study was to compare the biomechanical performance of a shape memory PEEK fixation device with metal and polymer-based interference devices in two clinical applications: ACL reconstruction and tenodesis.

Methods and Materials: ACL Tibial Interference devices: The following devices were used in this study: 9 x 25 mm RCI metallic interference screw (Smith and Nephew), 9 x 23 mm PEEK interference screw (Arthrex), 30 mm Intrafix tibial polyethylene sheath with 7-9 mm PLLA screw (Depuy Mitek), 9 x 30 mm ExoShape PEEK sheath-and-bullet device (MedShape). Resultant force: A custom test setup was mounted in an Instron test machine (#5567, 5kN) to measure the resultant normal force generated upon device insertion, a measurement of radial force[4]. Synthetic bone blocks (Sawbone, 20 PCF) were machined in half along with a centered 10 mm hole. Bovine extensor tendons (Animal Technologies), sized to 8 mm, were whip-stitched together for 30 mm and each free end was individually sutured 20 mm using size #2 braided polyester fiber sutures (Ethicon). Each device was inserted according to manufacturer's recommendations with manual tension of the tendons into the synthetic bone blocks and the load was measured as a function of time (n=5/device). F_{RMAX} was defined as the maximum resultant force and F_{RF} was defined as the final resultant force after 10 minutes post-fixation. ACL Pull out strength: Synthetic bone blocks with a 3 mm fiberglass layer were used. A 10 mm tunnel was drilled at 30° to the cortex. For porcine tibia (Animal Technologies), a 9 mm hole was drilled from the original ACL footprint to the medial surface of the tibia using a drill guide. As previously described, whip-stitched tendons were passed into the synthetic bone blocks or porcine tibia and fixated with each device. Synthetic bone blocks and tibiae were mounted to custom clamps and the free tendon ends were secured to custom soft-tissue clamps (Instron 5567). The tendon was pre-loaded to 5N, then pulled to failure at 50 mm/min (n=10/device). Pullout out strength was defined as the maximum load.

Tenodesis Interference Devices: Eclipse Soft Tissue Anchors (9x20mm, 4x10mm) (MedShape) and Bio-Tenodesis Screw (9x23mm, 4.75x15mm) (Arthrex) were used. Tunnels were drilled in synthetic bone block (10 pcf with 20 pcf cortical layer) to the match the size of the devices. Bovine extensor tendons were sized to match the device size and inserted into the tunnel along with the device. Pullout strength was measured following the previous procedure. One-way ANOVA with Tukey's post-hoc tests was performed ($p<0.05$). Pullout strength was plotted against F_{RMAX} and regression analysis performed to determine correlation and Pearson coefficient.

Results: Representative curves of resultant force generated during device insertion are shown in Figure 1 for ACL interference devices. Each device displayed a maximum resultant force upon full insertion. The curves for the RCI and PEEK screws had a jagged shape, while the curves for the Intrafix and ExoShape showed a two-stage response. After full insertion, the force decreased for each device. Figure 2 provides the values for F_{RMAX} and F_{RF} for each device. Overall, the F_{RF} increased as the F_{RMAX} increased. The F_{RMAX} and F_{RF} of both Intrafix and ExoShape were significantly greater than the RCI and PEEK screws. The F_{RMAX} of ExoShape was significantly greater than Intrafix's F_{RMAX}.

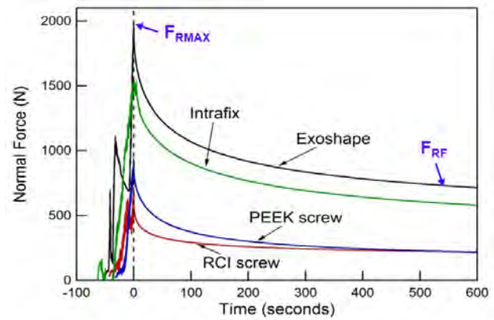

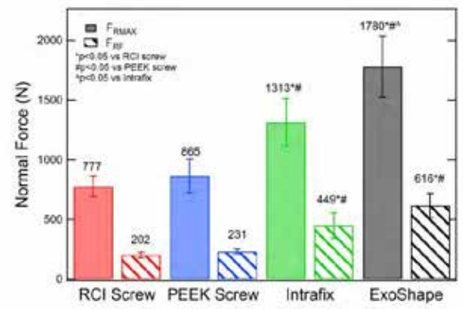

The pullout strengths in both synthetic bone block and porcine tibia are given in Table 1 for ACL interference devices. Both ExoShape and Intrafix had significantly greater pullout strength than the RCI screw and PEEK screw. The Pearson correlation coefficient of pullout strength vs F_{RMAX} was 0.89 with a p value of <0.001. The pullout strength of tenodesis fixation devices in synthetic bone block is given in Table 2. The shape memory PEEK devices show higher average pullout strengths than screw devices for a given comparable device size.

Table 1. Pullout Strength for ACL Fixation Devices

	Synthetic (N)	Porcine (N)
RCI Screw	883±125	1024±102
PEEK Screw	716±249*	696±143*
Intrafix	1147±142*#	1332±133*#
ExoShape	1233±190*#	1254±246*#

*p<0.05 vs RCI Screw. #p<0.05 vs PEEK Screw

Table 2. Pullout Strength of Tenodesis Fixation Devices

	Synthetic (N)
Eclipse Soft Tissue Anchor 9 x 20 mm	443±49
Arthrex Bio-Tenodesis Screw 9 x 23 mm	354±98
Eclipse Soft Tissue Anchor 4 x 10 mm	115±28
Arthrex Bio-Tenodesis Screw 4.75 x 15 mm	80±24

Discussion: The results suggest that the resultant force generated during interference fixation is device dependent even with devices of similar size. This work showed that expandable sheath-based devices, such as ExoShape, are able to generate higher radial force and display less graft relaxation post-fixation compared with screw devices. Analysis revealed a positive correlation between resultant force and pullout strength for the devices. After full insertion, tendon relaxation occurs, thus the resultant force decreases. The devices with higher F_{RMAX} are able to sustain higher F_{RF} during the tendon relaxation. Screw devices have limited contact area due to threads, which reduces radial force. The sheath-based devices expand radially allowing for a higher degree of circumferential compression of the graft, and increased contact area is suggested to enhance graft-to-bone healing[5]. The ACL interference devices fixate two grafts, while the tenodesis devices fixate a single graft in a bone tunnel. The tenodesis devices must effectively fixate to both the bone tunnel and the graft. The shape-memory expansion of the ExoShape and Eclipse devices allow for an increase in device size within the tunnel, thus a higher pullout strength than the screw devices. Shape-memory PEEK fixation devices show increased pullout strength due to increased normal force from the expanding contact area.

References:

1. Millennium Research Group. U.S. Market Ortho. 2009.
2. Millennium Research Group. U.S. Market Ortho. 2012.
3. Yakacki CM. Polymer. 2011. 52. 4947-4954.
4. Smith KE. Knee. 2012. 19: 786-792.
5. Nagarkatti DG. Am J Sports Med. 2001. 29:67-71.

Acknowledgements: This work was supported by the National Science Foundation (#750247) and Solvay Advanced Polymers.

The Use of PEEK-on-UHMWPE and CFR-PEEK-on-UHMWPE as a Bearing Combination in Total Knee Arthroplasty

TS Adesina, S Ajami, MJ Coathup and GW Blunn[1]
[1]John Scales Centre for Biomedical Engineering, Institute of Orthopaedics and Musculoskeletal Sciences, Division of Surgery and Interventional Science, UCL. The Royal National Orthopaedic Hospital, Stanmore, UK.
temitope.adesina.12@.ucl.ac.uk

Introduction

Modulus mismatch with subsequent stress shielding, wear induced aseptic loosening and metal ion release generated by metal-on-metal bearings are all significant causes of failure in joint arthroplasty. To improve survivorship, the use of low modulus materials may be a suitable alternative to hard bearing prostheses. Due to its favorable mechanical properties and clinical success when used in spinal surgery and in some prosthetic hip applications there is considerable research interest in the use of polyetheretherketone (PEEK) as a bearing surface in an all polymer total knee arthroplasty (TKA). Reported wear performance suggests a low wear rate and therefore the aim of this study was to use a pin on plate wear test to investigate the wear performance of PEEK and carbon fibre reinforced PEEK (CFR-PEEK) articulating against ultra high molecular weight polyethylene (UHMWPE) at contact stresses reported for TKA. Our hypothesis was that reduced wear is generated from PEEK or CFR-PEEK on UHMWPE bearings when compared with metal on UHMWPE bearings and that this combination may provide a suitable alternative in TKA.

Methods and Materials

This study compared the wear properties of the following material combinations: 1) PEEK-on-UHMWPE, 2) CFR-PEEK-on-UHMWPE and 3) CoCr-on-UHMWPE (n=3). Using a previously validated modification of the ASTM F732 pin on plate test [1], 20mm diameter PEEK or CFR-PEEK spherically ended pins with a radius of 25mm were articulated against flat circular plates composed of UHMWPE and measuring 40 mm in diameter. A load of 1000N was applied to generate a contact stress of ≈70MPa using a servo hydraulic system which provided reciprocating motion using a motor-crank mechanism. The lubricant used was 25% newborn calf serum containing 0.3% sodium azide to retard bacteria growth and 20mM EDTA to prevent calcium deposition. Pin on plate combinations (including unloaded soaked controls) were tested for 2 million cycles at a cycle frequency of 1Hz and a stroke length of 10 mm. Gravimetric wear analyses of both the pin and plate were carried out every 250,000 cycles where results were converted to volumetric wear using material density.

Results and Discussion

Results showed a linear wear rate of UHMWPE discs over the test period. CFR-PEEK-on-UHMWPE tests were terminated after 1.65 Million cycles (Mc) due to excessive wear of the UHMWPE disc (Figure 1). Wear volume was measured to be 4 times higher with the PEEK-on-UHMWPE combinations and more than 250 times higher in the CFR-PEEK-on-UHMWPE combinations when compared with CoCr-on-UHMWPE.

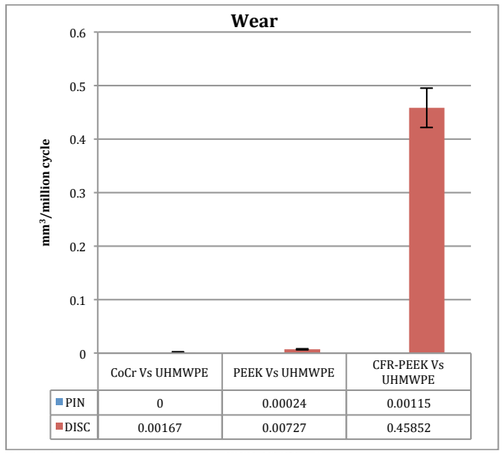

	CoCr Vs UHMWPE	PEEK Vs UHMWPE	CFR-PEEK Vs UHMWPE
PIN	0	0.00024	0.00115
DISC	0.00167	0.00727	0.45852

Fig 1: Volumetric wear loss in UHMWPE discs

Conclusion

In this pin on plate test conducted with contact stresses similar to that measured in the knee, PEEK and CFR-PEEK when articulating against UHMWPE plates generated more volumetric wear when compared with CoCr-on-UHMWPE bearings.
While isoelasticity and reduced wear are desirable in TKA, PEEK with or without carbon fibre reinforcement may be an inappropriate material for use in an all polymer TKA. Further tribological testing with PEEK against other potential materials and at suitable stresses, will be necessary to identify an appropriate combination in an all plastic knee joint.

Reference

1. Walker PS, Blunn GW and Lilley, Wear testing of materials and surfaces for Total Knee Replacement. J Biomedical Mater Res, 1996, 33.159-175.

The Tribological Performance of PEEK Polymer on Polymer Bearings: A Comparison to Conventional Orthopedic Bearing Couples

[2]Baykal D, [1,2]Siskey R, [2]Underwood R, [1,2]Kurtz SM
[1]Drexel University, Philadelphia, PA, [2]Exponent Inc., Philadelphia, PA,
Corresponding author rsiskey@exponent.com

Introduction

Orthopedic bearing materials have remained relatively unchanged for the past two decades. However, market pressures are now forcing manufactures to look to alternative materials to reduce implant cost and improve implant performance. All-polymer bearings involving PEEK are also being considered[1,2]. The objective of this study was to evaluate the wear rate of PEEK and PEEK composites under controlled laboratory conditions and to compare these alternative bearing couples with standard of care bearing couples such as highly-crosslinked polyethylene against CoCr.

Materials and Methods

Twenty pin-on-disc material combinations were tested using the 100 station Phoenix Tribology T87 Multi-station Pin-on-Disc Machine[3-5]. ASTM F732 "Standard Test Method for Wear Testing of Polymeric Materials Used in Total Joint Prostheses" was used as a guide. The materials tested were polyether ether ketone (PEEK Optima, Motis and $BaSO_4$ impregnated), ultrahigh molecular weight polyethylene samples (UHMWPE, HXLPE and Vitamin E blended) and cobalt chromium. Each material combination was tested in five wear stations and one load soak station, which was used to compensate for fluid uptake. The test matrix is summarized in Table 1.

Table 1. Summary of pin and disc material combinations.

Pin Material	Disc Material	Wear Stations	Load Soak Stations
VE UHMWPE	$BaSO_4$	n = 5	n = 1
HXLPE	CoCr	n = 5	n = 1
UHMWPE	CoCr	n = 5	n = 1
VE UHMWPE	CoCr	n = 5	n = 1
CoCr	HXPLE	n = 5	n = 1
Motis	HXPLE	n = 5	n = 1
Optima	HXPLE	n = 5	n = 1
HXPLE	Motis	n = 5	n = 1
UHMWPE	Motis	n = 5	n = 1
VE UHMWPE	Motis	n = 5	n = 1
HXPLE	Optima	n = 5	n = 1
UHMWPE	Optima	n = 5	n = 1
VE UHMWPE	Optima	n = 5	n = 1
CoCr	UHMWPE	n = 5	n = 1
Motis	UHMWPE	n = 5	n = 1
Optima	UHMWPE	n = 5	n = 1
$BaSO_4$	VE UHMWPE	n = 5	n = 1
CoCr	VE UHMWPE	n = 5	n = 1
Motis	VE UHMWPE	n = 5	n = 1
Optima	VE UHMWPE	n = 5	n = 1

The T87 Multi-station Pin-on-Disc Machine is a 100 station pin-on-disc machine manufactured by Phoenix Tribology Ltd (Newbury, England) based on the design of Dr. Saikko (Laboratory of Machine Design, Helsinki University of Technology). A photograph of the TE87 SuperPOD is shown in Figure 1. Validation studies of the T87 SuperPOD have been published by Dr V Saikko[4,5]. Water is circulated through the test bath at 37±3^{0}C. A lubricant chamber (volume 15 ml) is mounted around each disc, so that each station has an independent volume of bovine serum lubricant. The load applied to each pin is 128 N, giving a nominal contact pressure of 2.01 MPa (pin diameter 9 mm).

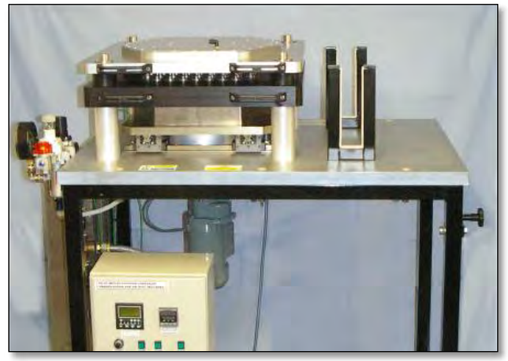

Figure 1. Photograph of Phoenix Tribology T87 Multi-station Pin-on-Disc Machine "SuperPOD"

An elliptical slide track (10 mm major axis, 5 mm minor axis) was employed to facilitate multidirectional wear up to 2 million cycles at 1 Hz. Sliding speed was 24.2 mm/s. The pins are subjected to full cross shear, but the discs are only subjected to cross shear in the limited zone in the middle of the "worn area" where the wear track crosses itself during each cycle.

Every 0.25 MC, up to 2.0 MC, the wear test was stopped for interval analysis and the test specimens removed for characterization. The pins and discs were cleaned and dried using the procedure described in ASTM F1714 "Standard Guide for Gravimetric Wear Assessment of Prosthetic Hip Designs in Simulator Devices." The cumulative volumetric was calculated for each pin and disc for each interval throughout the test. The cumulative wear was averaged for the five wear stations (load soak corrected) for each of the 20 material combinations tested. The wear rate (volumetric wear per million cycles) for each pin and disc was calculated by applying a linear regression algorithm at each interval analysis and averaged for each material combination. .

Results

The resulting wear rates have been summarized in Table 2 and Figure 2. All polymeric samples demonstrated burnishing of the articulating surfaces. For the pins, the entire surface was burnished whereas the discs only showed burning in the region of contact. Discs made from PEEK or PEEK composites demonstrated mass gain due to fluid absorption whereas UHMWPE discs demonstrated wear and cobalt chrome discs demonstrated no wear.

UHMWPE pins with and without vitamin E demonstrated average volumetric wear rates ranging from 6 mm^3/MC, against cobalt chromium, to 33 mm^3/MC, against Motis. Wear rates for the UHMWPE pins with and without vitamin E were only slightly higher when a PEEK Optima disc was substituted for a cobalt chromium disc (8 versus 6 mm^3/MC, respectively). When the UHMWPE is crosslinked, the wear rate of the pins reduced

to as low as 0.4 mm^3/MC when tested against PEEK Optima. When the pins were made from cobalt chromium, PEEK or PEEK composites, they were shown to wear minimally while the UHWMPE counterfaces, with and without vitamin E, demonstrated wear rates expected for the contact conditions applied (range 5-8 mm^3/MC). When those same pins were tested against highly crosslinked counterfaces, the wear rates dropped to 1-2 mm^3/MC.

Table 2. Summary of wear results for pins and discs by bearing couple after 2.0 MC. A positive number represents a mass loss. The results for the wear test samples were corrected at each interval using those of the load soak samples. All results are reported as average ± standard deviation.

Pin Material	Volumetric Wear Rate (mm^3/MC)	Disc Material	Volumetric Wear Rate (mm^3/MC)
UHMWPE	33 ± 15	Motis	-1 ± 0
UHMWPE	8 ± 1	Optima	-1 ± 0
UHMWPE	7 ± 1	CoCr	0 ± 0
Vitamin E	26 ± 7	Motis	0 ± 0
Vitamin E	10 ± 1	BaSO4	-1 ± 0
Vitamin E	8 ± 2	Optima	-1 ± 0
Vitamin E	6 ± 1	CoCr	0 ± 0
HXPLE	2 ± 1	Motis	-1 ± 0
HXLPE	1 ± 0	CoCr	0 ± 0
HXPLE	0 ± 0	Optima	-1 ± 0
Motis	0 ± 0	Vitamin E	8 ± 2
Motis	0 ± 0	UHMWPE	7 ± 2
Motis	0 ± 0	HXPLE	2 ± 1
Optima	0 ± 0	Vitamin E	7 ± 1
Optima	0 ± 0	UHMWPE	5 ± 2
Optima	0 ± 0	HXPLE	5 ± 2
BaSO4	0 ± 0	Vitamin E	6 ± 1
CoCr	0 ± 0	VE UHMWPE	4 ± 1
CoCr	0 ± 0	VE UHMWPE	8 ± 2
CoCr	0 ± 0	VE UHMWPE	7 ± 1

Discussion

Overall the values for UHMPWE materials serve as good experimental controls and provide values consistent with previously published studies summarized by Baykal et al.[6] PEEK composites appear to show wear rates comparable to CoCr with the exception of Motis, which when paired with uncrosslinked UHMWPE shows wear rates much higher than conventional bearing combinations. PEEK Optima performed well when paired with conventional UHMWPE forms and showed a lower wear rate than cobalt chrome when paired with highly crosslinked UHMWPE.

These results suggest that PEEK and PEEK composites should continue to be explored as potential orthopedic bearing materials. This study only investigated these bearing materials as a single set of contact and lubrication conditions. To explore more and less demanding applications in orthopedics, further investigation is warranted.

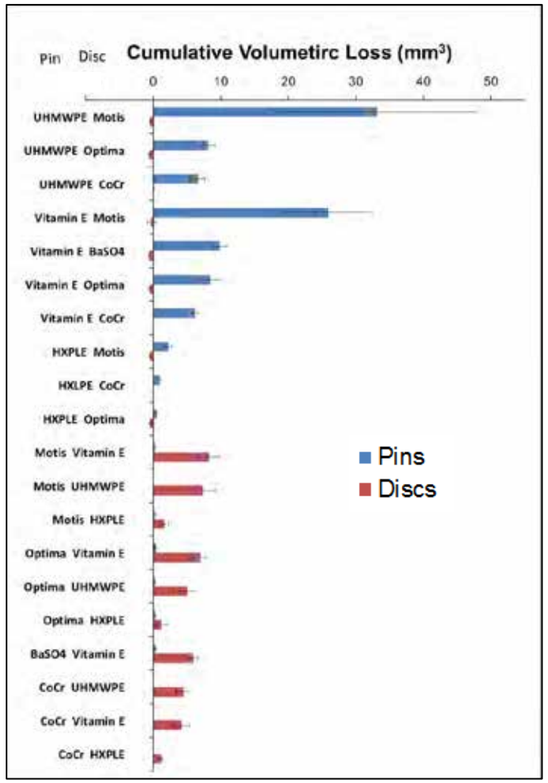

Figure 2. - Average volumetric wear rate (mm^3/MC) for all pin and disk materials. Error bars represent ± one standard deviation.

Acknowledgements

This research was supported by Invibio.

References

1. A. Wang et al. Wear 225–229 (1999) 724–727
2. G. Langohr et al. Proc. IMechE., Part J 225 (2011), 499-513
3. Saikko V. A multidirectional motion pin-on-disk wear test method for prosthetic joint materials, 1998.
4. Saikko, V., A hip wear simulator with 100 test stations. Proceedings of the Institution of Mechanical Engineers, Part H: Journal of Engineering in Medicine, 2005.
5. Saikko, V., Performance analysis of an orthopedic biomaterial 100-station wear test system. Proceedings of the Institution of Mechanical Engineers, Part C: Journal of Mechanical Engineering Science, 2010.
6. Baykal et al, Advances in tribological testing of artificial joint biomaterials using multidirectional pin-on-disk testers. Journal of the mechanical Behavior of Biomedical Materials, 2014.

PEEK Optima as an Alternative Bearing Material to Cobalt Chrome in Total Knee Replacement

Cowie RM[1], Briscoe A[2], Fisher J[1], Jennings LM[1].
[1] Institute of Medical and Biological Engineering, University of Leeds, Leeds, UK. [2] Invibio Biomaterial Solutions Ltd., Lancashire, UK.
r.cowie@leeds.ac.uk

Introduction: PEEK Optima® has been considered as an alternative bearing material for use in joint arthroplasty due to its potentially low wear rates and the low biological activity of its wear debris [1]. In this study, the use of PEEK as the femoral component in total knee arthroplasty was investigated, to give a metal free knee replacement. The wear of all-polyethylene tibial components articulating against moulded PEEK femoral components was compared to the wear against cobalt chrome femorals in a knee simulator. It was hypothesised that the wear of UHMWPE would be similar against cobalt chrome and PEEK femoral components of similar geometry and surface topography.

Methods and Materials: 3 cobalt chrome femoral components and 3 PEEK Optima® (Invibio Biomaterial Solutions, UK) femoral components were tested against all-polyethylene GUR 1020 (conventional, unsterilised) tibial components in a 6 station ProSim knee simulator (Simulation Solutions, UK). The femoral components were set up on the distal centre of rotation and tested under displacement control using Leeds Intermediate kinematics [2] with a maximum anterior-posterior displacement of 5mm. The PEEK femoral components were injection moulded and had an initial mean surface roughness (Ra) of 0.018±0.001µm; the cobalt chrome components were of a similar geometry and surface roughness (0.023±0.001µm). Tests were carried out for 3 million cycles (MC) using 25% bovine serum for lubrication, and wear of the tibial components was assessed gravimetrically after 1 and 3MC using unloaded soak controls to compensate for the uptake of moisture by the polyethylene. Surface roughness measurements of the bearing surfaces were taken pre- and post-test using a contacting Form Talysurf (Taylor Hobson, UK).

Statistical analysis was carried out using ANOVA; data was considered significant at $p<0.05$.

Results: Following 3MC of wear testing, the mean wear rate of UHMWPE articulating against cobalt chrome was 0.97±2.26 mm^3/MC and against PEEK was 2.45±0.77 mm^3/MC , there was no significant difference in the wear of the UHMWPE tibial components against the two different materials ($p=0.06$). Figure 1 shows a linear wear volume over the duration of the study for UHMWPE articulating against both PEEK and cobalt chrome. At the conclusion of the study, the UHMWPE tibial components had a clear wear scar where the machining marks had been removed and the surface of the tibial components were polished; there was light, linear scratching on the articulating surfaces of the PEEK components which had a post-test Ra of 0.240±0.206µm; the cobalt chrome components had a significantly lower ($P=0.009$) mean surface roughness, 0.031±0.036µm.

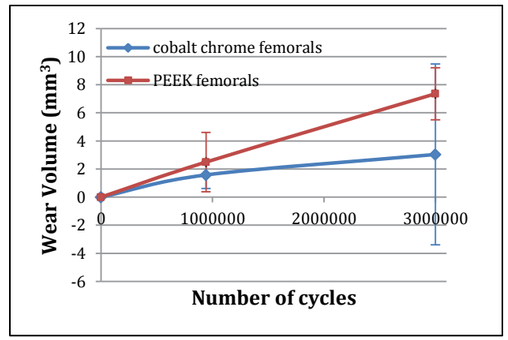

Figure 1: Mean wear volume (mm^3) of UHMWPE tibial components articulating against either cobalt chrome or moulded PEEK femoral components (n=3).

Discussion: The wear rate of UHMWPE tibial components was similar against both PEEK and cobalt chrome femorals. Following 3MC of wear testing, the surface roughness of the PEEK components was significantly higher than that of cobalt chrome; over the duration of this study, the wear rate of the UHMWPE against PEEK components was linear but more long term testing will be necessary to show whether the changes in surface topography during the wear test have an effect on wear rate and the longevity of the implant.

This study shows that under the test conditions used, the wear of UHMWPE tibial components articulating against PEEK Optima and cobalt chrome femoral components of similar surface topography and geometry was similar and that PEEK Optima® has the potential for use as the femoral component in metal free knees.

[1] Kurtz, S.M. Biomaterials, 2007, 28(32):4845-69
[2] McEwen, H.M.J J Biomechanics, 2005, 38(2):357-65

The Influence of Surface Roughness, Lubricant Protein Concentration and Temperature on the Wear of UHMWPE Articulating against PEEK Optima®

Cowie RM[1], Briscoe A[2], Fisher J[1], Jennings LM[1].
[1] Institute of Medical and Biological Engineering, University of Leeds, Leeds, UK. [2] Invibio Biomaterial Solutions Ltd., Lancashire, UK.
r.cowie@leeds.ac.uk

Introduction: PEEK Optima® has the potential for use as the hard bearing material in total knee arthroplasty due to its low wear rate when used in the appropriate tribological conditions and the bioinertness of its wear debris [1]. In this study, the wear of UHMWPE articulating against PEEK was investigated in a pin on plate reciprocating rig; the role of the surface topography of the plates, protein concentration in the lubricant and the temperature of testing were investigated in these simple geometry tests to better understand the wear mechanisms.

Methods and Materials: GUR 1020 UHMWPE pins with a flat 8mm contact face were tested against injection moulded PEEK Optima® (provided by Invibio Biomaterial Solutions Ltd., UK) and cobalt chrome plates in a 6 station multi axial pin on plate reciprocating rig. PEEK plates of varying surface topography (high Ra: 0.06µm and low Ra: 0.03µm) were tested with results compared to control tests carried out against highly polished cobalt chrome plates (Ra<0.01µm). The kinematic conditions were consistent throughout the studies; 1Hz, 20mm stroke length, ±20°rotation, 160N load giving a contact pressure of 3.18MPa. Tests were carried out at room temperature (as per standard practice at Leeds) and at a more physiologically relevant temperature (~36°C) and under varying concentrations of bovine serum (25% and 90%). The studies were run for 1 million cycles (MC) with the wear of the pins determined by gravimetric analysis every 0.3MC.

Statistical analysis was carried out using ANOVA, data was considered significant at $p<0.05$.

Results: Following 1MC of wear testing, the pins had a polished appearance at their contact surface where the machining marks had been removed. On the surface of the PEEK plates there was a wear scar which was more defined on the plates with a higher Ra; the cobalt chrome plates had light scratches in the contact area. Figure 1 shows the end of test wear factor of the UHMWPE pins.

- In 25% serum at room temperature, the wear of UHMWPE was similar ($p=0.10$) against the PEEK plates with low Ra and cobalt chrome plates and was significantly higher ($p=0.04$) against PEEK plates with high Ra.
- Testing in 90% serum at room temperature had no effect on the wear of UHMWPE (compared to tests in 25% serum) against PEEK but there was a significant increase in the wear against cobalt chrome ($p<0.01$).
- In 25% serum at increased temperature, the wear of UHMWPE against cobalt chrome and PEEK plates with low Ra was similar to room temperature tests but the wear rate against PEEK plates with high Ra was significantly lower ($p=0.02$) [2].
- Testing in 90% serum at increased temperature led to deposition of protein on the surface of cobalt chrome plates and against PEEK, the wear and change in surface topography was very variable.
- Improving the surface topography of the PEEK plates lowered the wear of UHMWPE under all environmental conditions.

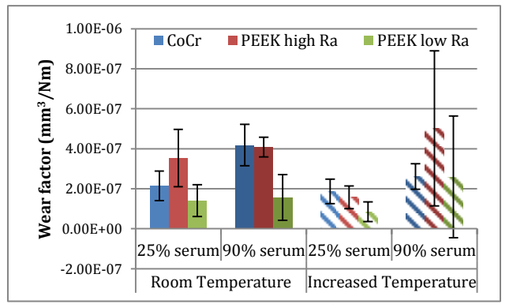

Figure 1: End of test wear factor (mm^3/Nm) of UHMWPE pins articulating against cobalt chrome and PEEK plates of varying surface topography under different serum concentration and temperature conditions.

Discussion: This study shows that surface topography, lubricant concentration and the temperature of the test all have an effect on the wear of UHMWPE. Under the different environmental conditions, the behavior of UHMWPE articulating against PEEK was not the same as against cobalt chrome, there are a multitude of factors contributing to the different wear mechanisms of the different bearing couples including changing lubrication regimes and protein deposition on the articulating surfaces.

This study highlights the importance of manufacturing arthroplasty bearing materials with the best possible surface topography to minimise wear and shows that environmental conditions can have a significant effect on wear performance so should be considered when testing new material combinations.

[1] Kurtz, S.M. Biomaterials, 2007, 28(32):4845-69
[2] Cowie, R.M. et al ORS 2014: Poster #932

PEEK-based Materials as Hip Replacement Bearing Surfaces: A Comparison of Wear and Wear Particles Generated by Injection Molded PEEK-based Materials with Cross Linked Polyethylene Sliding Against Metal and Ceramic Counterfaces.

Hammouche, S[1]; Tipper, JL[1]; Fisher, J[1]; Williams, S[1]
[1]University of Leeds, Leeds, UK
s.hammouche@doctors.org.uk

Introduction: Polyethylene (PE) on metal is the most frequently used bearing combination in total hip replacements (THR) in the US. PE THRs can fail due to late aseptic loosening; this is due to the macrophages' response to generated PE wear particles and the subsequent cytokine cascade. The degree of the response is determined by the wear volume and the chemical nature of wear particles, as well as their size and morphology [1-4]. The volumetric wear of a THR is dependent on the nature of the articulating surfaces and the mechanical environment. In terms of size and morphology, PE wear particles in the sub-micron size range seem to stimulate the highest cytokine response [4, 5]. However, the most bioactive size range was found to be different in other materials [4]. Therefore, a material that demonstrates low wear regardless of the mechanical environment, with fewer particles in its most bioactive size range would be advantageous.
There have been some preliminary investigations of PEEK (poly-ether-ether-ketone) in medical applications [6]. However, there has been very limited assessment of the wear behavior of injection molded PEEK-based resins and no full assessment of wear particle size and area distributions.
This study has compared the wear factors of injection molded unfilled and carbon fiber reinforced (CFR) PEEK against metallic counterfaces to that of cross-linked (XL) PE; and assessed the effect of changing the counterface to Biolox Delta and of increasing the contact stress on the wear factor of CFR-PEEK. Frequency and area distributions of wear particle size ranges of unfilled PEEK and XL PE were compared.

Methods and Materials: The following materials were studied: unfilled PEEK (OPTIMA, Invibio) and CFR-PEEK (MOTIS, Invibio) against high carbon (HC) CoCr or Biolox Delta ceramic plates. The comparative control material was a moderately XL PE (Marathon, DePuy Synthes).
A simple geometry wear study was undertaken. A rotational motion of ±30° across a sliding distance of ±28 mm (cross shear of 0.087), and contact pressures of 1.6 or 4 MPa were applied. The lubricant was 25% (v/v) bovine serum and the wear test was conducted for 1 million cycles at 1 Hz. Wear was assessed gravimetrically. A validated soak control method was used to adjust for serum absorption-induced mass changes during the wear test. Surface profilometry was assessed pre and post wear test.
The lubricant was removed at 600,000 cycles and stored at -18º C until required for wear particle isolation. Wear particles were isolated using the protocol described in ISO 17853 [7]. Briefly, samples of serum lubricant were defrosted; 10 ml of the lubricant was added to 40 ml of hydrochloric acid (37%, v/v). This solution was stirred at 50º C until it turned light purple; indicating complete serum digestion. A volume of 0.5 ml of the digest was added to 100 ml of methanol (100%). The resultant solution was filtered through 10 µm, 1 µm and 0.015µm filters consecutively. A section of each filter was coated with 10 nm of carbon, viewed and analyzed using a high performance cold field emission scanning electron microscopy (Hitachi SU8230) at a range of magnifications. Image Pro Plus® V 6 imaging software (Media Cybernetics Inc., USA) was used to measure the area and size of the particles. Measurements were combined to generate size and area distributions. Percentage data were arcsine transformed and then analyzed by one-way ANOVA.

Results: Unfilled PEEK produced a six-fold higher wear factor than XL PE against HC CoCr (p value <0.0001). CFR-PEEK articulating against Biolox Delta produced a two-fold lower wear factor than XL PE against HC CoCr (p value = 0.003). CFR-PEEK against Biolox Delta had the lowest wear factor among all studied combinations (Figure 1). Higher contact pressures led to a 30 % reduction in the wear factor of CFR-PEEK against Biolox Delta combination (p value = 0.048) (Figure 2). The wear of CFR-PEEK against HC CoCr was higher than XL PE against HC CoCr. The counterface surfaces were scratched following articulation against CFR-PEEK. This was more evident on CoCr plates, with the average surface roughness increasing from 0.005 µm to 0.32 µm (p value = 0.0048) and may provide a reason for the increased wear factor in the CFR-PEEK against HC CoCr combinations.
To maximize the number of particles available for analysis, the highest wear-producing PEEK-based material combination was analyzed (i.e. unfilled PEEK articulating against HC CoCr) and compared with XL PE wear particles articulating against HC CoCr plates. The number of wear particles isolated per material combination exceeded 1500 particles; with flake, fibril and granule-like morphology particles being observed. The XL PE wear particles were predominantly less than 100 nm in size (91%) compared with only 48% in the unfilled-PEEK (p value < 0.001). When unfilled PEEK articulated against HC CoCr, it generated greater percentages of wear particles in the 0.1-1 micron range (51% compared with 8.5% in the case of XL PE; p value < 0.001; Figure 3 a). Only 2% of XL PE and unfilled PEEK wear particles were in the > 1 micron size range.
As a function of volumetric concentration, XL PE articulating against HC CoCr generated significantly greater volumes of wear particles in the <0.1 µm range compared with the unfilled PEEK particles generated (p value <0.01). No statistically significant differences were observed in the volumetric concentration in the rest of the size ranges (Figure 3 b).

Discussion: This is one of the most comprehensive wear and wear particle analysis study to date of injection molded PEEK-based resins. It has shown that injection molded carbon fiber reinforced PEEK against Biolox Delta ceramic generated significantly lower wear compared with XL PE (even under higher contact pressures). Frequency distributions of wear particle size ranges showed that XL PE wear particles were predominately in the <100 nm size range while unfilled PEEK wear particles were more evenly distributed over the 1-0.1µm and <100 nm size ranges. Purportedly, UHMWPE wear particles in the submicron size range are more bioactive [4, 5, 8]. Based on reported size range bioactivity differences between PEEK and XL PE particles and based on what this study found in terms of particle frequency differences across size ranges, there might be functional bioactivity differences between XL PE and PEEK particles. The CFR-PEEK *vs.* Biolox Delta combination generated significantly less wear, and may have the potential to produce particles with less functional bioactivity (which is the subject of future work). The CFR-PEEK *vs.* Biolox Delta combination may have the potential to be used in longer lasting hip replacements. However, the effect of carbon fiber reinforcement should be accounted for; this will be the subject of further investigations.

References:

1. Heisel, C., M. Silva, and T. Schmalzried, *In vivo wear of bilateral total hip replacements: conventional versus crosslinked polyethylene.* Archives of Orthopaedic and Trauma Surgery, 2005. **125**(8): p. 555-557.
2. Kang, L., et al., *Quantification of the effect of cross-shear on the wear of conventional and highly cross-linked UHMWPE.* Journal of Biomechanics, 2008. **41**(2): p. 340-346.
3. Liu, A., *Determination of the biological response and cellular uptake mechanisms of nanometre-sized UHMWPE wear particles from total hip replacements*, 2012, University of Leeds.
4. Hallab, N.J., et al., *Macrophage reactivity to different polymers demonstrates particle size- and material-specific reactivity: PEEK-OPTIMA® particles versus UHMWPE particles in the submicron, micron, and 10 micron size ranges.* Journal of Biomedical Materials Research Part B: Applied Biomaterials, 2012. **100B**(2): p. 480-492.
5. Green, T.R., et al., *Polyethylene particles of a 'critical size' are necessary for the induction of cytokines by macrophages in vitro.* Biomaterials, 1998. **19**(24): p. 2297-2302.
6. Kurtz, S.M. and J.N. Devine, *PEEK biomaterials in trauma, orthopedic, and spinal implants.* Biomaterials, 2007. **28**(32): p. 4845-4869.
7. ISO, *ISO 17853:2011: Wear of implant materials -- Polymer and metal wear particles -- Isolation and characterization*, 2011.
8. McKellop, H.A., et al., *The Origin of Submicron Polyethylene Wear Debris in Total Hip Arthroplasty.* Clinical Orthopaedics and Related Research, 1995. **311**: p. 3-20.

Attached Figures:

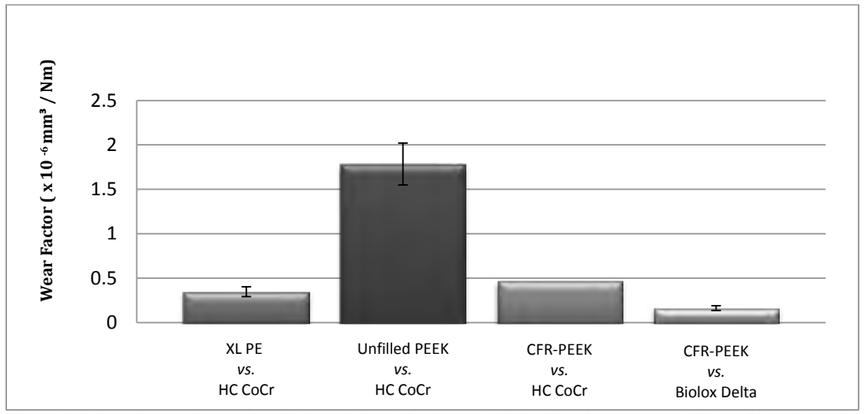

Figure (1): Mean pin wear factors of studied material combinations at 1.6 MPa. Error bars represent 95% confidence intervals.

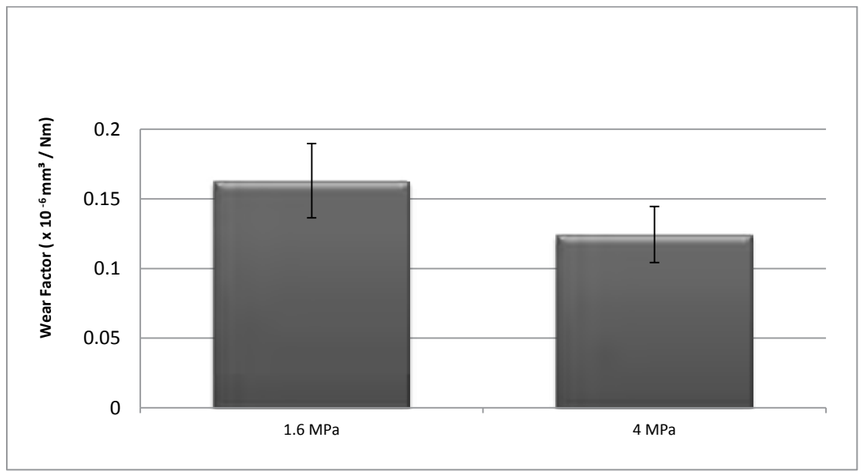

Figure (2): Mean pin wear factors of CFR-PEEK *vs.* Biolox Delta combinations at 1.6 MPa and 4 MPa. Error bars represent 95% confidence intervals.

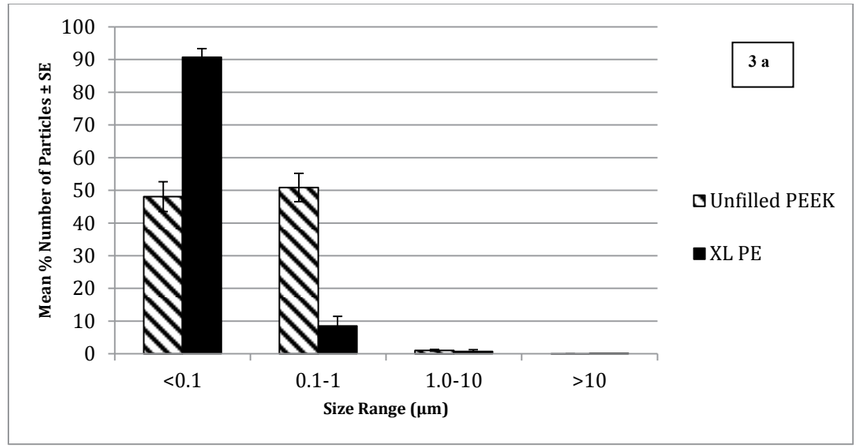

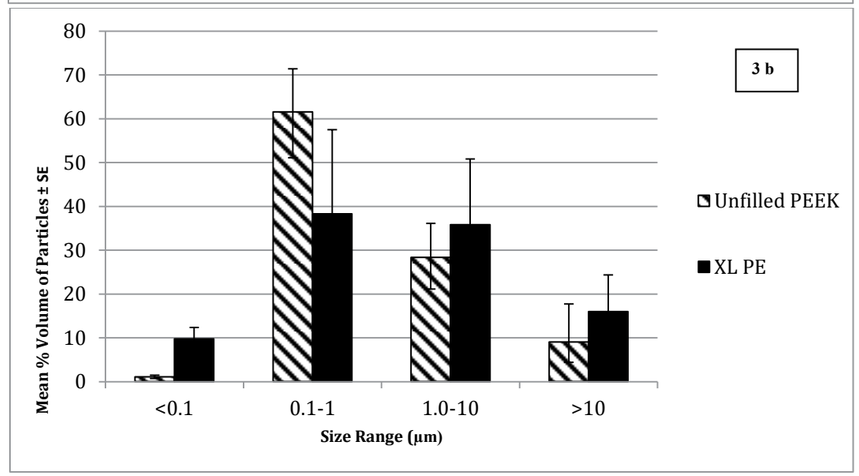

Figure (3 a): Frequency distributions (± standard error) as a function of particle size for wear particles from unfilled PEEK against HC CoCr and XL PE against HC CoCr wear stations. (Figure 3 b): Volumetric concentration distributions (± 95% standard error) as a function of particle size for wear particles from unfilled PEEK *vs*. HC CoCr and XL PE *vs*. HC CoCr wear stations.

Wear resistance of PMPC-grafted CFR-PEEK cups against ceramic femoral heads

Kyomoto, M[1,2,3], Yamane, S[1,2,3], Watanabe, K[2,3], Moro, T[2], Ishihara, K[1]
[1]Department of Materials Engineering, [2]Division of Science for Joint Reconstruction, The University of Tokyo, Tokyo, Japan
[3]Research Department, KYOCERA Medical Corporation, Osaka, Japan
kyomoto@mpc.t.u-tokyo.ac.jp

Introduction: The careful consideration of wear resistance for bearing couples or interfaces in artificial hip joint is very important. Studies have shown that poly(ether-ether-ketone) (PEEK) might be useful as an alternative bearing material. However, conventional PEEK cannot satisfy some requirements, e.g., wear resistance in artificial joint fabrication. Therefore, the use of PEEK as a reinforcing agent or surface modifier has been studied, focusing on the wear resistance of the polymer. Here, we propose a new and safer methodology for constructing a nanometer-scale modified surface layer of poly(2-methacryloyloxyethyl phosphorylcholine [MPC]) (PMPC) on the PEEK and carbon-fiber-reinforced PEEK (CFR-PEEK) substrates by self-initiated photoinduced graft polymerization [1–3]. In this study, we investigated the wear resistance of bearing couples of the PMPC-grafted CFR-PEEK acetabular cups against a ceramic femoral head to propose a better alternative.

Methods and Materials: Polyacrylonitrile (PAN) or Pitch-based CFR-PEEK (Sumiploy CK4600 or MOTIS) specimens were machined from extruded bar stocks. CFR-PEEK specimens were immersed in an aqueous 0.5 mol/L MPC solution. Photo-induced graft polymerization was performed at 60°C for 90 min on the CFR-PEEK surfaces under UV irradiation at 5 mW/cm^2 intensity [2]. A 12-station hip simulator with untreated and PMPC-grafted CFR-PEEK cups (n = 3 each) was used for the wear test of 3.0×10^6 cycles according to ISO 14242-3. A 26-mm Co–Cr–Mo alloy (K-MAX HH-02) or zirconia-toughened alumina (ZTA; Bioceram AZ209) ball was used as the femoral head. The wear particles were isolated by sequential filtering from the bovine serum solution used for lubrication, and they were observed using scanning electron microscopy. The features of the bearing surfaces of the femoral heads were observed using confocal laser scanning microscopy, a surface roughness tester, and a contour tracer.

Results: In the hip simulator wear test, the characteristics of the PMPC-grafted surface affected the durability of two types of CFR-PEEK cups (PAN and Pitch). During the hip simulator wear test, the PMPC-grafted CFR-PEEK (PAN) cup (mean ± 95% CI = –5.49 ± 1.62 mg/10^6 cycles) demonstrated less ($p < 0.05$) gravimetric wear rate than the untreated PEEK (PAN) cup (–2.46 ± 0.24 mg/10^6 cycles). In contrast, there was no significant difference in the wear rate of CFR-PEEK (Pitch) between the untreated (–0.01 ± 0.13 mg/10^6 cycles) and PMPC-grafted (0.13 ± 0.06 mg/10^6 cycles) cups. Significantly fewer wear particles were observed in the PMPC-grafted CFR-PEEK (Pitch) cup than in the untreated CFR-PEEK (Pitch) cup (Fig. 1). The surfaces of the ZTA femoral heads against the PMPC-grafted CFR-PEEK (Pitch) cups were smooth. In contrast, the surfaces against the untreated CFR-PEEK (Pitch) cups had a different morphology; the surface was worn and significantly more round ($p < 0.01$) than that against PMPC-grafted CFR-PEEK (Pitch) cups.

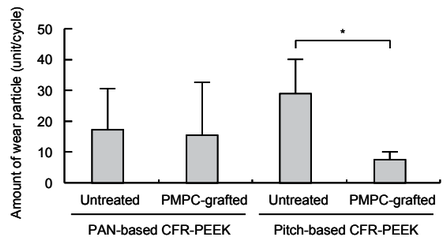

Fig. 1. Amount of wear particles isolated from lubricants of the hip simulator wear test. *$p < 0.05$.

Discussion: In the hip simulator wear test of the present study, the PMPC-grafted CFR-PEEK cups prevented wear particle production and counter femoral head surface damage. Regardless of the material used for the femoral head, the wear rate of the PMPC-grafted CFR-PEEK cups was almost zero. PMPC is water soluble because MPC is highly hydrophilic. Fluid film lubrication with the PMPC-grafted surface was therefore afforded by the hydrated layer. The carbon fiber content of the composite must be sufficient to achieve high wear resistance, and in this study, it scratched the counter surfaces that exhibited high degrees of femoral head wear [3]. In contrast, the counter surfaces against PMPC-grafted CFR-PEEK were smooth. It is assumed that the fluid film and/or hydrated layer produced by the PMPC graft suppressed direct contact between the counter-bearing face and the hard carbon fibers of the CFR-PEEK substrate. This prevented counter surface damage regardless of the carbon fiber content of CFR-PEEK.

In conclusion, PMPC-grafted CFR-PEEK and ZTA ceramic are suitable candidates for artificial hip joint development. Such investigations are of great importance for the design of lifelong artificial hip joints and obtaining a better understanding of the limitations resulting from the use of this material.

References: [1] Kyomoto M., *et al. Appl Mater Interfaces*. 2009:1;537-542; [2] Kyomoto M., *et al. Biomaterials*. 2010:31;1017-1024; [3] Kyomoto M., *et al. Biomaterials*. 2013:34;7829-7839.

Acknowledgments: This study was supported by the Strategic Promotion of Innovative Research and Development (JST).

Characterization of the invitro antimicrobial and in vivo antibiofilm properties of a PEEK-Silver Zeolite Composite in spine

Sankar, Sriram[1]; Crudden, Joseph[2]; Johns, W.Derrick[3]
DiFusion Technologies Inc., Georgetown, TX-USA.
sankar@difusiontech.com

Introduction: Polyether ether ketone (PEEK) demonstrates intrinsic inertness and hydrophobic properties, thereby resulting in an inherent susceptibility to bacterial infections and reduced fusion capacity within the intervertebral space due to fibrous encapsulation. CleanFuze™ (CF) is a bioactive PEEK- silver zeolite composite, which has recently received CE approval in Europe and is known to have infection resistive and osteoblast stimulative effects due to silver ions and ceramic zeolite particles respectively.

Aim: Evaluate the efficacy of CleanFuze in preventing in vitro bacterial colonization and in vivo biofilm formation relative to PEEK; without compromising the latter's attractive biomechanical properties.

Methods and Materials:

- **In vitro peri-operative contamination model:** Competitive colonization between a GFP (green fluorescent protein) induced MRSA (methicillin resistant staphylococcus aureus) strain and human MG-63 osteoblast-like cells (ATCC CRL-1427 TM) for a CleanFuze and PEEK disks (~1.23 cm2). Osteoblast proliferation characteristics on these MRSA inoculated surfaces were compared to their respective un-inoculated controls. GFP-MRSA strain was seeded onto the implants for 4hrs to initiate bacterial adhesion before the introduction of the osteoblasts. Osteoblast proliferation was quantified using Alamar Blue assay while bacterial viability was quantified using colony count technique. Both assays were carried out at two time points-Day 3 and Day 7. Any contribution to the Alamar assay by viable bacteria on the implant surfaces was subtracted by setting up a concentration vs. fluorescence standard curve using a UV-Vis micro plate reader.
- **In vivo Antibiofilm Testing using a Rabbit Spine infection Model:**

12 NZW female rabbits- 2.5-3 kg.

• Rabbits 1, 5, 9- PEEK; Rabbits 2,6,10 - Ag eluting CF; Rabbits 3,7,11,12- Surface Modified Ag eluting CF; Rabbits 4, 8 Ag-Zn surface modified CF.

•Implant screw placed across mammillary spinous process. L3- control site with defect but no implant/inoculum. L6- site with implant and infected with 500 cfu of MRSA.

•Equivalent implant sections explanted after a week and analysed for biofilm formation qualitatively via crystal violet biofilm assay.

- **Comparative Biomechanical Testing:** Gamma sterilized (60-80KGy) 22x8 PLIF CF and PEEK cages were tested for dynamic compression and torsion (ASTM F2267-03, F2267-04) in PBS at 37 ± 3°C. Unsterilized PEEK and CF samples were used for static impact (ASTM D256), flexural (ASTM D790) and tensile analysis (ASTM D638).

Results and Discussion:

In vitro peri-operative contamination model

CleanFuze being antimicrobial is able to protect osteoblasts from attack, infiltration and destruction by MRSA. Infected CleanFuze shows ~ 46 times greater osteoblast proliferation compared to infected PEEK & three times greater proliferation compared to even uninfected PEEK.

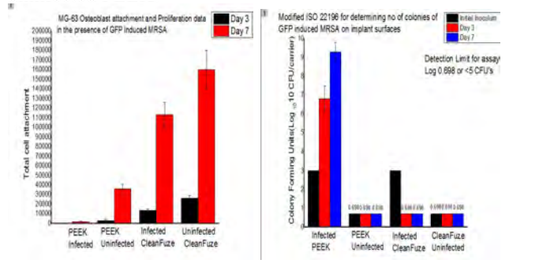

In vivo Antibiofilm Testing using a Rabbit Spine infection Model

PEEK implants show intense purple color indicative of biofilm formation. CleanFuze displays no purple coloration, i.e. absence of biofilm as show below.

Comparative Biomechanical Testing

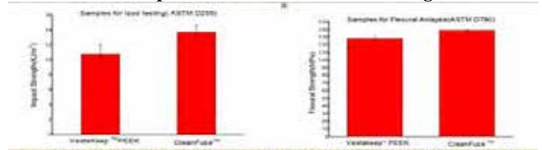

Conclusion: CleanFuze™ demonstrates enhanced osteoblast proliferation and anti-biofilm activity; while preserving PEEK's biomechanical properties, thereby allowing for an alternative biomaterial in spine and orthopedics with improved characteristics.

SEE YOU NEXT YEAR!

Thank you!

ORGANIZED BY

IRC
IMPLANT RESEARCH CENTER

Exponent®

SPONSORED BY

Invibio®
BIOMATERIAL SOLUTIONS